

13 June 2025

Dear Endocrine Society of Australia,

Re: Application for the ESA Young Investigator Scientific Article Award

Thank you for your consideration of our work for the 2025 ESA Young Investigator Scientific Article Award.

We would like to submit the following scientific article for consideration of this award:

Kim, A. S., Taylor, V. E., Castro-Martinez, A., Dhakal, S., Zamerli, A., Mohanty, S. T., ... & McDonald, M. M. (2025). Early and multiple doses of zoledronate mitigates rebound bone loss following withdrawal of RANKL inhibition. Journal of Bone and Mineral Research, zjaf008. (Published 23rd January 2025)

This manuscript represents the doctoral research of Dr Albert S. Kim, a PhD student at the Garvan institute of Medical Research, Sydney. The submitted work was conducted under the supervision of A/Prof Michelle McDonald, A/Prof Christian Girgis and Prof Jackie Center.

Dr Kim was responsible for the majority of the experimental work, with the assistance from lab members, including animal work (injections, live imaging, tissue dissection and harvesting), microCT scan and analysis, and biochemical assays (including TRAP5b and CTX ELISA). He led the writing and revision of the manuscript in consultation with the co-authors.

To support this application, we also enclose the following scientific articles that frame and extend the significance of the submitted publication:

1. *Kim, A. S., Taylor, V. E., Castro-Martinez, A., Dhakal, S., Zamerli, A., Mohanty, S., ... & McDonald, M. M. (2024). Temporal patterns of osteoclast formation and activity following withdrawal of RANKL inhibition. Journal of Bone and Mineral Research, 39(4), 484-497.*
 - This study provided the foundational mechanistic insights that informed the sequential therapy approach employed in the submitted manuscript.
2. *Kumar, S., Wang, M., Kim, A. S., Center, J. R., McDonald, M. M., & Girgis, C. M. (2025). Denosumab discontinuation in the clinic: implications of rebound bone turnover and emerging strategies to prevent bone loss and fractures. Journal of Bone and Mineral Research, zjaf037.*
 - This perspective article builds upon the submitted work to outline the clinical implications and future directions in the management following denosumab discontinuation.

Together, these articles represent a translational body of work spanning preclinical discovery to clinical application in a highly relevant field of endocrine research.

The global impact of this body of work has been recognised through invitation to present at leading international conferences, including ENDO, ASBMR and ECE. Dr Kim has received multiple competitive awards relating to the submitted work, most notably the ASBMR-AIMM John Haddad Young Investigator Award. Further, the senior author (A/Prof McDonald), has been invited to join the ASBMR Taskforce on Denosumab Discontinuation in recognition of the translational importance of this work.

Thank you again for your consideration.

Kind regards,

Dr Albert S Kim 

Victoria E Taylor *Victoria Taylor*


Ariel Casto-Martinez

Dr Suraj Dhakal *Suraj Dhakal*

Amjad Zamerli *Jad Zamerli*

Dr Sindhu T Mohanty *Sindhu Mohanty*

Ya Xiao 

Dr Marija K Simic *Marija Simic*

Alyssa Pantalone *Alyssa Pantalone*


Julian Chu

Dr Tegan L Cheng *Tegan Cheng*

Prof Peter I Croucher *Peter Croucher*

Prof Jacqueline R Center *Jacqueline Center*

A/Prof Christian M Girgis 

A/Prof Michelle M McDonald 

Early and multiple doses of zoledronate mitigates rebound bone loss following withdrawal of receptor activator of nuclear factor kappa-B ligand inhibition

Albert S. Kim^{1,2,3,4} , Victoria E. Taylor^{1,3}, Ariel Castro-Martinez^{1,5}, Suraj Dhakal¹, Amjad Zamerli¹, Sindhu T. Mohanty¹, Ya Xiao¹, Marija K. Simic^{1,6}, Alyssa Pantalone³, Julian Chu⁷, Tegan L. Cheng^{3,7}, Peter I. Croucher^{2,5}, Jacqueline R. Center^{2,5}, Christian M. Girgis^{3,4} , Michelle M. McDonald^{1,2,3,*}

¹Cancer Ecosystems Program, Garvan Institute of Medical Research, Sydney, NSW 2010, Australia

²Faculty of Medicine and Health, St Vincent's Clinical School, UNSW Sydney, Sydney, NSW 2010, Australia

³Faculty of Medicine and Health, University of Sydney, Sydney, NSW 2006, Australia

⁴Department of Diabetes and Endocrinology, Westmead Hospital, Sydney, NSW 2145, Australia

⁵Cancer Plasticity and Dormancy Program, Garvan Institute of Medical Research, Sydney, NSW 2010, Australia

⁶Department of Pathology, New York University Grossman School of Medicine, New York, NY 10016, United States

⁷Centre for Children's Bone and Musculoskeletal Health, The Children's Hospital at Westmead, Sydney, NSW 2145, Australia

*Corresponding author: Michelle M. McDonald, Faculty of Medicine and Health, Charles Perkins Centre, John Hopkins Drive, Camperdown, NSW 2006, Australia. (michelle.mcdonald@sydney.edu.au).

Abstract

Rebound bone loss following denosumab discontinuation is an important barrier in the effective long-term treatment of skeletal disorders. This is driven by increased osteoclastic bone resorption following the offset of RANKL inhibition, and sequential osteoclast-directed therapy has been utilized to mitigate this. However, current sequential treatment strategies intervene following the offset of RANKL inhibition and this approach fails to consistently prevent bone loss. Our previous work, using a mouse model of denosumab discontinuation, has shown that the processes that drive the rebound phenomenon occur earlier than when bone loss is detected, namely a rise and overshoot in serum tartrate-resistant acid phosphatase (TRAP). We identified that these changes in serum TRAP may provide an earlier window of opportunity to intervene with sequential therapy following RANKL inhibition withdrawal. Here, we show that early treatment with zoledronate (10 mg/kg, 3 wk following the last dose of OPG:Fc), preceding the rise and overshoot in serum TRAP, effectively mitigates rebound bone density loss through preventing the overshoot in serum TRAP. Further, we show that multiple doses of zoledronate (early treatment and during anticipated BMD loss) is superior in consolidating bone density gains made with RANKL inhibition and preventing rebound BMD loss as measured by DXA. Importantly, we demonstrate the efficacy of early and multi-dose zoledronate strategy in preventing bone loss in both growing and skeletally mature mice. MicroCT analysis showed improved trabecular bone structure in both the femur and lumbar vertebrae with zoledronate treatment compared with control. These increases in bone mass translated to increased fracture resistance in skeletally mature mice. This work provides a novel approach of early and multi-dose sequential treatment strategy following withdrawal of RANKL inhibition, contributing valuable insight into the clinical management of patients who discontinue denosumab therapy.

Keywords: sequential therapy, zoledronate, denosumab, osteoporosis, denosumab discontinuation

Lay summary

Stopping denosumab leads to loss of bone gained during treatment, due to increased bone resorption when denosumab wears off. Current strategies often fail to prevent this as they cannot stop osteoclasts resorbing bone. Our work using a mouse model has shown that processes that lead to bone loss start earlier than we can detect in the clinic. We show that early and multi-dose zoledronate treatment, another medication used to block osteoclasts, to target these earlier processes can prevent bone loss after stopping denosumab. This approach offers a new strategy for managing bone health in patients stopping denosumab.

Introduction

Neutralization of RANKL with denosumab has revolutionized the management of conditions requiring inhibition of bone resorption.¹ Continued use leads to sustained BMD gains and fracture risk reduction, with evidence of efficacy for up to 10 yr.² Denosumab is well tolerated and often preferred by patients over bisphosphonates,³ leading to widespread use globally.

Rare, but serious side effects, such as medication-related osteonecrosis of the jaw (MRONJ) and atypical femoral fractures (AFFs), arise from prolonged suppression of bone turnover with antiresorptive therapy. This led to the development of “drug holidays” (or monitored treatment break),⁴ which reduces the risk of these complications in those receiving long term bisphosphonates.⁵ However, “drug holidays” are not recommended with denosumab.

Received: September 21, 2024. Revised: December 20, 2024. Accepted: January 22, 2025

© The Author(s) 2025. Published by Oxford University Press on behalf of the American Society for Bone and Mineral Research.

This is an Open Access article distributed under the terms of the Creative Commons Attribution License (<https://creativecommons.org/licenses/by/4.0/>), which permits unrestricted reuse, distribution, and reproduction in any medium, provided the original work is properly cited.

Bisphosphonates are embedded into bone tissue, displaying durability of osteoclast inhibition,⁴ whereas denosumab binds systemically to soluble and membrane bound RANKL, and osteoclast inhibition is rapidly reversed following its clearance.

Upon stopping denosumab, rebound BMD losses are observed with a sharp rise and overshoot in the markers of bone turnover following the offset of RANKL inhibition.⁶ Rise in P1NP and CTX above pretreatment baseline levels are observed from 6 mo following the last denosumab dose, following the offset of RANKL inhibition. These elevated levels of bone turnover markers are sustained for 12 mo before returning to baseline levels and are associated with increased fracture risk during this time, particularly the risk of multiple vertebral fractures.⁷ Despite these risks, persistence and adherence to denosumab declines with longer treatment duration.⁸

Rebound increases in bone resorption following denosumab discontinuation are driven by a rapid overshoot in osteoclastic activity.⁹ Therefore, an appropriate approach would be to transition to an osteoclast-directed therapy, such as bisphosphonates. However, clinical studies examining the use of sequential zoledronate do not consistently prevent rebound bone loss, with longer denosumab treatment duration and greater BMD gains being important risk factors for bone loss.^{10–14}

Initial reports of rebound bone loss despite a “parting” dose of zoledronate¹² gave rise to the idea that sequential therapy should be withheld until bone turnover resumes (as measured by serum CTX). It was thought that this would allow bisphosphonates to be taken up in the newly opened resorption pits and thereby become available to osteoclasts.¹²

However, prospective randomized controlled studies utilizing sequential zoledronate following denosumab discontinuation could not show consistent prevention of bone loss and fractures.^{13–16} Despite these inconclusive studies, current expert advice¹⁷ align sequential zoledronate with a rise in serum CTX or when BMD loss is detected, and while repeated zoledronate doses are recommended,¹⁷ the specific parameters that warrant this are not clearly defined, leading to bone loss and fractures despite multiple doses of zoledronate.¹⁵ There is currently no evidence-based, efficacious sequential treatment strategy to consolidate BMD gained on denosumab treatment, mitigate the rebound phenomenon, and prevent resultant fractures. This absence of a safe approach is rendering patients to receive denosumab indefinitely, and importantly, hindering treatment uptake.

An improved sequential treatment strategy following denosumab discontinuation is needed—based on better understanding of the cellular mechanisms driving this phenomenon and improved methods to predict imminent bone loss. Clinical studies examining sequential therapies are observational, and placebo-controlled studies are not ethically feasible due to the increased risk of bone loss and fractures in those receiving placebo.

To address these limitations, we developed a murine model of denosumab discontinuation using osteoprotegerin(OPG:Fc), to mimic denosumab. In brief, OPG:Fc treatment leads to BMD gains and following the offset of its effect, there is rebound bone loss to vehicle levels. We showed that serum tartrate-resistant acid phosphatase (TRAP), a marker of osteoclast number and activity, rises prior to the rise in serum CTX and loss in BMD. We also revealed that a

pro-osteoclastogenic environment develops before bone loss is clinically detected, highlighting a potential early intervention window with sequential therapy analogous to a time within 6 mo of the last denosumab dose¹⁸ (Figure 1). These findings suggest that rising serum TRAP may predict imminent bone loss and therefore support an optimized therapeutic window for sequential therapy, rather than waiting until bone loss is underway.

In this study, we first aimed to determine whether a single dose of zoledronate in the current therapeutic window, when CTX levels are rising and BMD loss underway, would be ineffective in preventing bone loss following denosumab discontinuation. We hypothesized that earlier intervention with bisphosphonates, prior to the offset of RANKL inhibition, and preceding the rise and overshoot of serum TRAP, would prevent rebound bone loss. We also aimed to determine whether a multi-dose zoledronate strategy, both early and a follow-up dose, would provide a more efficacious regimen for preventing rebound BMD loss. To translate the findings of our model to the clinical context, we performed these studies in both growing and skeletally mature mice to examine the efficacy of this strategy at various stages of skeletal maturity. Taken together, our preclinical studies provide novel insights to guide sequential treatment strategies in patients undertaking denosumab discontinuation.

Materials and methods

Experimental mice

Animal experiments were performed in accordance with approved protocols from the Garvan Institute of Medical Research and St Vincent’s Hospital Animal Ethics Committee (ARA 18/03 and 21/17), as well as the Australian Code of Practice for the Care and Use of Animals for Scientific Purposes.

Female C57BL/6J or C57BL/KaLwRij (Harlan, Netherlands) mice were obtained from Australian BioResources. All mice were bred and maintained under specific-pathogen free (SPF) conditions. Animal experiments were performed at the Biological Testing Facility, Garvan Institute of Medical Research. Holding areas were maintained within a constant temperature of 21.4 °C with humidity range to avoid stress and minimize experimental variability. Circadian rhythms were stimulated with lighting mimicking 12 h day/night cycles. Mice were provided with standard chow and water ad libitum.

All mice entered their respective experiments aged 6–8 or 26 wk and group sizes were determined based on previous experiences with each model, in which power calculations were performed to estimate sample size. Using this, 7–10 mice were allocated to each group or otherwise as stated in the figure legends.

To examine the effects of sequential zoledronate following OPG:Fc withdrawal modeling current clinical practice, C57BL/KaLwRij mice were randomly allocated to receive zoledronate or saline at week 12, 10 wk following 2 wk of OPG:Fc or saline treatment, at a time where a rise in serum CTX and rebound BMD loss was anticipated based on previous studies.¹⁸

To examine and compare the effects of early sequential zoledronate and a multi-dose zoledronate strategy following OPG:Fc withdrawal in young growing mice, 6–7 wk old C57BL/6J mice were randomly allocated to receive OPG:Fc or saline for 2 wk followed by zoledronate or saline at week

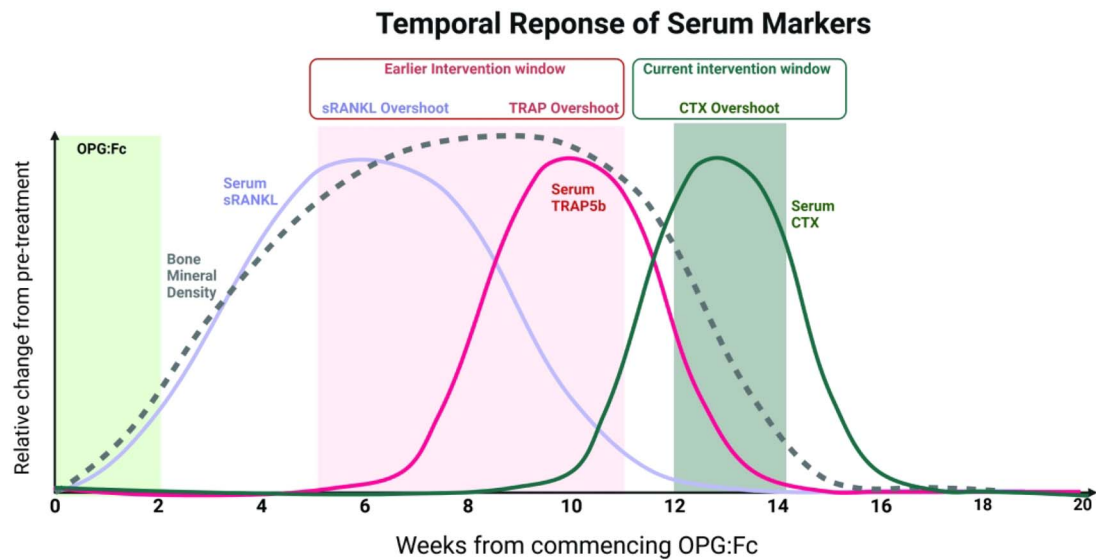


Figure 1. Pro-osteoclastogenic environment develops before a rise in CTX or BMD loss is detected following withdrawal of RANKL inhibition. Schematic summarizing our model of denosumab discontinuation utilizing OPG:Fc in growing mice showing the rebound phenomenon following withdrawal of RANKL inhibition.¹⁸ BMD and serum RANKL rise with OPG:Fc treatment, while serum TRAP and CTX are suppressed. As there is offset of RANKL inhibition, serum TRAP rises as BMD falls with a rise in CTX following this. Current sequential therapy strategies intervene at a time of CTX rise and/or BMD decline, at or later than 6 mo following the last denosumab dose, despite increased markers of osteoclast formation and activity preceding this. A rise in serum RANKL and TRAP may provide an earlier intervention window to prevent BMD loss analogous to within 6 mo of the last denosumab dose. Created in Biorender.com.

5 only, or week 5 and again at week 12 where CTX rise and BMD loss was anticipated in mice treated with OPG:Fc only.

To examine and compare the effects of early sequential zoledronate and a multi-dose zoledronate strategy following OPG:Fc withdrawal in skeletally mature mice, 26 wk old C57BL/6J mice were randomly allocated to receive OPG:Fc or saline for 4 wk, which was followed by zoledronate or saline at week 7 only, or week 7 and again at week 13.

Mice underwent DXA imaging and retro-orbital bleeds fortnightly or 3-weekly throughout the study. At the end of the study, tissue was harvested for their respective experiments outlined below.

OPG:Fc and zoledronate treatment

OPG:Fc (Amgen Inc.) was administered at a dose of 10 mg/kg i.p. twice weekly for 2 wk in young growing mice (6-8 wk old). OPG:Fc was administered 3 times weekly for 4 wk in aged, skeletally mature mice (26 wk old) at a higher dose and for a longer duration to achieve a significant difference between vehicle and OPG:Fc-treated mice. OPG:Fc was administered at a dose confirmed to ablate osteoclasts.¹⁹ Vehicle mice received saline 2-3 times weekly at the same frequency as the OPG:Fc doses in the corresponding treatment groups.

Zoledronate (Novartis Pharma) was administered at a dose of 0.1 mg/kg i.p. once or repeated as outlined above, at a dose determined based on the adult therapeutic dose and confirmed to increase BMD in our previous work.²⁰

DXA analysis of BMD

DXA (Faxitron Ultrafocus DXA, Hologic) was performed fortnightly or 3-weekly on anesthetized mice under 3%-5% inhaled isoflurane. Hindlimb analysis was performed using VisionDXA (Hologic) and a manually drawn ROI

encompassing the hindlimb excluding the foot was used to quantify BMD.

MicroCT

Formalin-fixed right femora and the L4 vertebrae were imaged with the SkyScan 1772 microCT scanner (Bruker) at a resolution of 4.3 μm , 0.5 mm aluminum filter, 50 kv voltage, and 200 μA tube current. Images were captured every 0.4° through 360° and were reconstructed and analyzed using NRecon software (SkyScan). Bone structural parameters and nomenclature were utilized according to standardized guidelines.²¹ Three-dimensional reconstructed images of femora were generated using Drishti imaging software version 2.4 (ANU). ROI selection and analyses were performed using CTAn software (Bruker).

To examine the changes in femoral bone parameters trabecular bone parameters were calculated from scans performed at a voxel resolution of 5 μm in a 1 mm region beginning 200 μm proximal to the distal femoral growth plate to reduce the contribution of the primary spongiosa in the analysis. Cortical bone parameters were calculated from scans performed at a voxel resolution of 5 μm in a 0.5 mm region beginning 300 μm proximal to the distal femoral growth plate.

Changes in vertebral bone trabecular and cortical parameters were calculated from scans performed at a voxel resolution of 5 μm in an ROI calculated by measuring the distance between 0.2 mm offset from the point of 50% spongiosa and trabecular bone on both ends of the vertebral body.

Measurement of TRAP5b and CTX

Serum collected by retro-orbital bleeds throughout animal phases, under anesthesia with isoflurane, was stored at -70° and then assessed for TRAP5b and CTX levels using ELISA kits (Immunodiagnostic Systems) following the manufacturer's instructions.

Mechanical testing

Compression testing of L4 vertebrae performed as described previously.²² In brief, the L4 vertebrae were warmed to room temperature and the vertebral processes were removed. Samples underwent mechanical testing on an Instron 5966 (Instron Inc.) by compression until failure. Testing was performed at 3 mm/min until breaking with a 100 N load cell. Data were collected using BlueHill 3 version 3 (Instron Inc.) and the load displacement curve were plotted with the maximum load to first failure calculated.

Analysis of bone histomorphometry

Quantitative histomorphometry

Preparation of femora samples for paraffin histomorphometric analysis and TRAP staining was performed as described previously.¹⁸ Briefly, femora were fixed in paraformaldehyde for 24 h then decalcified in EDTA. Samples were then processed in paraffin and sections were cut and stained for TRAP to identify osteoclasts from other resident bone cells.¹⁸

Right femora sections were scanned on the Aperio Scanscope CS2 model. An area of interest was indicated by a rectangle placed on the Macro image. Utilizing an Olympus UPLXAPO objective lens at a 20x objective, high-quality digital slides were created. Digital slides were modified on Aperio ImageScope (v12.3.2.8013) to show 3 ROI's: 900 μ m at 2.2x objective, 300 μ m at 9.8x objective, and 300 μ m at 7x objective.

Quantification of osteoclast populations among the trabecular bone were performed with BioQuant Osteo (Version v21.5.60). Utilizing a Zeiss Axioplan Microscope (Zeiss) with a high-resolution Jenoptik Camera at 10X objective, an ROI capturing a 3 mm region of trabecular bone, 1 mm from the top of the growth plate junction within the cortices was analyzed for each sample. TRAP-positive osteoclasts (bright pink cytoplasmic appearance) were marked, and their cell surface-bone contact perimeters and trabecular bone surfaces were recorded. The total bone surface, number of osteoclasts per total bone surface, and osteoclasts per total bone surface were determined. The structural and cellular parameters were calculated and expressed according to the ASBMR standardized nomenclature.²¹

Statistical methods

Results were analyzed using GraphPad Prism (Version 9, GraphPad Prism). One-way ANOVA and multiple comparisons were performed using Tukey correction, and unpaired t-tests were performed when comparing 2 populations. All data are expressed as mean with error bars representing standard deviation and *p*-values less than .05 were considered statistically significant.

Results

Sequential zoledronate at the time of CTX rise does not prevent bone loss

Serum CTX rise or BMD reduction has been used to guide the timing of sequential treatment¹³ due to concerns that earlier bisphosphonate administration would not be taken up onto bone surfaces.¹² To model the current clinical practice, we treated mice with OPG:Fc or saline for 2 wk and administered zoledronate or saline at week 12, a time in our model of expected CTX rise from post treatment levels (Figure 2A).

Treatment with OPG:Fc (10 mg/kg) twice weekly for 2 wk significantly increased hindlimb BMD, which continued to rise for 6 wk following treatment reaching levels 21% higher than vehicle ($p < .0001$) before declining to vehicle levels over 4 wk between week 8 and 12. Zoledronate (0.1 mg/kg) or saline was administered at week 12, although BMD was equivalent between groups at this time point as rebound BMD loss had already occurred (Figure 2B).

Serum TRAP was 54% and 85% lower than vehicle at week 8 in mice treated with OPG:Fc ($p < .05$ and $p < .001$ in OPG and OPG + ZOL groups, respectively), though levels were rising from being fully suppressed following OPG:Fc treatment, indicating increasing osteoclast activity (Figure 2Di). Serum TRAP in OPG:Fc treated mice was 56% and 53% higher than vehicle at week 10 ($p < .01$ and $p < .05$, respectively, Figure 2Dii) and both serum TRAP and CTX were significantly higher than vehicle at week 12, when zoledronate was administered (Figures 2Ci and 2Diii). This elevation in TRAP and CTX above vehicle levels persisted in mice that received OPG:Fc-only at week 14, whereas administration of zoledronate at week 12 led to suppression of TRAP levels to significantly below vehicle levels ($p < .001$ OPG + ZOL vs Vehicle, Figure 2Div), and serum CTX to vehicle levels (Figure 2Cii), indicating reduced osteoclast activity.

These data confirm that the current intervention timing of sequential therapy, at a time of CTX rise or BMD loss, was too late to prevent rebound BMD loss following the offset of RANKL inhibition. This indicates that sequential bisphosphonate therapy may be more effective if administered before CTX levels rise, as our model showed that this is preceded by a rise in serum TRAP.

Early and multiple sequential zoledronate consolidates BMD attained with RANKL inhibition and prevents the overshoot in serum TRAP

Our previous work showed that the processes that drive the rebound phenomenon occur before BMD loss is detected.¹⁸ We hypothesized that early intervention with zoledronate to prevent the rise and overshoot in serum TRAP would be able to prevent rebound BMD loss. Further we hypothesized that a repeated zoledronate dose at week 12, where we would expect rebound BMD loss based on our model, would be superior to the single early dose.

To examine this, mice were treated with OPG:Fc or saline for 2 wk and received zoledronate or saline at week 5, while serum TRAP remained suppressed, and a group of mice received a second dose at week 12 when rebound BMD loss was occurring to assess the effectiveness of multiple zoledronate doses (Figure 3A). Mice treated with OPG:Fc experienced BMD gains for 8 wk following treatment, peaking at week 10, 22% higher than vehicle ($p < .0001$, Figure 3B). BMD loss was observed in OPG:Fc treated mice reaching vehicle levels just 2 wk later at week 12. Mice treated with a single dose of zoledronate at week 5 experienced a 27% reduction in BMD from its peak at week 10 but levels remained significantly higher than vehicle and OPG:Fc-only mice until the end of the study at week 17. Mice that received a dose of zoledronate at both week 5 and week 12 maintained the peak BMD attained with OPG:Fc treatment and levels remained higher than all other groups until the end of the study at week 17 ($p < .0001$, Figure 3B).

Longitudinal TRAP analysis showed suppressed serum TRAP levels in mice treated with OPG:Fc at week 5 when

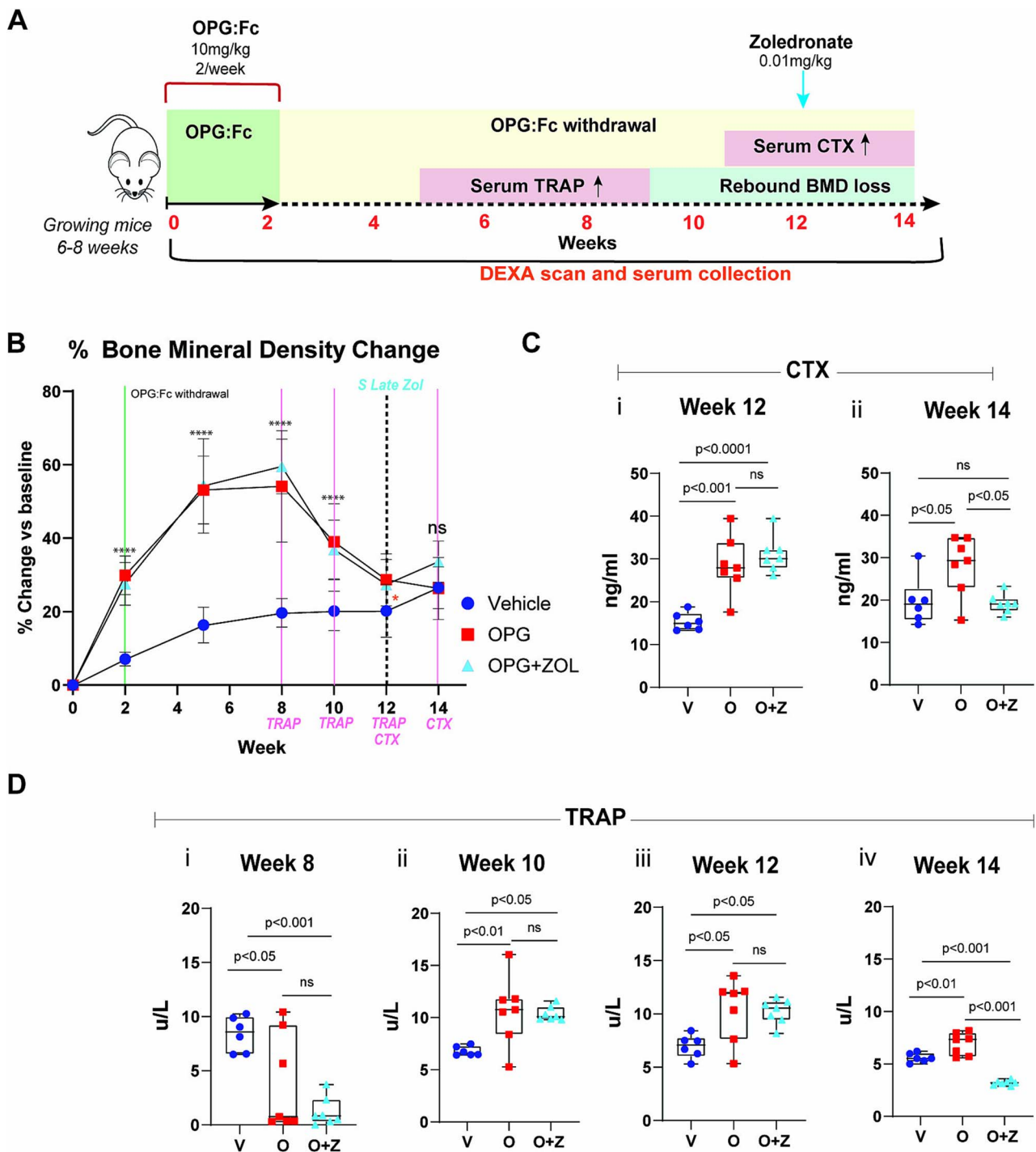


Figure 2. Sequential zoledronate at the time of CTX rise does not prevent bone loss. (A) Schematic of the experimental design to assess the effect of sequential zoledronate following OPG:Fc treatment in growing mice. Expected timing of a rise in serum TRAP, P1NP, CTX, and rebound bone loss highlighted. (B) BMD changes following OPG:Fc treatment and sequential treatment at week 12, at a time of expected CTX rise. BMD shown as percentage change from baseline levels following treatment with OPG:Fc or saline followed by zoledronate or saline at week 12 ($n = 6$ in vehicle, $n = 7$ per intervention group). Timing of zoledronate is denoted by a vertical dotted line at week 12. The vertical lines at weeks 8, 10, 12, and 14 denote time of CTX and TRAP analysis. Data are represented as mean \pm SD. The asterisks indicate p -values $< .05$ (* $p < .05$, ** $p < .01$, **** $p < .0001$). (C) Serum CTX measured by ELISA at (i) week 12 and (ii) week 14. Data are represented as mean \pm SD. (D) Serum TRAP measured by ELISA at (i) week 8, (ii) 10, (iii) 12, and (iv) 14. Data are represented as mean \pm SD.

the first zoledronate dose was administered (Figure 3C). Consistent with our model of denosumab treatment and discontinuation, a rapid rise and overshoot in serum TRAP above vehicle levels was observed in mice treated with OPG:Fc only, reaching levels 68% higher than vehicle levels at week

12 ($p < .0001$, Figure 3C). Mice that received a single dose of zoledronate at week 5 also experienced a rise in serum TRAP levels but only to vehicle levels and remained equivalent to vehicle levels until the end of the study (Figure 3C). Similarly, mice receiving zoledronate at both weeks 5 and 12 also

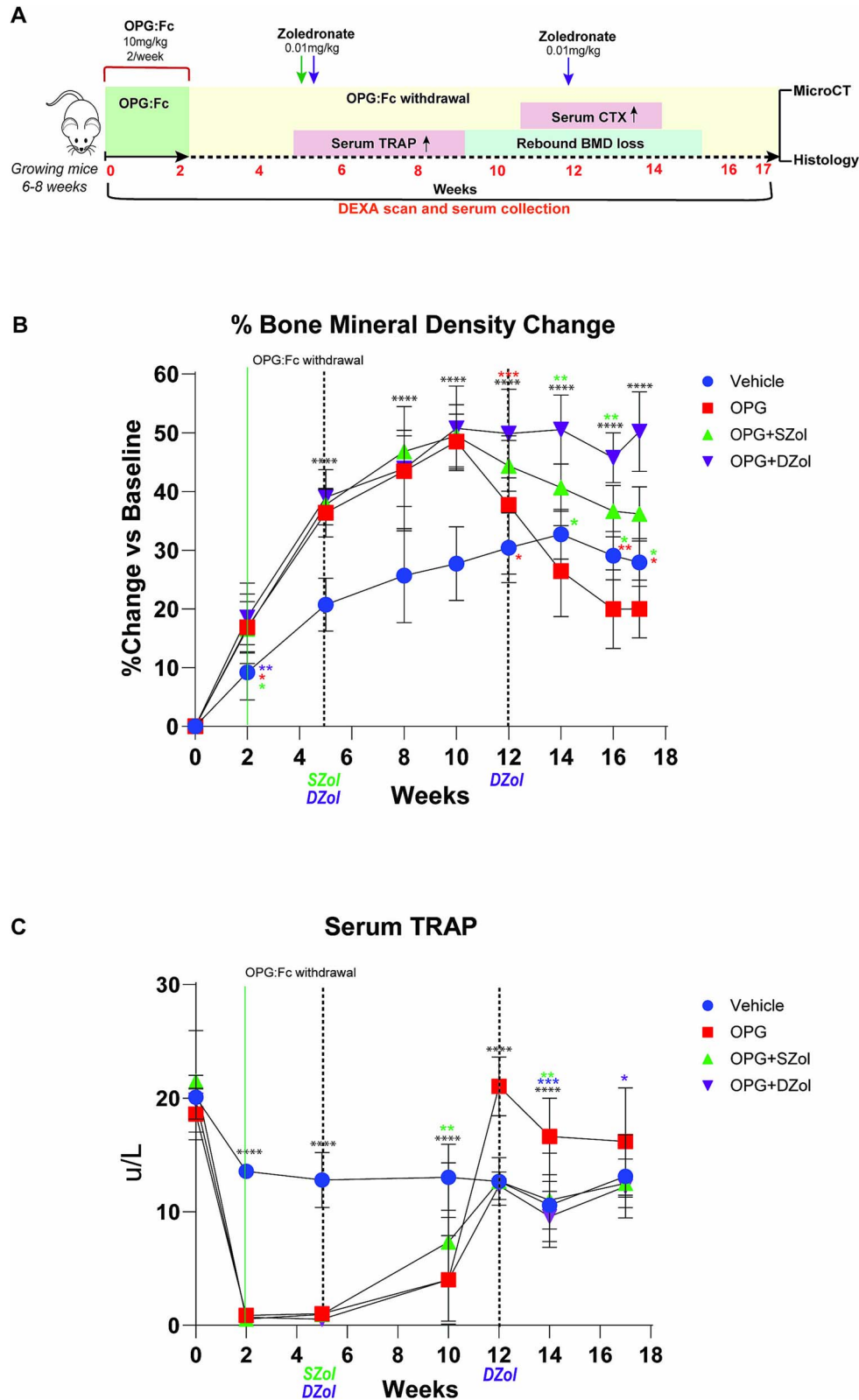


Figure 3. Early and multiple doses of sequential zoledronate prevents rebound BMD loss and the rise and overshoot in serum TRAP in growing mice. (A) Schematic of the experimental design to assess the effect of sequential zoledronate following OPG:Fc treatment in growing mice. Expected timing of a rise in serum TRAP, P1NP, CTX, and rebound bone loss is highlighted. (B) BMD changes following OPG:Fc treatment and sequential zoledronate as early single dose at week 5 or multiple doses at weeks 5 and 12. BMD shown as a percentage change from baseline levels following treatment with OPG:Fc or saline followed by zoledronate or saline at weeks 5 and 12 ($n = 8$ per group). Data are represented as mean \pm SD. The asterisks indicate p -values $< .05$ (* $p < .05$, ** $p < .01$, *** $p < .001$, **** $p < .0001$). (C) Longitudinal serum TRAP measured by ELISA at baseline and following 2 wk treatment with OPG:Fc or saline followed by zoledronate or saline at weeks 5 and 12. Data are represented as mean \pm SD. The asterisks indicate p -values $< .05$ (* $p < .05$, ** $p < .01$, *** $p < .001$, **** $p < .0001$).

showed a rise in serum TRAP levels to control levels which was maintained until the end of the study (Figure 3C).

Sequential zoledronate attenuates rebound bone loss following OPG:Fc withdrawal in skeletally mature mice

Our model utilizes young, growing mice and therefore the effect of normal skeletal growth is an important consideration. To address this limitation and to confirm the effect of sequential zoledronate following OPG:Fc withdrawal, we treated 26-wk-old, skeletally mature mice with OPG:Fc or saline for 4 wk until there was a significant increase in BMD between treated mice compared with controls (Figure 4A). Three weeks following the end of the treatment period, mice were treated with zoledronate or saline at week 7, and a group received a second dose of zoledronate at week 13 when a significant decline in BMD was occurring (Figure 4B). BMD loss was observed in the vehicle mice throughout the study. BMD increased in all OPG:Fc treated mice, peaking at week 4 at 9.4% above vehicle levels ($p < .0001$). A decline in BMD was noted in the mice treated with OPG:Fc-only from week 7, reaching vehicle levels by week 13. Both the vehicle and OPG:Fc-only mice had lower BMD at the end of the study compared with at that start of the study (-6.7% and -6.8% from baseline, respectively). Mice that received zoledronate maintained significantly higher BMD compared with vehicle throughout the study. In the mice that received a single dose of zoledronate at week 7, BMD loss was observed from week 16, though this remained significantly higher than vehicle and OPG:Fc-only mice. Mice that received a second dose of zoledronate at week 13 maintained significantly higher BMD and reached levels higher than mice that received a single dose at the end of the study (4.3% higher vs single dose ZOL, $p < .05$) (Figure 4B).

At week 7, at the time of the first zoledronate dose, serum TRAP was below vehicle levels in most of the OPG:Fc treated mice though some mice in each group had started to experience a rebound overshoot in serum TRAP above vehicle levels (Figure 4C). Four weeks later at week 11, serum TRAP levels were below vehicle levels in mice treated with zoledronate. However, in mice treated only with OPG:Fc, serum TRAP levels rose to vehicle levels with more mice experiencing an overshoot in serum TRAP compared with week 7. By week 13, serum TRAP in OPG:Fc-only mice had overshoot above vehicle levels and this persisted until the end of the study. Mice treated with zoledronate maintained serum TRAP levels below vehicle at week 15, but mice treated with a single dose of zoledronate experienced a rise in serum TRAP by week 20, which was equivalent to vehicle and OPG:Fc-only mice at this timepoint. Notably, mice treated with a second dose of zoledronate at week 13 had significantly lower serum TRAP levels compared with all other groups at week 15, and this remained lower than vehicle levels at the end of the study (Figure 4C).

Taken together, these results show that even a single early dose of zoledronate was able to attenuate the rise and overshoot in serum TRAP, and the rebound BMD loss following withdrawal of RANKL inhibition. A second dose of zoledronate was able to consolidate the BMD gains made during treatment with RANKL inhibition and prevent the rebound bone loss. Importantly, the efficacy of this treatment strategy was seen in both young, growing mice and older, skeletally mature mice.

Early sequential and multiple zoledronate therapy maintains bone gains in both trabecular and cortical compartments in the femur

The rebound phenomenon following denosumab discontinuation leads to the loss of bone gained during treatment to pretreatment levels. To examine the effect of early and multiple zoledronate treatment on consolidating bone gains made during RANKL inhibition, we harvested femora at the end of the study for ex vivo analysis with microCT.

Trabecular parameters were calculated in the distal metaphyseal region to reduce the contribution of the primary spongiosa in this analysis (Figure 5A). Comparing the femurs harvested at the end of the study following completion of rebound bone loss, there was no difference in trabecular volume (BV/TV), thickness, or number between control and mice treated with OPG:Fc in both growing and skeletally mature mice, aligning with DXA data showing the OPG:Fc group had rebounded to vehicle levels at this time. However, trabecular parameters were significantly higher in both growing and mature mice treated with zoledronate compared with vehicle and OPG:Fc treated mice that did not receive zoledronate (Figure 5B). Growing mice that received 2 doses of zoledronate had significantly higher trabecular volume ($p < .01$) and thickness ($p < .001$) compared with those that received a single dose, though the trabecular number was equivalent (Figure 5Bi-iii). In skeletally mature mice, those that received 2 doses of zoledronate had significantly higher trabecular thickness ($p < .001$) but equivalent volume and number compared with mice that received a single dose of zoledronate (Figure 5Biv-vi).

In the cortical compartment at the distal diaphysis, there was increased cortical volume in mice treated with zoledronate in both growing and skeletally mature mice compared with OPG:Fc-only and vehicle (Figure 5C). Growing mice that received 2 doses of zoledronate had significantly higher cortical volume compared with those that received a single dose ($p < .05$), but this difference was not seen in skeletally mature mice where the cortical volume was equivalent between those that received a single dose and multiple doses of zoledronate. Cortical thickness also showed different results between growing and skeletally mature mice. Growing mice treated with OPG:Fc-only or with a single dose zoledronate had significantly reduced cortical thickness compared with vehicle ($p < .0001$). Cortical thickness was significantly higher in mice treated with 2 doses of zoledronate compared with OPG:Fc-only ($p < .0001$) or single dose zoledronate ($p < .0001$), where skeletally mature mice treated with 2 doses of zoledronate had significantly higher cortical thickness compared with all other groups (Figure 5C). Endosteal and periosteal perimeters at the cortical ROI were significantly higher in all mice treated with OPG:Fc compared with vehicle (Figure S1). There were no differences in periosteal perimeter between all groups in the skeletally mature mice. Endosteal perimeters were also equivalent between groups except in skeletally mature mice that received 2 doses of zoledronate, which was significantly lower (Figure S1).

These results show that both trabecular and cortical parameters return to untreated, vehicle levels in mice that did not receive any sequential therapy following OPG:Fc withdrawal. Sequential zoledronate treatment improved both trabecular and cortical parameters compared with mice that did not

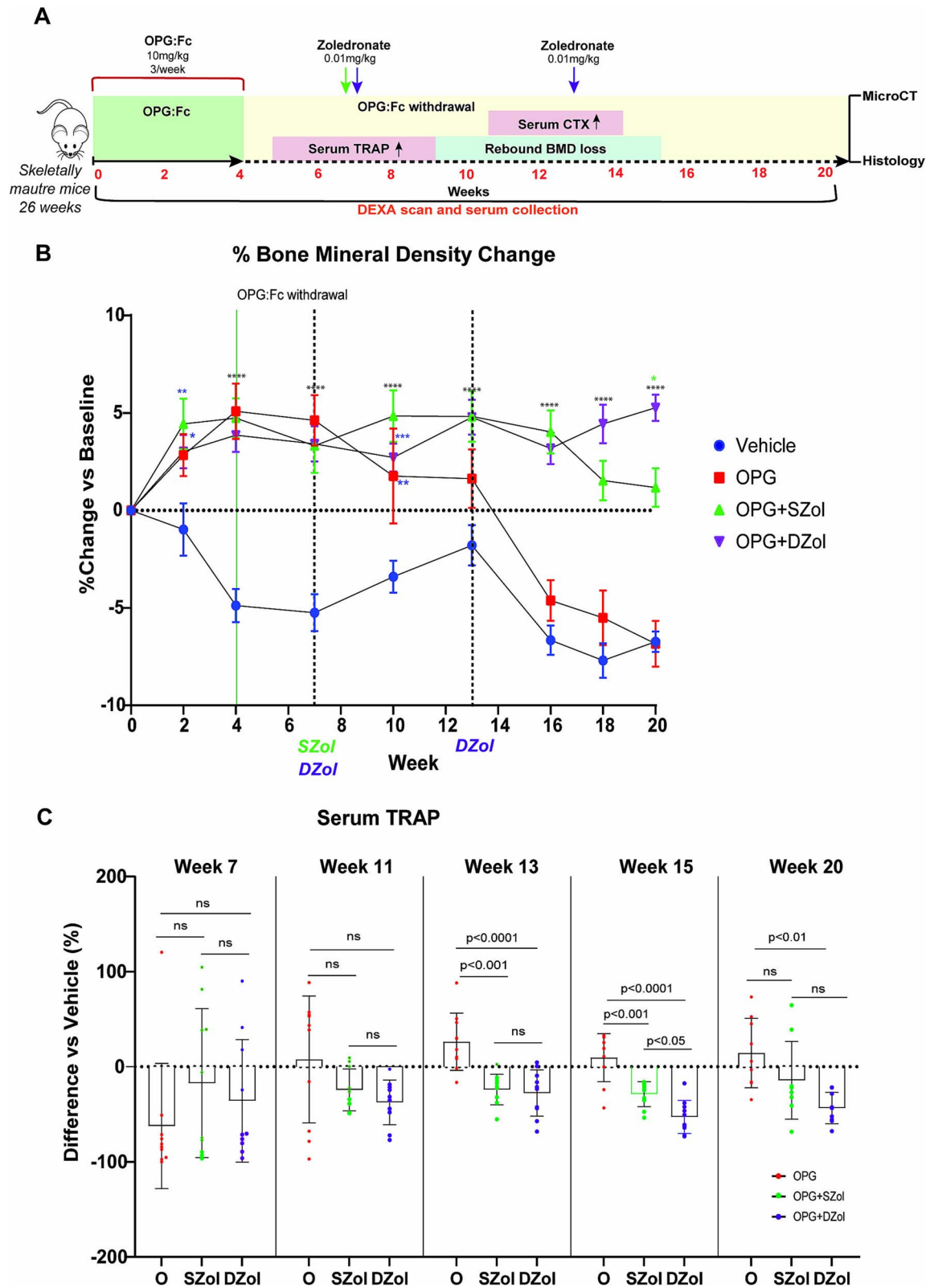


Figure 4. Early and multiple doses of sequential zoledronate prevents rebound BMD loss and the rise and overshoot in serum TRAP in skeletally mature mice. (A) Schematic of the experimental design to assess the effect of sequential zoledronate following OPG:Fc treatment in skeletally mature mice. Expected timing of a rise in serum TRAP, P1NP, CTX, and rebound bone loss is highlighted. (B) BMD changes following OPG:Fc treatment and sequential treatment at weeks 7 and 13. BMD is shown as a percentage change from baseline levels following treatment with OPG:Fc or saline followed by zoledronate or saline at weeks 7 and 13 ($n = 10$ per group). Data are represented as mean \pm SD. The asterisks indicate p -values $< .05$ (* $p < .05$, ** $p < .01$, **** $p < .0001$). (C) Serum TRAP measured by ELISA in mice treated with OPG:Fc and sequential treatment at each timepoint compared with vehicle ($n = 7$ -10 per group), expressed as a percentage difference compared with the vehicle mean. The boxplots represent mean \pm SD. The displayed p -values indicate statistical significance between treatment groups at each timepoint.

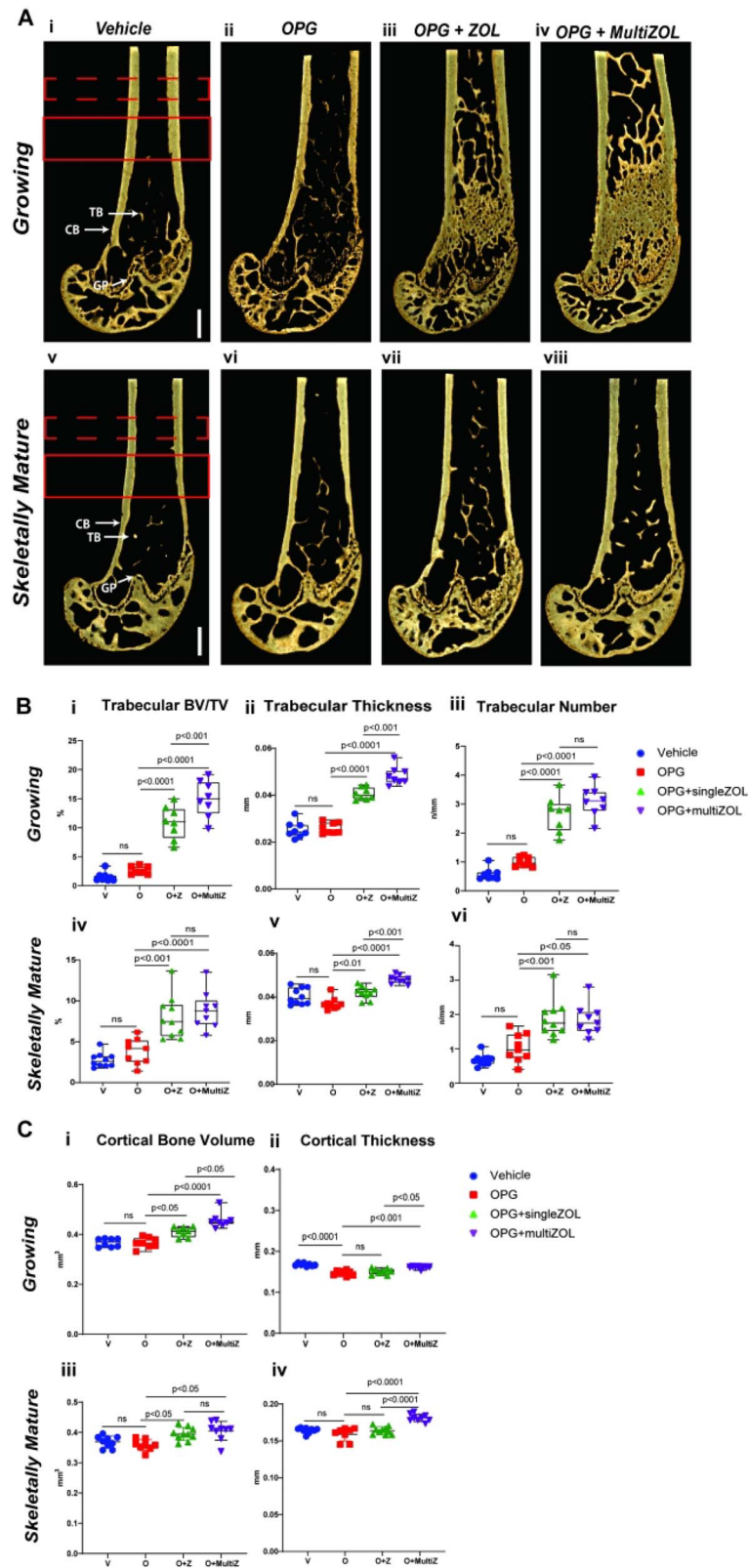


Figure 5. Changes in bone microarchitecture in the femur following OPG:Fc treatment and sequential zoledronate therapy. (A) Representative 3D images of harvested femora showing differences in bone microarchitecture between mice treated with saline and OPG:Fc followed by zoledronate or saline in (i-iv) growing and (v-viii) skeletally mature mice. The dashed red box denotes a ROI examined at a 0.5 mm section located 3 mm above the growth plate (GP) where the cortical parameters are calculated. The solid red box denotes ROI examined at a 1 mm section located 2 mm above the growth plate where the trabecular parameters are calculated. (B) Differences in trabecular volume (i, iv), thickness (ii, v), and number (iii, vi) between growing mice or skeletally mature mice treated with saline (vehicle) or OPG:Fc followed by sequential zoledronate. The boxplots represent mean \pm SD. (C) Differences in cortical volume (i, iii) and thickness (ii, iv) between growing mice or skeletally mature mice treated with saline (vehicle) or OPG:Fc followed by sequential zoledronate. The boxplots represent mean \pm SD. Abbreviations: CB, cortical bone, TB, trabecular bone.

receive any sequential therapy, particularly in mice given multiple doses of zoledronate.

Early sequential zoledronate therapy increased vertebral fracture resistance in skeletally mature mice

Vertebral fractures are a significant concern in the management of patients following denosumab discontinuation. To assess how differences in bone microarchitecture alter fracture resistance following OPG:Fc treatment and sequential zoledronate, the L4 vertebrae underwent *ex vivo* microCT analysis and compression mechanical testing in both growing and skeletally mature mice.

Representative 3D microCT reconstructed images of the L4 vertebrae harvested at the end of the study are shown in Figure 6A. Higher trabecular volume and number were seen in growing mice that received zoledronate compared with those that did not, and this was higher in mice that received 2 doses of zoledronate. Trabecular number was equivalent in growing mice that received a single or multiple doses of zoledronate. A similar pattern was observed in skeletally mature mice though the trabecular volume was equivalent between mice that received single and 2 doses of zoledronate (Figure 6B).

There were no differences in the vertebral cortical volume or thickness between groups in growing mice (Figure 6Ci-ii). In skeletally mature mice, there was no difference in cortical thickness between groups; however, a significantly higher cortical volume was noted in mice that received 2 doses of zoledronate compared with OPG:Fc treated mice that did not receive any zoledronate ($p < .05$, Figure 6Ciii).

Despite the significant differences in the trabecular parameters, there was no difference in the maximum load to failure between groups in growing mice (Figure 6Di). In skeletally mature mice, there was a significantly higher maximum load in mice treated with either single or multiple doses of zoledronate compared with control and OPG:Fc-only groups (Figure 6Dii). There was no difference in the maximum load to failure between skeletally mature mice that received a single dose zoledronate to those that received 2 doses (Figure 6Dii) despite increased cortical bone volume seen in skeletally mature mice that received multiple doses of zoledronate compared with a single dose.

Taken together, these results show sustained increases in trabecular parameters with sequential zoledronate following OPG:Fc treatment in both growing and skeletally mature mice. However, these results translated into increased fracture resistance only in skeletally mature mice that received zoledronate.

Abundant TRAP-positive osteoclasts are observed following sequential zoledronate, discordant with serum TRAP levels

To examine the differences in the number of osteoclasts following rebound bone loss and sequential zoledronate treatment, TRAP-positive cells were quantified on the trabecular bone surfaces in the distal femora at the end of the study (Figure 7A).

TRAP-positive osteoclasts were more abundant in the distal femora of growing mice treated with zoledronate compared with control (Figure 7Bi). When normalized for increased bone surface, there was a trend for fewer osteoclasts per bone surface in growing mice treated with zoledronate;

however, this was not statistically significant (Figure 7Bii). There was no difference in the number of TRAP-positive osteoclasts seen in the distal femora of skeletally mature mice (Figure 7Biii-iv). No differences were seen in osteoclast surfaces between groups in both growing and skeletally mature mice (Figure S2).

While the quantification of osteoclasts was not possible in the most distal metaphyseal region of the femur, due to the retention of the primary spongiosa, TRAP-positive osteoclasts were higher in abundance in this region in growing mice that received zoledronate (Figure 7C). This difference was less pronounced in skeletally mature mice that received zoledronate.

Interestingly, higher TRAP-positive osteoclast numbers were observed despite equivalent serum TRAP between growing mice that received saline, OPG:Fc-only, or a single dose of zoledronate at the end of the studies (Figure 3C). While serum TRAP was significantly lower in mice treated with 2 doses of zoledronate, there were more TRAP-positive osteoclasts seen in growing mice that received 2 doses of zoledronate compared with OPG:Fc-only and single zoledronate treated mice. A similar pattern in serum TRAP was seen in skeletally mature mice receiving saline, OPG:Fc-only, or a single dose of zoledronate (Figure 4C) but without a difference in TRAP-positive osteoclast numbers. Skeletally mature mice that received 2 doses of zoledronate had lowest serum TRAP between the treatment groups but there was no difference in TRAP-positive osteoclast numbers.

These results show that although osteoclast number was increased in mice treated with zoledronate, when normalized to trabecular bone surface, this was no longer the case. Interestingly, differences in the number of TRAP-positive osteoclasts seen in mice treated with zoledronate did not necessarily correlate with differences in serum TRAP levels.

Discussion

The rebound phenomenon following denosumab discontinuation is an important clinical challenge. However, an optimized sequential strategy that can consistently prevent the rapid rise and overshoot in bone resorption does not yet exist. We have previously developed and utilized an animal model of denosumab discontinuation to show that a pro-osteoclastogenic environment is present and osteoclast enzymatic activity (measured by serum TRAP) is elevated prior to the rise in serum CTX and P1NP, and serum TRAP is elevated prior to clinically detectable bone loss as measured by DXA.¹⁸ These results, combined with clinical studies showing bisphosphonate treatment at the time of CTX rise were inconsistent in preventing BMD loss, led us to hypothesize that earlier administration of osteoclast-directed therapy may be more effective in attenuating the rebound phenomenon, and a multiple dose strategy may be superior.

In this study, we utilized our model of denosumab discontinuation to explore the effects of early sequential and multi-dose bisphosphonate therapy and directly examine the changes in osteoclast activity and bone microarchitecture in response to this treatment strategy.

Consistent with real-world observation, administration of sequential zoledronate at a time of rise in serum CTX did not prevent rebound bone loss in our model. In addition, at the time of serum CTX rise, significant BMD loss had already occurred. We have again shown that a rise in serum TRAP from post-treatment suppressed levels precedes BMD loss and

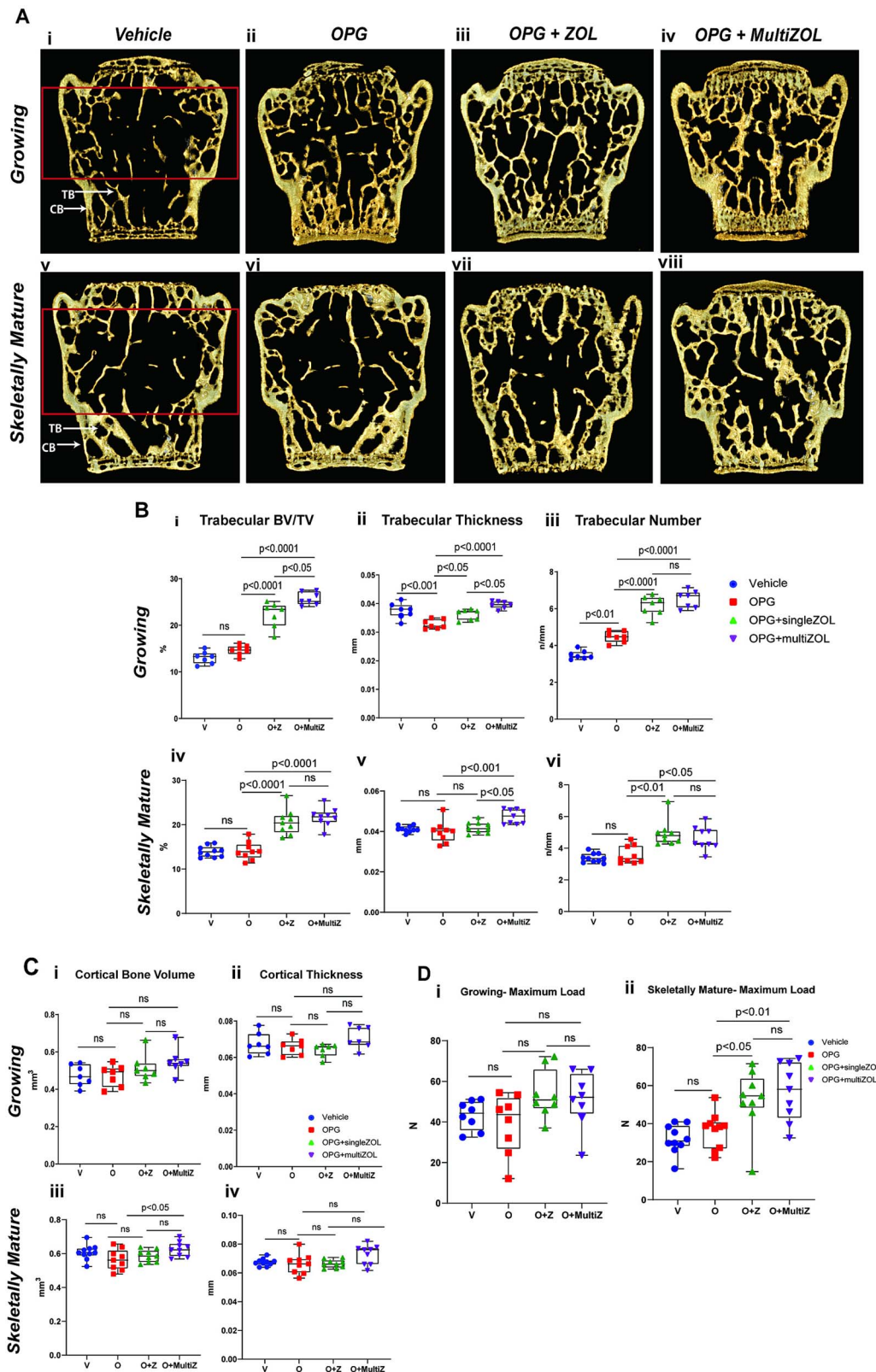


Figure 6. Sequential zoledronate following OPG:Fc prevented trabecular bone loss and improved fracture resistance in skeletally mature mice, but not in growing mice. (A) Representative 3D images of harvested L4 vertebrae showing differences in bone microarchitecture between mice treated with saline and OPG:Fc followed by zoledronate or saline in (i-iv) growing and (v-viii) skeletally mature mice. The solid red box denotes ROI examined at a distance between 0.2 mm offset from the point of 50% spongiosa and trabecular bone on both ends of the vertebrae. (B) Differences in trabecular volume (i, iv), thickness (ii, v), and number (iii, vi) between growing mice or skeletally mature mice treated with saline (vehicle) or OPG:Fc followed by sequential zoledronate. The boxplots represent mean \pm SD. (C) Differences in cortical volume (i, iii) and thickness (ii, iv) between growing mice or skeletally mature mice treated with saline (vehicle) or OPG:Fc followed by sequential zoledronate. The boxplots represent mean \pm SD. (D) Maximum load to failure (N) of L4 vertebrae from each treatment group in growing mice (i) and skeletally mature mice (ii). Boxplots represent mean \pm SD. Abbreviations: CB, cortical bone, TB, trabecular bone.

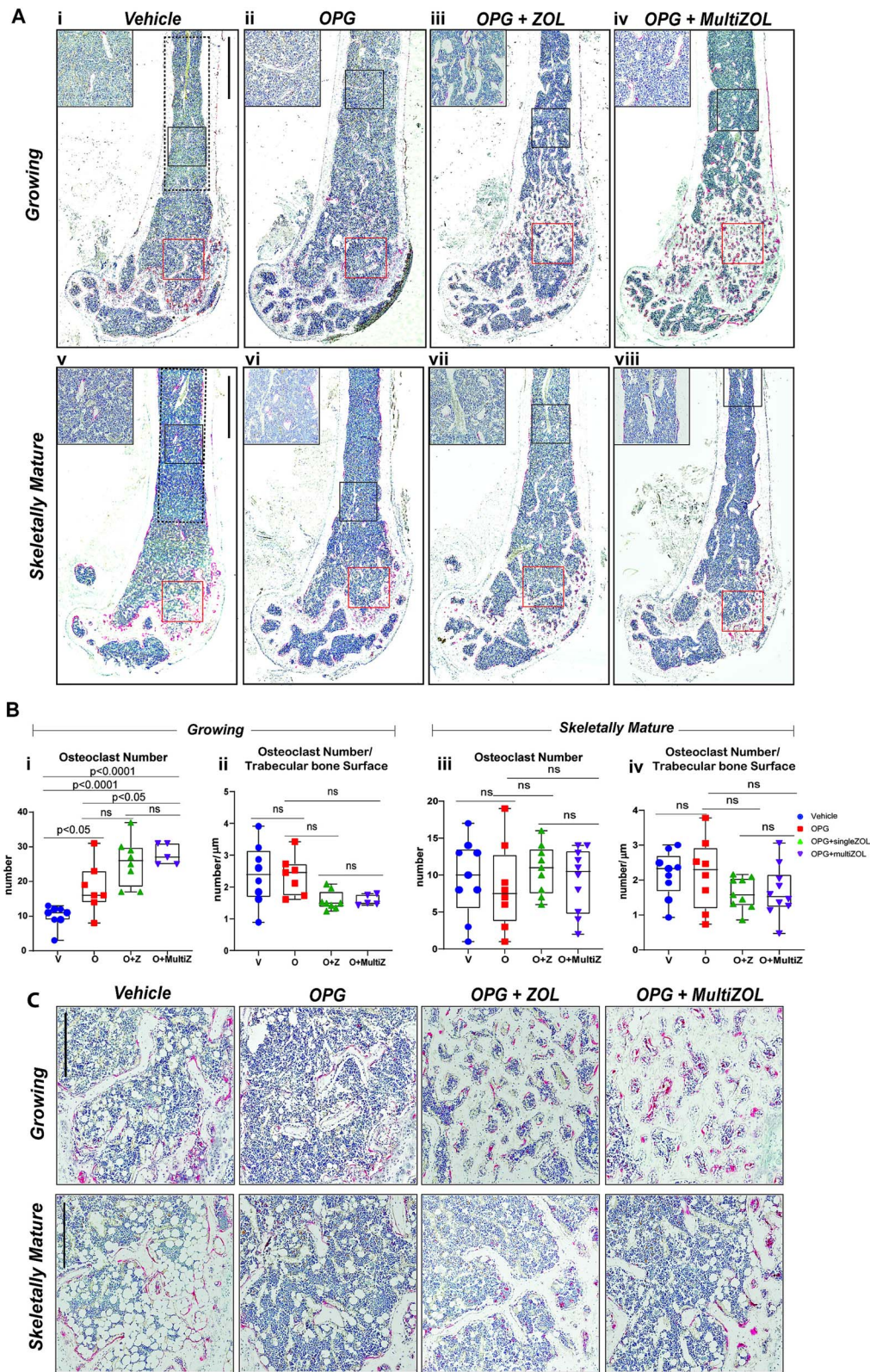


Figure 7. Differences in osteoclast number following OPG:Fc treatment and sequential zoledronate. (A) Representative histological images of femora stained with TRAP (red) harvested following treatment with saline or OPG:Fc. Analysis of osteoclast parameters on trabecular bone was performed within the ROI defined by the dotted line (scale bar 900 μm at 2.2x magnification). Representative high magnification images are shown in the top left corner and their corresponding ROIs are shown in the black box (scale bar 300 μm at 9.8x magnification). The red box denotes osteoclasts observed on trabecular bone surfaces as shown in magnified images in Figure 7C. (B) Quantification of number of osteoclasts (i, iii) and osteoclast surface (ii, iv) per trabecular bone surfaces in growing and skeletally mature mice. The boxplots represent mean \pm SD. (C) Representative images of osteoclasts observed on trabecular bone surfaces throughout the study in the ROI marked by the red box in Figure 7A (scale bar 300 μm at 7x magnification).

CTX rise. Further, we showed that earlier administration of zoledronate, while RANKL inhibition remained active, was able to suppress and prevent the overshoot in serum TRAP observed in our model.

Early administration of zoledronate following OPG:Fc treatment, even prior to the offset of RANKL inhibition, was able to mitigate rebound BMD loss, and an additional dose was able to prevent BMD loss, consolidating and maintaining BMD gains made on treatment in both growing and skeletally mature mice. These findings challenge the prevailing concern that early zoledronate administration would not be taken up while turnover is suppressed. Indeed, tracking uptake using fluorescent analogs *in vivo*, bisphosphonates have been shown to bind to so-called “quiescent” bone surfaces such as osteoclast lacunae as well as bone marrow monocytes.²³

We utilized both growing and skeletally mature mice to allow examination of differences in the rebound phenomenon and the effects of sequential zoledronate across skeletal maturity. Growing mice receiving OPG:Fc experienced greater BMD gains compared with mature mice, reflecting contribution of normal skeletal growth. Greater BMD gains on treatment are an established risk factor for BMD loss following denosumab discontinuation.²⁴ Our model previously demonstrated that longer OPG:Fc treatment, and therefore greater BMD gains, led to accelerated BMD loss.¹⁸ This, and increased TRAP-positive osteoclasts seen in growing mice, may explain why severe hypercalcemia is more commonly observed in pediatric patients discontinuing denosumab compared with adults.²⁵ Growing bones accumulate greater bone mass with denosumab, which is then resorbed *en masse* by newly formed osteoclasts, releasing calcium. This aligns with observations where multiple bisphosphonate doses were required to treat post-denosumab severe hypercalcaemia in children.^{26,27}

Multiple doses of zoledronate following denosumab discontinuation in adults was examined by Grassi et al.¹⁵ in a retrospective analysis of participants that received repeated doses of zoledronate in accordance with current recommendations, which did not prevent BMD loss and vertebral fractures. Importantly, the first dose of zoledronate was administered 7 mo following the last denosumab dose, which is likely too late to act on osteoclasts already formed and driving BMD loss. Notably, BMD remained stable in those with lower serum CTX (<280 ng/L), suggesting that zoledronate administered prior to a rise in serum CTX, and perhaps targeting the rise in serum TRAP, was able to better attenuate rebound BMD loss.

Our previous work showed that the rise and overshoot in serum TRAP accompanies rebound BMD loss, leading to our hypothesis that targeting this rise in serum TRAP with earlier intervention would mitigate BMD loss. In this work, early zoledronate administration indeed prevented the overshoot in serum TRAP and did not exceed vehicle levels in mice receiving zoledronate.

Cross-sectional analyses of serum TRAP, CTX, and RANKL at 6, 9, and 12 mo following the last denosumab dose were performed by Sølling et al.²⁸ This showed significantly lower serum TRAP at 6 mo compared with 9 and 12 mo, whereas serum RANKL was significantly higher at 6 mo. The authors concluded that elevated RANKL levels most likely result in increased osteoclasts (measured by TRAP), consistent with findings in our model.¹⁸

Utility of serum TRAP as a marker following denosumab discontinuation was explored by Makras et al.,²⁹ where serum

TRAP and CTX were measured 6 mo following the last denosumab dose. The authors did not find a relationship between the duration of denosumab and serum TRAP or the TRAP:CTX ratio and concluded that serum TRAP was not a useful early marker. However, this negative finding may be due to the timing of sampling. Serum samples were collected 6 mo following the last dose, whereas our model indicates that the rise and overshoot in serum TRAP may occur earlier. Serum TRAP measurement earlier than 6 mo following the last denosumab dose, as acknowledged by the authors, and clinical studies examining the longitudinal changes in serum TRAP may provide a better assessment of its value as a marker of osteoclast activity in this context.

Interestingly in our study, there was an increased number of TRAP-positive osteoclasts throughout the femora of mice that received sequential zoledronate, discordant with differences in serum TRAP. This suggests that serum TRAP reflects the enzymatic activity of resorbing osteoclasts, rather than the number of osteoclasts present.³⁰ This was particularly evident in mice that received 2 doses of zoledronate as serum TRAP was lowest despite higher or equivalent osteoclast numbers. We observed an increased number of non-attached, TRAP-positive osteoclasts in both growing and skeletally mature mice treated with zoledronate (data not shown). In a model of MRONJ, where rats were treated with zoledronate, Nagata et al.³¹ showed greater TRAP-positive multinucleated cells in the dental sockets with a significantly higher proportion of non-attached osteoclasts. These results suggest that bisphosphonate therapy impairs osteoclast activity but not the formation and activation of osteoclasts.

Patients are at increased risk of fractures, especially vertebral fractures, following denosumab discontinuation. MicroCT analysis at the end of our study showed a return to control levels in both trabecular and cortical parameters in mice that received OPG:Fc alone without sequential zoledronate, whereas mice that received zoledronate had significantly improved trabecular microarchitecture in both the femur and the vertebrae. However, when the lumbar vertebrae were subject to compression mechanical testing to assess fracture resistance, the increased trabecular parameters in zoledronate treated mice did not translate to higher maximal load to failure in young, growing mice, though a significantly higher maximal load to failure was observed in skeletally mature mice that received zoledronate. This may be due to the timing of mechanical testing as this was performed at the end of the study when rebound BMD loss was complete and there was continued skeletal growth in growing mice. Compression mechanical testing during rebound BMD loss may have revealed differences in fracture resistance between groups. Nonetheless, these differences in microCT parameters and maximal load to failure support the use of sequential zoledronate following denosumab discontinuation to improve bone microarchitecture and fracture resistance, especially in older patients.

Anabolic therapies promoting osteoblastic bone formation have expanded the therapeutic options available to improve bone mass.³² Despite their efficacy, it remains unclear if sequential anabolic therapy can effectively mitigate rebound bone loss following denosumab discontinuation. Several studies have examined sequential anabolic therapy using teriparatide³³ or romosozumab^{34–36} with mixed results, and the optimal sequence and timing of anabolic therapies following denosumab discontinuation remains unclear.

Our studies were performed in eugonadal mice, whereas most patients treated for osteoporosis are postmenopausal women, and this represents a limitation in the clinical translation of our findings. However, our murine models consistently show that the processes driving the rebound phenomenon following the offset of RANKL inhibition occurs earlier than when we can detect rebound bone loss in the clinic. Therefore, clinical studies defining the temporal changes in osteoclast activity, specifically changes in serum TRAP and its association with changes in CTX and BMD, in the setting of denosumab discontinuation and sequential therapy are needed to translate the findings of our studies to clinical practice. As no effective strategy currently exists to prevent exposing patients discontinuing denosumab to potential harm, prospective clinical trials comparing earlier vs standard timing of sequential therapy would be highly informative.

Overall, our findings show that targeting osteoclasts earlier with sequential zoledronate can mitigate rebound BMD loss following the withdrawal of RANKL inhibition, and a multi-dose strategy is superior in preventing BMD loss. Future studies examining sequential therapy following denosumab discontinuation should therefore consider intervening earlier than 6 mo following the last denosumab dose and incorporate measurements of serum TRAP as a biomarker heralding imminent BMD loss.

Acknowledgments

OPG:Fc used in this study was provided by Amgen Inc. and zoledronate was provided by Novartis Pharma.

Author contributions

Albert S. Kim (Conceptualization, Data curation, Formal analysis, Investigation, Methodology, Writing—original draft, Writing—review & editing), Victoria E. Taylor (Data curation, Formal analysis), Ariel Castro-Martinez (Data curation, Methodology), Suraj Dhakal (Data curation, Formal analysis), Amjad Zamerli (Data curation), Sindhu T. Mohanty (Data curation), Ya Xiao (Data curation), Marija K. Simic (Data curation, Methodology), Alyssa Pantalone (Data curation), Julian Chu (Data curation), Tegan L. Cheng (Data curation), Peter I. Croucher (Funding acquisition, Supervision, Writing—review & editing), Jacqueline R. Center (Conceptualization, Investigation, Supervision, Writing—review & editing), Christian M. Girgis (Conceptualization, Investigation, Writing—review & editing), and Michelle M. McDonald (Conceptualization, Formal analysis, Funding acquisition, Investigation, Supervision, Writing—review & editing).

Supplementary material

Supplementary material is available at *Journal of Bone and Mineral Research* online.

Funding

A.S.K. is supported by the UNSW Sydney University Postgraduate Award, Australian Government Research Training Program Scholarship, and received financial support from the Australia and New Zealand Bone and Mineral Society and the Endocrine Society of Australia. This work is supported by the Mrs. Janice Gibson and the Ernest Heine Family Foundation and Cancer Council NSW project grant R20-05, American Society of Bone and Mineral Research Rising Star Award and Bone Health Foundation, and Australia and New Zealand Bone and Mineral Society Grant in Aide.

Conflicts of interest

M.M.M. has received honoraria for speaking from Amgen Inc.

Data availability

All raw data files can be provided on request.

References

- Cummings SR, Martin JS, McClung MR, et al. Denosumab for prevention of fractures in postmenopausal women with osteoporosis. *N Engl J Med*. 2009;361(8):756–765. <https://doi.org/10.1056/NEJMoa0809493>
- Bone HG, Wagman RB, Brandi ML, et al. 10 years of denosumab treatment in postmenopausal women with osteoporosis: results from the phase 3 randomised FREEDOM trial and open-label extension. *Lancet Diabetes Endocrinol*. 2017;5(7):513–523. [https://doi.org/10.1016/S2213-8587\(17\)30138-9](https://doi.org/10.1016/S2213-8587(17)30138-9)
- Freemantle N, Satram-Hoang S, Tang E-T, et al. Final results of the DAPS (denosumab adherence preference satisfaction) study: a 24-month, randomized, crossover comparison with alendronate in postmenopausal women. *Osteoporos Int*. 2012;23(1):317–326. <https://doi.org/10.1007/s00198-011-1780-1>
- Wang M, Wu YF, Girgis CM. Bisphosphonate drug holidays: evidence from clinical trials and real world studies. *JBRM Plus*. 2022;6(6):e10629. <https://doi.org/10.1002/jbm4.10629>
- Black DM, Geiger EJ, Eastell R, et al. Atypical femur fracture risk versus fragility fracture prevention with bisphosphonates. *N Engl J Med*. 2020;383(8):743–753. <https://doi.org/10.1056/NEJMoa1916525>
- McClung MR, Wagman RB, Miller PD, Wang A, Lewiecki EM. Observations following discontinuation of long-term denosumab therapy. *Osteoporos Int*. 2017;28(5):1723–1732. <https://doi.org/10.1007/s00198-017-3919-1>
- Burckhardt P, Faouzi M, Buclin T, Lamy O, The Swiss Denosumab Study G. Fractures after denosumab discontinuation: a retrospective study of 797 cases. *J Bone Miner Res*. 2021;36(9):1717–1728. <https://doi.org/10.1002/jbmr.4335>
- Koller G, Goetz V, Vandermeer B, et al. Persistence and adherence to parenteral osteoporosis therapies: a systematic review. *Osteoporos Int*. 2020;31(11):2093–2102. <https://doi.org/10.1007/s00198-020-05507-9>
- Kim AS, Girgis CM, McDonald MM. Osteoclast recycling and the rebound phenomenon following denosumab discontinuation. *Curr Osteoporos Rep*. 2022;20(6):505–515. <https://doi.org/10.1007/s11914-022-00756-5>
- Anastasilakis AD, Polyzos SA, Yavropoulou MP, et al. Comparative effect of zoledronate at 6 versus 18 months following denosumab discontinuation. *Calcif Tissue Int*. 2021;108(5):587–594. <https://doi.org/10.1007/s00223-020-00785-1>
- Tutaworn T, Nieves JW, Wang Z, Levin JE, Yoo JE, Lane JM. Bone loss after denosumab discontinuation is prevented by alendronate and zoledronic acid but not risedronate: a retrospective study. *Osteoporos Int*. 2023;34(3):573–584. <https://doi.org/10.1007/s00198-022-06648-9>
- Reid IR, Horne AM, Mihov B, Gamble GD. Bone loss after denosumab: only partial protection with zoledronate. *Calcif Tissue Int*. 2017;101(4):371–374. <https://doi.org/10.1007/s00223-017-0288-x>
- Sølling AS, Harsløf T, Langdahl B. Treatment with zoledronate subsequent to denosumab in osteoporosis: a 2-year randomized study. *J Bone Miner Res*. 2020;36(7):1245–1254. <https://doi.org/10.1002/jbmr.4305>
- Lee C-C, Wang C-Y, Yen H-K, et al. Zoledronate sequential therapy after denosumab discontinuation to prevent bone mineral density reduction: a randomized clinical trial. *JAMA Netw Open*. 2024;7(11):e2443899-e. <https://doi.org/10.1001/jamanetworkopen.2024.43899>
- Grassi G, Ghielmetti A, Zampogna M, et al. Zoledronate after denosumab discontinuation: is repeated administrations more effective than single infusion? *J Clin Endocrinol Metab*. 2024;109(10):e1817–e1826. <https://doi.org/10.1210/clinem/dgae224>

16. Anastasilakis AD, Papapoulos SE, Polyzos SA, Appelman-Dijkstra NM, Makras P. Zoledronate for the prevention of bone loss in women discontinuing denosumab treatment. A prospective 2-year clinical trial. *J Bone Miner Res.* 2019;34(12):2220–2228. <https://doi.org/10.1002/jbmr.3853>
17. Tsourdi E, Zillikens MC, Meier C, et al. Fracture risk and management of discontinuation of denosumab therapy: a systematic review and position statement by ECTS. *J Clin Endocrinol Metab.* 2021;106(1):264–281. <https://doi.org/10.1210/clinem/dgaa756>
18. Kim AS, Taylor VE, Castro-Martinez A, et al. Temporal patterns of osteoclast formation and activity following withdrawal of RANKL inhibition. *J Bone Miner Res.* 2024;39(4):484–497. <https://doi.org/10.1093/jbmr/zjae023>
19. McDonald MM, Morse A, Mikulec K, et al. Matrix metalloproteinase-driven endochondral fracture union proceeds independently of osteoclast activity. *J Bone Miner Res.* 2013;28(7):1550–1560. <https://doi.org/10.1002/jbmr.1889>
20. McDonald MM, Reagan MR, Youlten SE, et al. Inhibiting the osteocyte-specific protein sclerostin increases bone mass and fracture resistance in multiple myeloma. *Blood.* 2017;129(26):3452–3464. <https://doi.org/10.1182/blood-2017-03-773341>
21. Dempster DW, Compston JE, Drezner MK, et al. Standardized nomenclature, symbols, and units for bone histomorphometry: a 2012 update of the report of the ASBMR Histomorphometry nomenclature committee. *J Bone Miner Res.* 2013;28(1):2–17. <https://doi.org/10.1002/jbmr.1805>
22. Simic MK, Mohanty ST, Xiao Y, et al. Multi-targeting DKK1 and LRP6 prevents bone loss and improves fracture resistance in multiple myeloma. *J Bone Miner Res.* 2020;38(6):814–828. <https://doi.org/10.1002/jbmr.4809>
23. Roelofs AJ, Coxon FP, Ebetino FH, et al. Fluorescent risedronate analogues reveal bisphosphonate uptake by bone marrow monocytes and localization around osteocytes in vivo. *J Bone Miner Res.* 2010;25(3):606–616. <https://doi.org/10.1359/jbmr.091009>
24. Anastasilakis AD, Polyzos SA, Makras P, Aubry-Rozier B, Kaouri S, Lamy O. Clinical features of 24 patients with rebound-associated vertebral fractures after denosumab discontinuation: systematic review and additional cases. *J Bone Miner Res.* 2017;32(6):1291–1296. <https://doi.org/10.1002/jbmr.3110>
25. Boyce AM. Denosumab: an emerging therapy in pediatric bone disorders. *Cur Osteoporos Rep.* 2017;15(4):283–292. <https://doi.org/10.1007/s11914-017-0380-1>
26. Liu X, Xie Y, Tang J, Zhong J, Lan D. Hypercalcemia in children following a discontinuation of denosumab therapy: a case report and literature review. *Clin Pediatr.* 2024;63(6):750–754. <https://doi.org/10.1177/00099228231194427>
27. Sydlík C, Dürr HR, Pozza SB-D, Weißenbacher C, Roeb J, Schmidt H. Hypercalcaemia after treatment with denosumab in children: bisphosphonates as an option for therapy and prevention? *World J Pediatr.* 2020;16(5):520–527. <https://doi.org/10.1007/s12519-020-00378-w>
28. Sølling AS, Harsløf T, Jørgensen NR, Langdahl B. Changes in RANKL and TRAcP 5b after discontinuation of denosumab suggest RANKL mediated formation of osteoclasts results in the increased bone resorption. *Osteoporos Int.* 2023;34(3):599–605. <https://doi.org/10.1007/s00198-022-06651-0>
29. Makras P, Yavropoulou MP, Polyzos SA, et al. The relationship between length of denosumab treatment for postmenopausal osteoporosis and serum TRAcP5b measured six months after the last injection. *Osteoporos Int.* 2024;35(2):365–370. <https://doi.org/10.1007/s00198-023-06931-3>
30. Schini M, Vilaca T, Gossiel F, Salam S, Eastell R. Bone turnover markers: basic biology to clinical applications. *Endocr Rev.* 2023;44(3):417–473. <https://doi.org/10.1210/endo/rev/bnac031>
31. Nagata MJH, Messori MR, Antoniali C, et al. Long-term therapy with intravenous zoledronate increases the number of nonattached osteoclasts. *J Craniofac Surg.* 2017;45(11):1860–1867. <https://doi.org/10.1016/j.jcms.2017.08.011>
32. Cosman F, Crittenden DB, Adachi JD, et al. Romosozumab treatment in postmenopausal women with osteoporosis. *N Engl J Med.* 2016;375(16):1532–1543. <https://doi.org/10.1056/NEJMoa1607948>
33. Leder BZ, Tsai JN, Uihlein AV, et al. Denosumab and teriparatide transitions in postmenopausal osteoporosis (the DATA-Switch study): extension of a randomised controlled trial. *Lancet.* 2015;386(9999):1147–1155. [https://doi.org/10.1016/S0140-6736\(15\)61120-5](https://doi.org/10.1016/S0140-6736(15)61120-5)
34. McClung MR, Bolognese MA, Brown JP, et al. Skeletal responses to romosozumab after 12 months of denosumab. *JBMR Plus.* 2021;5(7):e10512. <https://doi.org/10.1002/jbm4.10512>
35. Kumar S, Gild ML, McDonald MM, Kim AS, Clifton-Bligh RJ, Girgis CM. A novel sequential treatment approach between denosumab and romosozumab in patients with severe osteoporosis. *Osteoporos Int.* 2024;35:1669–1675. <https://doi.org/10.1007/s00198-024-07139-9>
36. Ebina K, Etani Y, Tsuboi H, et al. Effects of prior osteoporosis treatment on the treatment response of romosozumab followed by denosumab in patients with postmenopausal osteoporosis. *Osteoporos Int.* 2022;33(8):1807–1813. <https://doi.org/10.1007/s00198-022-06386-y>

Temporal patterns of osteoclast formation and activity following withdrawal of RANKL inhibition

Albert S. Kim^{1,2,3,4}, Victoria E. Taylor¹, Ariel Castro-Martinez¹, Suraj Dhakal¹, Amjad Zamerli¹, Sindhu Mohanty¹, Ya Xiao¹, Marija K. Simic^{1,5}, Jinchen Wen⁶, Ryan Chai^{1,2} , Peter I. Croucher^{1,2}, Jacqueline R. Center^{1,2}, Christian M. Girgis^{3,4}, Michelle M. McDonald^{1,2,4,*}

¹Skeletal Diseases Program, Garvan Institute of Medical Research, Sydney, NSW, 2010, Australia

²Faculty of Medicine, St Vincent's Clinical School, UNSW Sydney, Sydney, NSW, 2010, Australia

³Department of Diabetes and Endocrinology, Westmead Hospital, Sydney, NSW, 2145, Australia

⁴Faculty of Health and Medicine, University of Sydney, Sydney, NSW, 2050, Australia

⁵Department of Pathology, New York University Grossman School of Medicine, New York, NY, 10016, United States

⁶Department of Psychology and Neuroscience, Duke University, Durham, NC, 27708, United States

*Corresponding author: Michelle M. McDonald, School of Medical Sciences, Faculty of Medicine and Health, University of Sydney, Science Rd, Camperdown, NSW, 2050, Australia (michelle.mcdonald@sydney.edu.au).

Abstract

Rebound bone loss following denosumab discontinuation is an important clinical challenge. Current treatment strategies to prevent this fail to suppress the rise and overshoot in osteoclast-mediated bone resorption. In this study, we use a murine model of denosumab treatment and discontinuation to show the temporal changes in osteoclast formation and activity during RANKL inhibition and withdrawal. We show that the cellular processes that drive the formation of osteoclasts and subsequent bone resorption following withdrawal of RANKL inhibition precede the rebound bone loss. Furthermore, a rise in serum TRAP and RANKL levels is detected before markers of bone turnover used in current clinical practice. These mechanistic advances may provide insight into a more defined window of opportunity to intervene with sequential therapy following denosumab discontinuation.

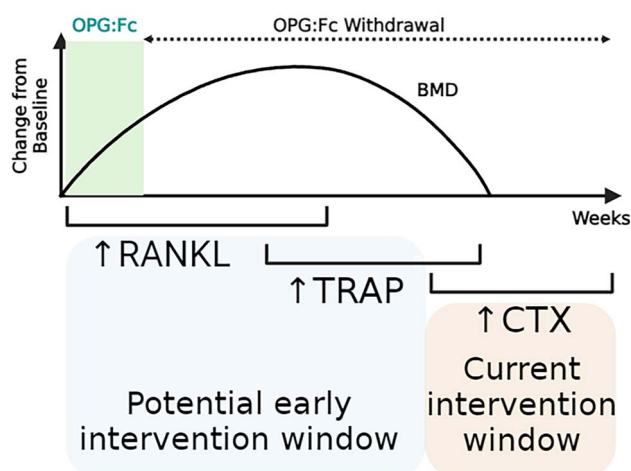
Keywords: osteoclast, RANKL, Denosumab, osteoporosis

Lay Summary

Stopping denosumab, a medication commonly used to improve bone mass by blocking formation of bone resorbing osteoclasts, leads to a rebound loss in the bone which was gained during treatment. Current strategies to prevent this bone loss fail in most cases as they are unable to prevent the rise and overshoot in bone resorption by osteoclasts. This stems from an incomplete understanding of how osteoclasts behave during denosumab treatment and after treatment is discontinued. We use a mouse model of this phenomenon to show how osteoclast formation and activity changes throughout this process. We show that increases in the processes that drive the formation of osteoclasts can be detected in the circulation before bone loss occurs. These findings could therefore provide insight into a targeted 'window of opportunity' to intervene and prevent the rebound bone loss following stopping denosumab in patients.

Graphical Abstract

Temporal changes following RANKL inhibition



Received: November 5, 2023. Revised: January 15, 2024. Accepted: January 25, 2024

© The Author(s) 2024. Published by Oxford University Press on behalf of The American Society for Bone and Mineral Research.

This is an Open Access article distributed under the terms of the Creative Commons Attribution Non-Commercial License (<https://creativecommons.org/licenses/by-nc/4.0/>), which permits non-commercial re-use, distribution, and reproduction in any medium, provided the original work is properly cited.

For commercial re-use, please contact journals.permissions@oup.com

Introduction

Therapeutic agents inhibiting osteoclasts have revolutionized treatment of bone diseases including osteoporosis. Osteoclasts are highly specialized cells that differentiate from hematopoietic stem cells under local and systemic influences. The RANKL) its receptor RANK, and the decoy receptor osteoprotegerin (OPG) form the RANKL/RANK/OPG pathway, which plays a critical role in the differentiation and activation of osteoclasts, and therefore regulation of bone turnover.¹ Inhibiting this interaction leads to increased bone mass and reduced bone resorption and has been the target of bone-directed therapies for conditions where suppression of osteoclast-mediated bone resorption is desired.

Denosumab is a fully human monoclonal antibody that binds to and inhibits RANKL, leading to inhibition of osteoclast differentiation and bone resorption. Denosumab has revolutionized the treatment of osteoporosis, and its continued use leads to continuous BMD gains with up to 10 yr of treatment.²

However, discontinuation of denosumab treatment leads to a rapid reversal of its therapeutic effects and a transient overshoot in bone turnover, which eventually returns to pre-treatment levels.³ This results in a net bone loss during this time and appears to be driven by osteoclast-mediated bone loss as measured by elevated markers of collagen breakdown, namely, CTX.³ However, why this rapid overshoot of bone turnover and bone loss following denosumab discontinuation occurs is unknown.

Clinical studies using sequential antiresorptive agents to inhibit this increase in bone resorption following denosumab discontinuation are predominantly observational or post hoc analyses and are therefore limited in providing a mechanism to explain this phenomenon nor a potential solution to manage these patients.⁴⁻⁷ Duration of denosumab treatment appears to impact outcomes following cessation, with patients receiving denosumab for a longer duration experiencing greater rates of bone loss and increased risk of vertebral fractures during the off-treatment period.^{8,9} Placebo-controlled randomized studies to examine the efficacy of interventions to prevent this bone loss are not ethically feasible due to the risk of bone loss and fractures in the control group.

Clinicians are faced with a dilemma, having to weigh risks associated with long-term anti-resorptive treatment, such as atypical femoral fractures, against the risks of bone loss and fractures if denosumab is discontinued. This problem stems from an incomplete understanding of osteoclast biology following withdrawal of RANKL inhibition, highlighting the need for pre-clinical investigations into the underlying mechanisms. Indeed, the discovery that osteoclasts undergo recycling via fission into osteomorphs, and re-fusion into active osteoclasts, and that during RANKL inhibition these fission products and osteoclast precursors may accumulate, provides new insight into this phenomenon.¹⁰

In the presence of RANKL inhibition, suppressed serum tartrate-resistant acid phosphatase (TRAP) levels reflected inhibition of osteoclast formation. Following cessation of RANKL inhibition, a rapid rise in serum TRAP preceded a dramatic loss in BMD in mice,¹⁰ confirming clinical findings that enhanced bone resorption follows treatment withdrawal. However, the cellular processes and changes in osteoclast biology that drive this rapid rise in serum TRAP are unclear,

and the temporal relationship between serum TRAP and typical bone turnover markers CTX and P1NP has not yet been defined.

To address this, we aimed to define the key regulators of osteoclast formation and activity, and the longitudinal changes in bone turnover markers, to examine how these correlate with changes in BMD and bone microarchitecture during RANKL inhibition and following its cessation. We also examined these changes following longer periods of RANKL inhibition and compared the utility of serum TRAP, a marker of osteoclast activity, with markers of bone turnover utilized in clinical practice. We performed these studies using mice which respond to OPG:Fc with changes in serum bone turnover markers which are relevant to the human biological processes we aim to examine. Taken together, our preclinical investigations provide essential mechanistic insight to guide the timing of sequential therapy in patients discontinuing denosumab.

Materials and methods

Experimental mice

Animal experiments were performed in accordance with approved protocols from the Garvan Institute and St Vincent's Hospital Animal Ethics Committee (ARA 18/03 and 21/17). All experiments were conducted in accordance with the Australian Code of Practice for the Care and Use of Animals for Scientific Purposes.

Female C57BL/KaLwRij (Harlan, Netherlands) or C57BL/6J mice were obtained from the Australian BioResources. All mice were bred and maintained on a C57BL/KaLwRij background or C57BL/6J background under specific-pathogen free conditions. Animal experiments were performed at the Garvan Institute Biological Testing Facility. All animal holding areas in both facilities are maintained within a constant temperature of 21.4 °C with humidity range to avoid animal stress and to minimize experimental variability. Lighting mimics 12-h d/night cycles to stimulate circadian rhythms. Mice were acclimatized for 3 d upon arrival, and standard chow and water were provided ad libitum.

All mice entered their respective experiments aged 6–8 wk and group sizes were determined based on previous experiences with each model. This included studies of the effect of OPG:Fc in these models, in which power calculations were performed to estimate sample size. Using this, 8–10 mice were allocated to each group or otherwise as stated in the figure legends.

To compare the effects of OPG:Fc and anti-mouse RANKL antibody, C57BL/KaLwRij mice were randomly allocated to treatment groups. OPG:Fc or anti-mouse RANKL antibody was administered for 2 wk, and mice were culled at the end of the treatment phase at week 2 where tissue was harvested for their respective experiments outlined below.

To examine the effect of longer duration of RANKL inhibition, C57BL/KaLwRij mice were treated with OPG:Fc for 8 wk and were culled at the end of the study at week 23. Mice underwent DXA imaging and retro-orbital bleeds fortnightly or 3-weekly throughout the study.

To allow contemporaneous measurements of serum markers of osteoclast activity, C57BL6 mice were treated with OPG:Fc for 2 wk and were culled at week 2, 8, 11, and 13 to allow for collection of a large volume of serum. Throughout the study, mice underwent DXA imaging and retro-orbital

bleed fortnightly. At each cull timepoint, a large volume of blood was collected through retro-orbital bleeding, and tissue was harvested for their respective experiments outlined below.

OPG:Fc and anti-mouse RANKL antibody treatment

OPG:Fc (Amgen Inc) was administered at a dose of 10 mg per kg i.p. 2-3 times weekly for 2 or 8 wk, a dose confirmed previously to abrogate osteoclasts.¹¹ Anti-mouse RANKL antibody (BioXcell, BE0191) was administered at a dose of 5 mg per kg i.p. thrice weekly for 2 wk. Vehicle mice received saline.

DXA analysis of BMD

DXA (Faxitron Ultrafocus DXA, Hologic) was performed fortnightly or 3-weekly on anaesthetized mice under 3%-5% inhaled isoflurane. Analysis of the hind limb was performed using Vision DXA (Hologic) using a manually drawn region of interest encompassing the hindlimb to quantify the BMD.

Micro-computed tomography

Formalin-fixed right femora were imaged with the SkyScan 1772 micro-computed tomography (microCT) scanner (Bruker) at a resolution of 4.3 μm , 0.5 mm aluminum filter, 50 kv voltage, and 200 μA tube current. Images were captured every 0.4° through 360° and were reconstructed and analyzed using NRecon software (SkyScan). Bone structural parameters and nomenclature were utilized according to standardized guidelines.¹² Three-dimensional reconstructed images of femora were generated using Drishti imaging software version 2.4 (ANU).

ROI selection and analyses were performed using CTAn software (Bruker). To compare the effect of OPG:Fc and mouse anti-RANKL antibody, trabecular and cortical bone parameters were calculated from scans performed at a voxel resolution of 5 μm in a 1 mm region of the trabecular compartment beginning 100 μm proximal to the distal femoral growth plate.

To examine the changes in bone parameters following treatment and during rebound bone loss following OPG:Fc withdrawal, trabecular bone parameters were calculated from scans performed at a voxel resolution of 5 μm in a 1 mm region beginning 200 μm proximal to the distal femoral growth plate to reduce the contribution of the primary spongiosa in the analysis. Cortical bone parameters were calculated from scans performed at a voxel resolution of 5 μm in a 0.5 mm region beginning 300 μm proximal to the distal femoral growth plate.

Measurement of TRAP5b, P1NP, CTX, and RANKL

Serum collected by retro-orbital bleeds, under isoflurane anesthesia, throughout animal phases was stored at -70° and then assessed for TRAP5b, P1NP, and CTX levels using ELISA kits (Immunodiagnostic Systems) or assessed for RANKL levels using ELISA kits (R&D Systems) following the manufacturer's instructions.

Analysis of bone histomorphometry

Sectioning/TRAP staining of osteoclasts

Right femora samples were prepared for paraffin histomorphometric analysis by fixing in 4% paraformaldehyde for 24 h at 4 °C, then decalcifying samples in 0.34 M EDTA in PBS (pH 8.0). Samples were then processed for paraffin histology, and 3 μm sections were cut using a Leica Microtome

Model RM2265. Paraffin femora sections were stained for TRAP to identify osteoclasts from other resident bone cells. The TRAP staining solution was prepared, comprising of 1000 μL of 0.20 g per mL sodium nitrite added to 1000 μL of the basic fuchsin solution until small bubbles appeared. The sodium nitrite/fuchsin solution was added to 0.35 g of tartaric acid dissolved in 350 mL 1 M sodium acetate buffer pH 5.4. Then, 0.20 g naphthol ASBI phosphate dissolved in 20 mL dimethylformamide was added until the solution turned bright pink. The mixed solution was filtered prior to immediate staining using a 0.22 μm vacuum filter unit (Corning).

Following dewaxing in xylene, sections were incubated in 1 M Tris-HCL buffer (pH 9.4) at 40 °C for 1 h. Throughout incubation, 350 mL of TRAP staining solution was incubated for 15 min at 37 °C. Sections were counterstained with hematoxylin then cover slipped with Eukitt.

Aperio image scanning

Right femora sections on Superfrost PLUS glass slides were scanned on the Aperio Scanscope CS2 model. An area of interest was indicated by a red rectangle placed on the Macro image. Utilizing an Olympus UPLXAPO objective lens at a 20 \times objective, high quality digital slides were created. Digital slides were modified on Aperio ImageScope (v12.3.2.8013) to show 3 ROI's: 900 μm at 2.2 \times objective, 300 μm at 9.8 \times objective, and 300 μm at 7 \times objective.

Quantification of osteoclasts and osteoblasts

Quantification of osteoclast populations among the trabecular bone was performed with BioQuant Osteo (Version v21.5.60). Utilizing a Zeiss Axioplan Microscope (Zeiss, Germany) with a high resolution Jenoptik Camera at 10 \times objective, an ROI capturing a 3 mm region of trabecular bone, 1 mm from the top of the growth plate junction within the cortices was analyzed for each sample. TRAP-positive osteoclasts (bright pink cytoplasmic appearance) and cuboidal hematoxylin-stained osteoblasts were marked, and their cell surface-bone contact perimeters and trabecular bone surfaces were recorded. The total bone surface, no. of osteoclasts or osteoblasts per total bone surface, and osteoclast or osteoblast surface per total bone surface were determined. The structural and cellular parameters were calculated and expressed according to the ASBMR standardized nomenclature.¹²

RNA extraction

Harvested femora were frozen in liquid nitrogen and homogenized using the Polytron homogenizer probe (Kinematica) in TriReagent RNA isolation reagent (Sigma-Aldrich). RNA was sequentially precipitated from the homogenized sample by first separating the aqueous phase following the addition of chloroform and further precipitation with isopropanol and 3 M sodium acetate. The precipitated RNA was washed with 70% ethanol, resuspended in nuclease-free water, and stored at -70 °C.

Reverse transcription and quantitative polymerase chain reaction (qPCR)

Isolated RNA was used to generate cDNA using the Tetro cDNA synthesis kit (Meridian Life Science Inc) following the manufacturer's instructions.

The following gene-specific TaqMan probes were used: mouse *Rankl* (mm00441906_m1), mouse *Opg* (mm00435454_m1), and mouse *B2m* (mm00437762_m1) for qPCR. The qPCR reaction was performed using TaqMan Gene Expression MasterMix (Thermo Fisher Scientific) and Life Technologies QuantStudio 7 instrument. For each sample, the threshold cycle (CT) values were processed according to the 2(-Delta Delta C(T)) method.¹³ Gene expression levels were normalized to the expression of the housekeeping gene *B2m* and presented relative to untreated vehicle controls.

Statistical methods

Results were analyzed using GraphPad Prism (Version 9, GraphPad Prism V9). One-way analysis of variance (ANOVA) and multiple comparisons were performed using Tukey's correction, and unpaired *t*-tests were performed when comparing 2 populations. All data are expressed as mean with error bars representing standard deviation. For all statistical analyses, *P*-values < .05 were considered to be statistically significant.

Results

OPG:Fc models denosumab treatment and discontinuation in mice

Denosumab is a fully humanized monoclonal antibody against RANKL and does not bind murine RANKL, whereas human OPG is capable of binding directly to murine RANKL¹⁴ and able to reduce bone resorption and increase BMD.^{15,16} We have previously demonstrated RANKL inhibition and rebound bone loss following treatment withdrawal using OPG:Fc.¹⁰ To confirm this, we directly compared the efficacy of OPG:Fc and murine anti-RANKL antibody in wild-type mice in suppressing osteoclast activity and driving rebound bone loss upon discontinuation.

Treatment of mice with twice-weekly OPG:Fc (10 mg/kg) or thrice-weekly murine anti-RANKL antibody (5 mg/kg) (Figure 1A) for 2 wk significantly increased hindlimb BMD, which continued to increase for 6 wk following treatment. BMD peaked at week 8 in treated mice and the mean BMD was 12.7% and 15.2% higher than vehicle mean in OPG:Fc and murine anti-RANKL antibody-treated mice, respectively (*P* < 0.01 compared to vehicle). This was followed by a decrease in BMD to vehicle levels over the next 4 wk, (Figure 1Bi). Throughout the study, there was no significant difference in hindlimb BMD between mice treated with OPG:Fc and murine anti-RANKL antibody.

Serum TRAP was completely suppressed following 2 wk of treatment with either OPG:Fc or murine anti-RANKL antibody (*P* < .0001, Figure 1Bii), confirming suppression of osteoclast activity with either treatment.

MicroCT analysis of the femur was performed at a 1 mm region of interest in the distal femur to compare the effects of treatment with OPG:Fc or murine anti-RANKL antibody on the bone microarchitecture. This showed significantly increased trabecular bone structure at the end of 2 wk of treatment in both OPG:Fc and murine anti-RANKL antibody-treated mice compared to vehicle (Figure 1C, week 2). Trabecular volume (BV/TV) was 52.7% and 75.7% higher (*P* < 0.01 and *P* < 0.0001, respectively Figure 1Di), and trabecular number was 51.2% and 84.4% higher than vehicle levels in mice treated with OPG:Fc and murine anti-RANKL antibody, respectively (*P* < .05 and *P* < .0001, respectively, Figure 1Dii). The trabecular number was significantly higher in the murine

anti-RANKL antibody group compared to the OPG:Fc group (*P* < .05, Figure 1Dii). There was no difference in trabecular thickness between all groups (Figure 1Diii). There was no significant difference between trabecular bone volume and thickness between mice treated with OPG:Fc or murine anti-RANKL antibody.

At week 17, following bone loss in treated mice, and when hindlimb BMD was equivalent in all groups, there was no difference in the trabecular microCT parameters between vehicle and mice treated with OPG:Fc or murine anti-RANKL antibody (Figure 1D, week 17). Cortical bone volume in the distal femur was increased in mice treated with OPG:Fc at the end of treatment compared to vehicle and murine anti-RANKL antibody-treated mice but was equivalent in all groups at week 17 (Supplementary Figure S1). This shows a similar response in trabecular bone structural parameters to both OPG:Fc and murine anti-RANKL treatment, with return to untreated vehicle levels following withdrawal.

Longer treatment with OPG:Fc increases the rate of bone loss following withdrawal

Increased duration of treatment with denosumab has been associated with increased risk of rebound bone loss and fractures.^{8,9} To examine this in our mouse models, we treated mice with OPG:Fc or saline for 8 wk instead of 2 wk (Figure 2A). In the longer treatment group, hindlimb BMD increased and continued to increase until week 16, where this reached levels 51.1% higher than vehicle levels from baseline (*P* < .001). This was followed by a rapid decline in BMD to vehicle levels with a decrease of 24.5% over a 4-wk period (weeks 16-20) (Figure 2B), which was greater than the rate of bone loss observed with 2 wk of treatment of 12.6% over a 4 wk period (Figure 1B). Interestingly, BMD continued to decline below vehicle levels between week 20 and 23, though there was no significant difference between the groups during this period.

Once again, we demonstrated that serum TRAP was suppressed with OPG:Fc treatment, remained markedly suppressed between week 8 and 14 (*P* < .01), and then showed a rapid overshoot in serum to 73.3% (*P* < .001) higher than vehicle just 2 wk later (Figure 2C). Serum TRAP remained significantly above vehicle levels between weeks 16-20, while BMD loss was ongoing, before dropping to vehicle levels by the end of the study at week 23. We again demonstrated that the rapid rise and overshoot above vehicle levels in serum TRAP (week 14-16) preceded the rebound loss in hindlimb BMD (from week 16).

Serum TRAP is elevated prior to P1NP and CTX following withdrawal of treatment with OPG:Fc

We have demonstrated that OPG:Fc treatment and withdrawal are representative of denosumab treatment and discontinuation in our model. Following our observation of serum TRAP rising prior to decline in hindlimb BMD, we sought to investigate how BMD and serum TRAP changes correlate with bone turnover markers used in clinical practice, namely CTX and P1NP, which are currently utilized to guide sequential therapy following denosumab discontinuation.

As shown previously, longitudinal analyses following 2 wk of OPG:Fc revealed suppressed serum TRAP to week 8 and a rise to control levels at week 10, prior to BMD loss between weeks 10 and 13 (Figure 3B and C). As expected, serum TRAP, P1NP, and CTX were all suppressed below control levels at the end of OPG:Fc treatment at week 2, and all markers

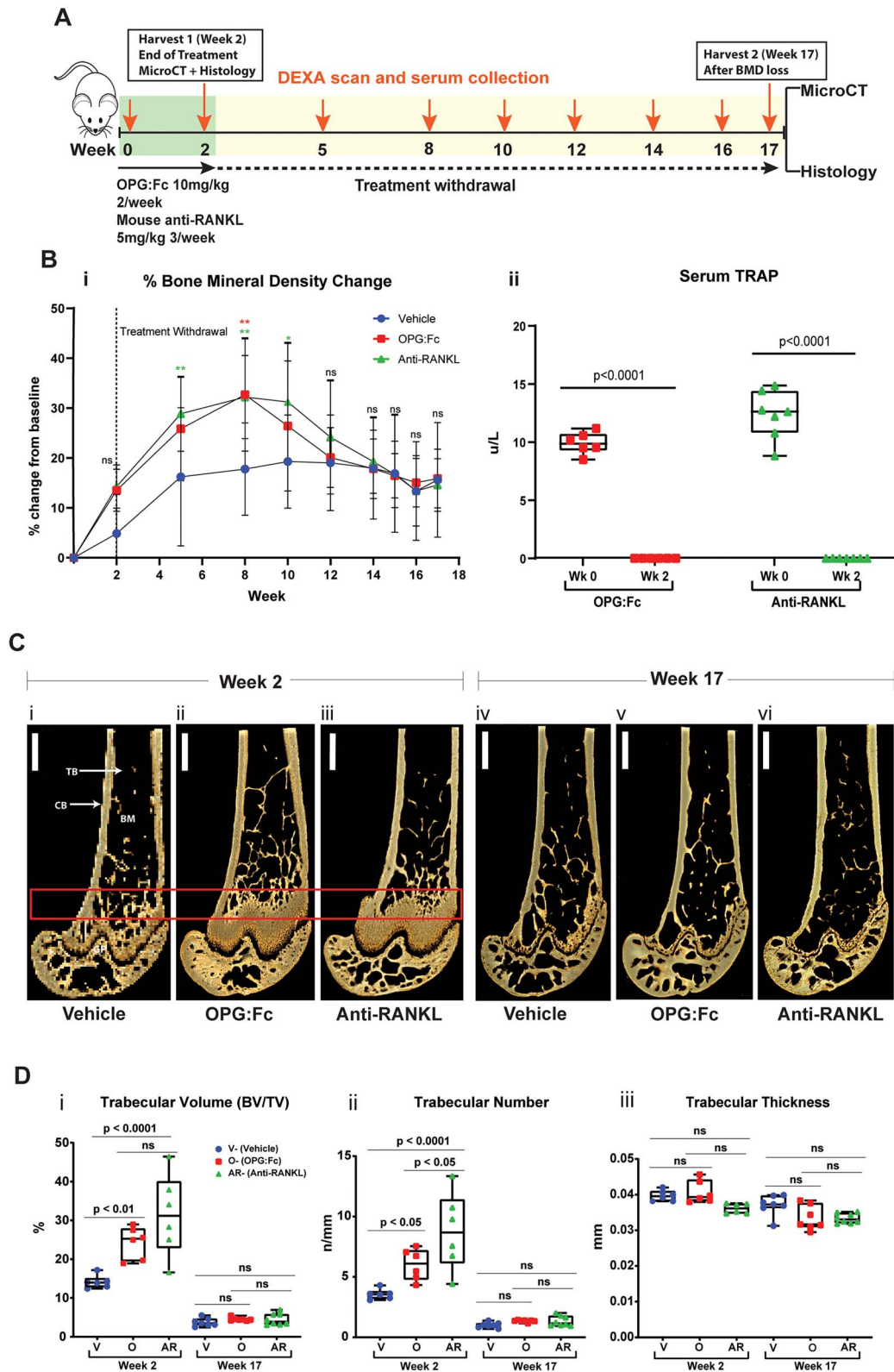


Figure 1. RANKL inhibition with OPG:Fc increases BMD, and treatment withdrawal leads to loss of bone mass and density. (A) Schematic of the experimental design to assess the effect of treatment with OPG:Fc or murine anti-RANKL antibody. (B) BMD and TRAP changes following treatment. (i) BMD shown as a percentage change from baseline levels following treatment with OPG:Fc ($n = 9$), murine anti-RANKL antibody ($n = 9$), or saline (vehicle, $n = 9$). Dotted line showing the end of treatment at week 2. Data represented as mean \pm SD. Asterisks indicate P -values $< .05$ ($*P < .05$, $**P < .01$). (ii) Serum TRAP measured by ELISA at baseline and following 2 wk of treatment with OPG:Fc ($n = 6$) or murine anti-RANKL antibody ($n = 7$). Boxplots represent mean \pm SD. (C) Representative 3D microCT reconstructed images of the right femur at the end of 2 wk of treatment (i)–(iii) and at the end of the study (iv)–(vi). Box highlighting the region of interest. CB, cortical bone; TB, trabecular bone; BM, bone marrow. (D) MicroCT analysis of the region of interest showing trabecular volume (i), number (ii), and thickness (iii) at the end of treatment (week 2, $n = 6$ –7 per group) and at the end of the study (week 17, $n = 9$ per group). Boxplots represent mean \pm SD. V, vehicle; O, OPG:Fc; AR, anti-RANKL.

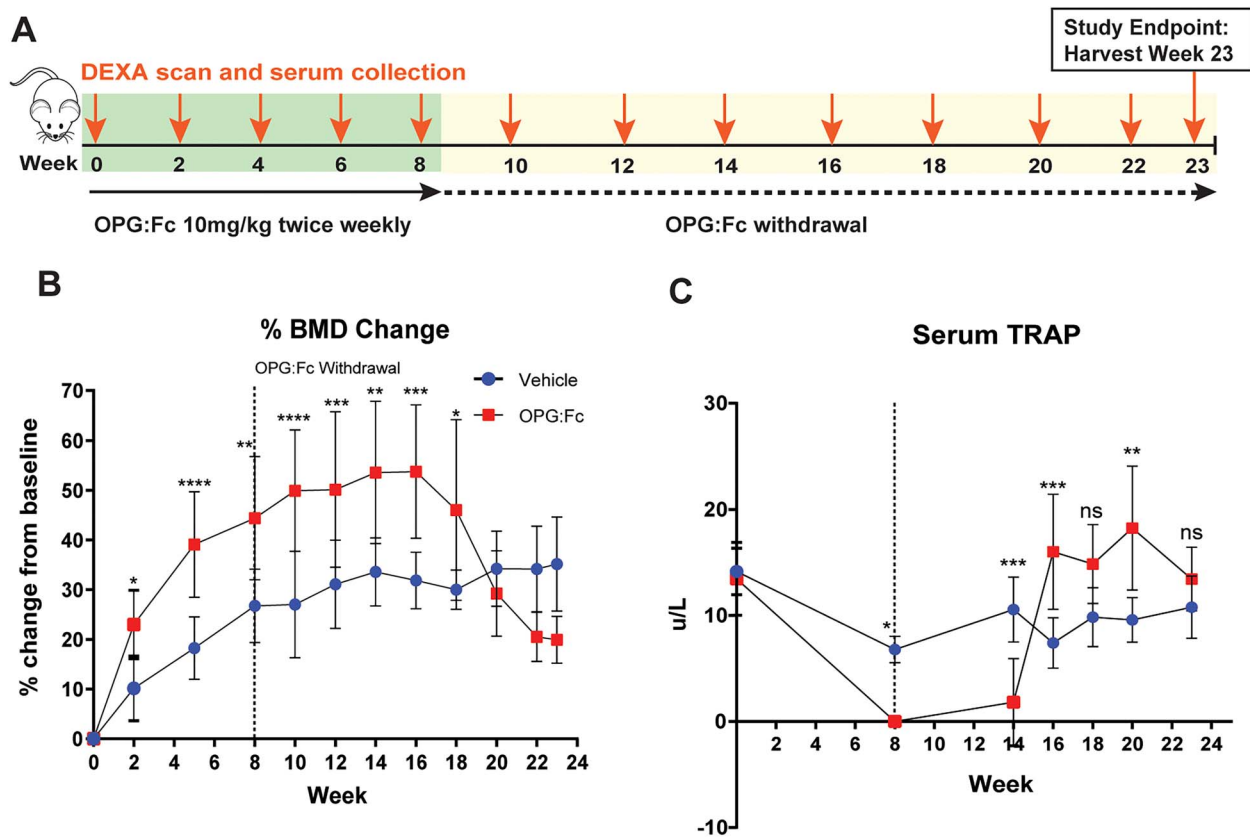


Figure 2. Longer duration of RANKL inhibition increases the rate of BMD loss and leads to sustained increases in serum TRAP following treatment withdrawal. (A) Schematic of the experimental design to assess the effect of longer duration of treatment with OPG:Fc on BMD and serum TRAP. $N = 10$ per group. (B) Longitudinal change in BMD presented as percentage change from baseline. Dotted line showing end of treatment at week 8. Data presented as mean \pm SD. Asterisks indicate P -values $< .05$ (* $P < .05$, ** $P < .01$, *** $P < .001$, **** $P < .0001$). (C) Longitudinal serum TRAP throughout the study. Dotted line showing end of treatment at week 8. Data presented as mean \pm SD. Asterisks indicate P -values $< .05$ (** $P < .01$, *** $P < .001$).

remained suppressed at week 8 (Figures 3D and S2). At week 11, following the peak in BMD, serum TRAP was significantly elevated 34.8% above mean control levels, while serum P1NP and CTX had risen to reach control levels (Figures 3D and S2). By week 13, when BMD had returned to control levels in mice treated with OPG:Fc, serum TRAP remained significantly higher than control levels and it was only at this timepoint where serum P1NP and CTX were also significantly higher than vehicle levels (Figures 3D and S2).

Overall, this shows that an increase in osteoclast number and overshoot in osteoclast enzyme activity, as measured by serum TRAP, parallels bone loss more closely and was detected earlier than an overshoot in markers of bone turnover used in clinical practice, P1NP, and CTX.

Relative deterioration of bone microarchitecture is observed during rebound bone loss

To investigate the changes in bone microarchitecture during rebound bone loss following OPG:Fc treatment, harvested femora were examined with microCT (Figure 4A). Mice treated with OPG:Fc were harvested at time-points following treatment and during rebound bone loss (Figure 3A).

Trabecular bone volume, number, and thickness in the distal metaphyseal region were significantly higher in the femora of mice treated with OPG:Fc compared to their controls throughout the study (Figure 4B). Notably this difference was less evident by week 13 indicating a relative loss in trabecular volume during rebound BMD loss.

Cortical bone volume in the distal diaphysis was significantly higher in OPG:Fc-treated mice compared to vehicle at week 2 following treatment, at week 8 prior to the decline in BMD, and at week 11 while BMD loss was occurring (Figure 4Ci) but was equivalent to vehicle mice at week 13 following rebound bone loss. There was no difference in cortical thickness following treatment at week 2 but it was significantly lower in OPG:Fc-treated mice at each timepoint thereafter (Figure 4Cii). The endosteal and periosteal perimeters were equivalent at the end of treatment but were higher in treated mice at each time-point thereafter (Figure S3). These changes in cortical parameters suggest that there is increased cortical volume initially, but there is increased bone resorption on the endosteal surface, leading to a thinner cortex and increased endosteal and periosteal perimeter.

Together, these results show that, following an initial improvement in bone microarchitecture following OPG:Fc treatment, loss in trabecular and cortical bone is observed while rebound BMD loss is occurring following the offset of RANKL inhibition.

Abundant osteoclasts are observed during rebound bone loss

To examine the changes in osteoclast number during OPG:Fc treatment and rebound bone loss, TRAP-positive cells were quantified in the distal femora at each harvest time point (Figure 5A).

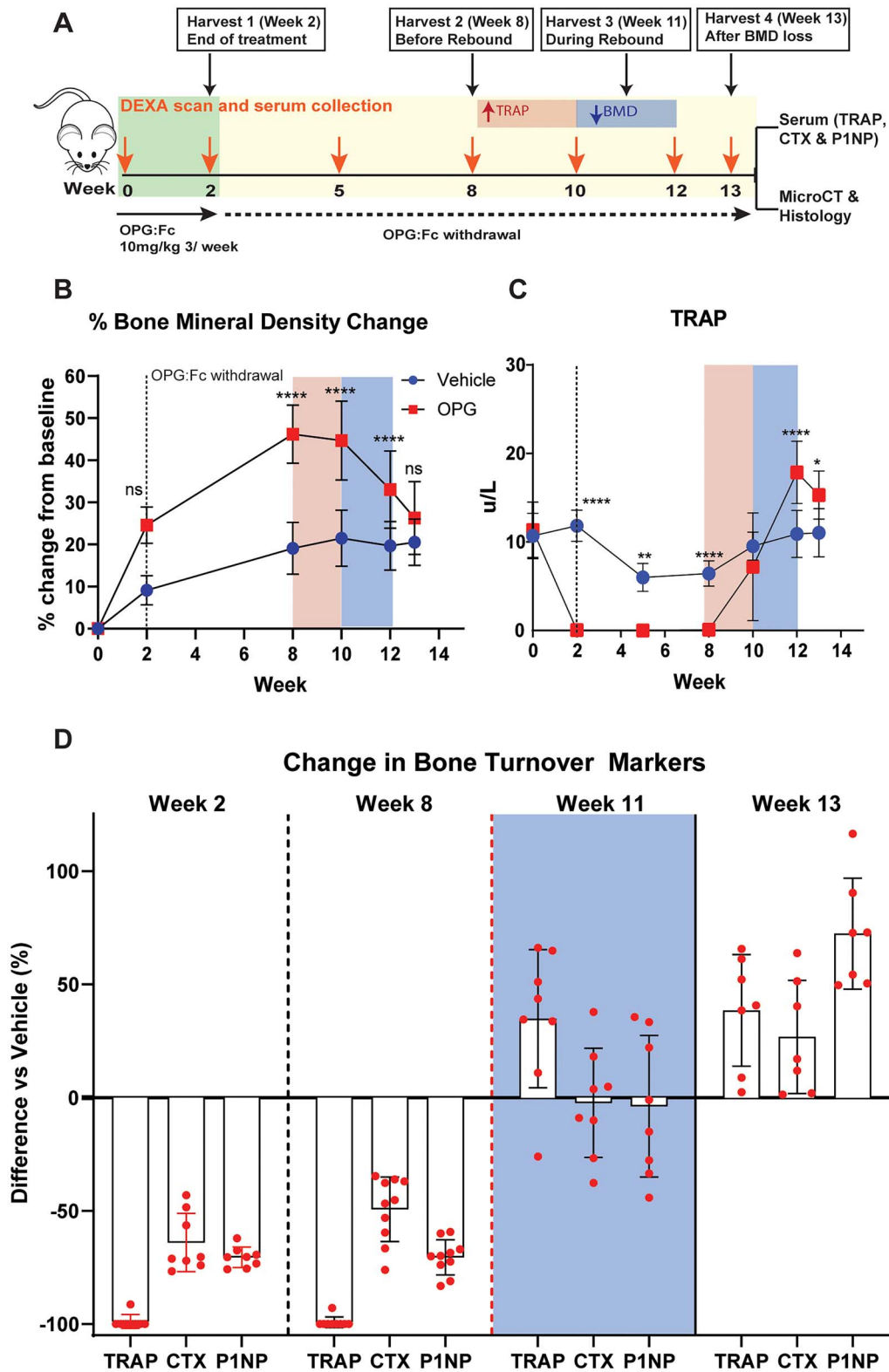


Figure 3. Serum TRAP rises above vehicle levels before P1NP and CTX following withdrawal of RANKL inhibition. (A) Schematic of the study design to harvest cohorts of mice at specific intervals following 2 wk of OPG:Fc treatment to allow for contemporaneous measurements of bone turnover markers, changes in bone microarchitecture, and histology. Pink box (left) highlights a time at which serum TRAP is rising from post treatment levels, while the blue box (right) highlights the time during which BMD loss is occurring. (B) Longitudinal changes in BMD. Data presented as mean \pm SD. Asterisks indicate P -values $< .05$ (* $P < .05$, ** $P < .01$, *** $P < .001$, **** $P < .0001$). (C) Longitudinal changes in serum TRAP. Data presented as mean \pm SD. Asterisks indicate P -values $< .05$ (* $P < .05$, ** $P < .01$, *** $P < .001$, **** $P < .0001$). (D) Changes in the bone turnover markers (TRAP, CTX, and P1NP) in mice treated with OPG:Fc compared to vehicle at each harvest timepoint, expressed as % change compared to vehicle mean. Week 11 highlighted in the blue box represents the time during which BMD loss is occurring.

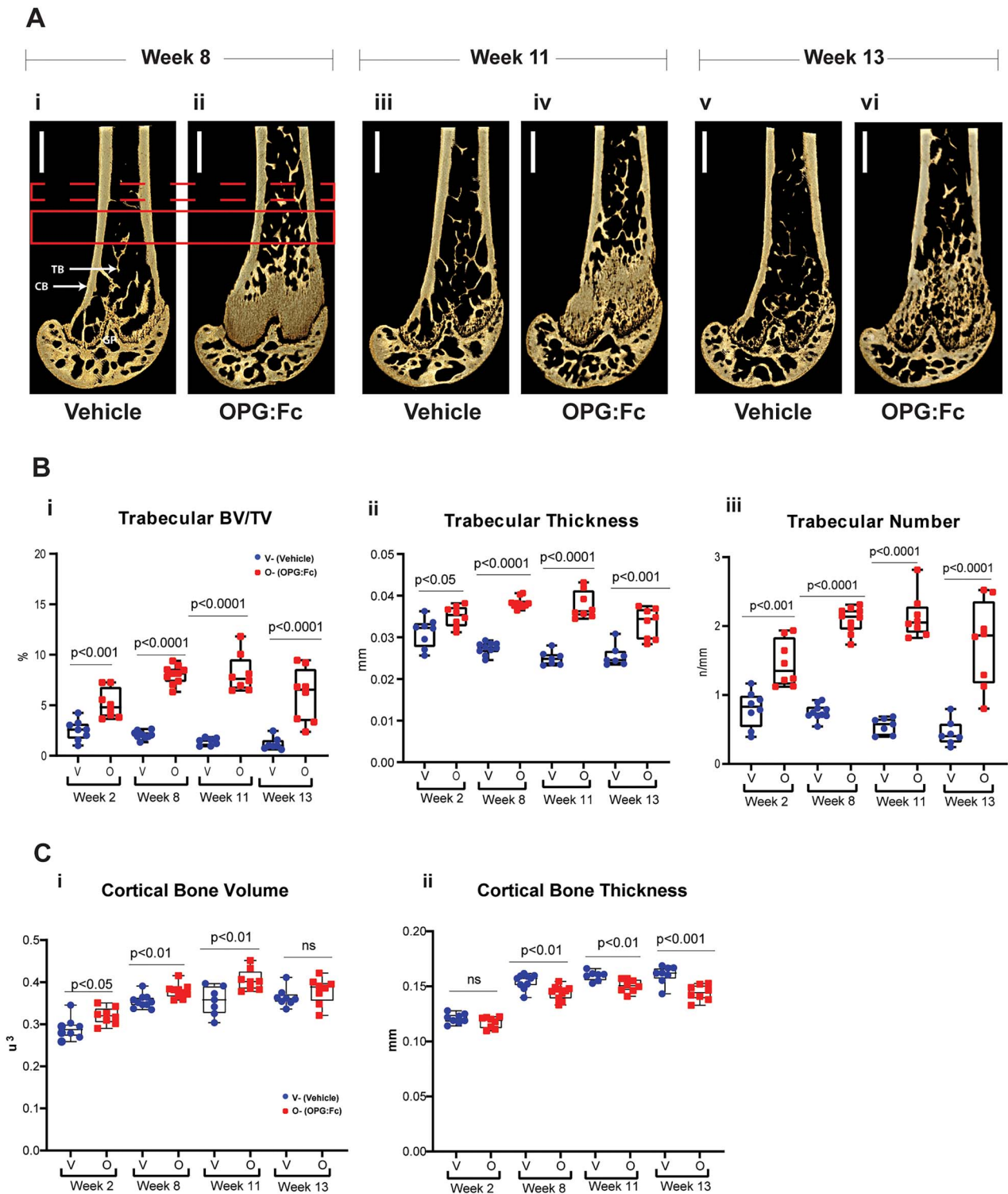


Figure 4. Changes in bone microarchitecture during rebound bone loss following withdrawal of RANKL inhibition with OPG:Fc. (A) Representative 3D images of harvested femora showing differences in bone microarchitecture between mice treated with saline and OPG:Fc. Dashed red box denotes a region of interest examined at a 0.5 mm section located 3 mm above the growth plate (GP). Solid red box denotes region of interest examined at a 1 mm section located 2 mm above the growth plate. CB, cortical bone; TB, trabecular bone. (B) Differences in trabecular volume (i), number (ii), and thickness (iii) between mice treated with saline (vehicle) and OPG:Fc at the harvest timepoints. Boxplots represent mean \pm SD. (C) Differences in cortical volume (i) and thickness (ii) between mice treated with saline (vehicle) and OPG:Fc at the harvest timepoints. Boxplots represent mean \pm SD.

Following treatment with 2 wk of OPG:Fc, there was a complete absence of osteoclasts. Osteoclasts were detectable at week 8 but remained reduced in number compared to control. However, by week 11, osteoclast numbers were

significantly higher than control levels, remaining elevated at week 13 (Figure 5Bi). When osteoclast numbers were normalized to trabecular bone surfaces, and the increase in trabecular bone volume with OPG:Fc treatment was

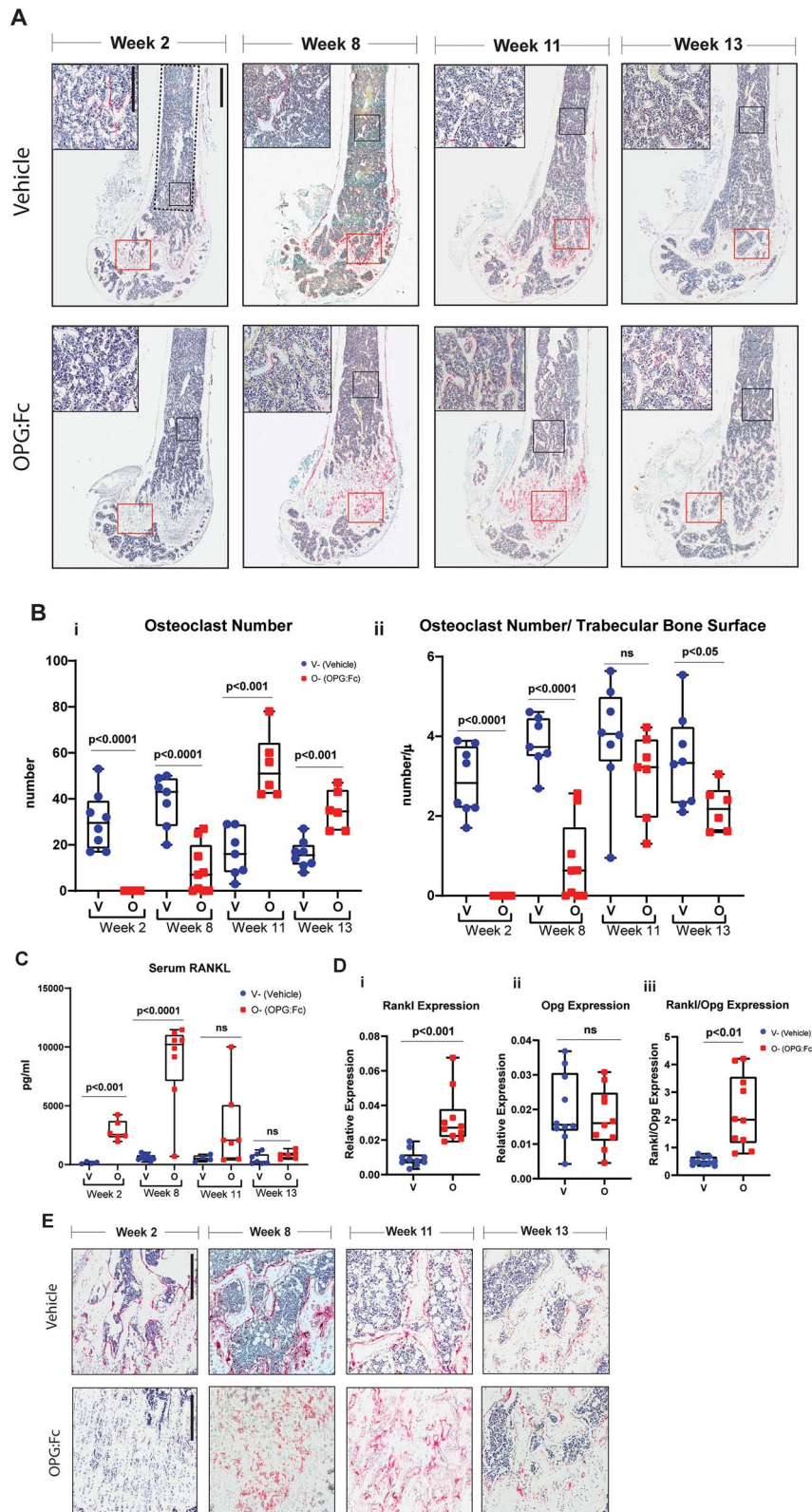


Figure 5. Changes in osteoclast number and activity during rebound bone loss following withdrawal of RANKL inhibition with OPG:Fc. (A) Representative histological images of femora stained with TRAP (red) harvested following treatment with saline or OPG:Fc. Analysis of osteoclast parameters on trabecular bone was performed within the ROI defined by the dotted line (scale bar 900 μ m at 2.2 \times magnification). Representative high magnification images shown in top left corner and its corresponding ROI shown in the black box (scale bar 300 μ m at 9.8 \times magnification). Red box (near bottom of image) denotes osteoclasts observed on trabecular bone surfaces as shown in magnified images in Figure 5E. (B) Quantification of number of osteoclasts (i) and osteoclast surface (ii) per trabecular bone surfaces at harvest timepoints week 2, 8, 11, and 13. Boxplots represent mean \pm SD. (C) Quantification of serum RANKL following OPG:Fc treatment. Boxplots represent mean \pm SD. (D) Quantification of mRNA expression of (i) *Rankl*, (ii) *Opg*, and (iii) *Rankl:Opg* in marrow depleted femora of mice treated with saline or OPG:Fc harvested at week 8. Boxplots represent mean \pm SD. Representative images of osteoclasts observed on trabecular bone surfaces throughout the study in the ROI marked by the red box in Figure 5A (scale bar 300 μ m at 7 \times magnification).

accounted for (Figure 4B), osteoclasts numbers per trabecular bone surface were equivalent or lower in treated mice during rebound bone loss (Figure 5Bii). Osteoclast surfaces were also increased during rebound bone loss. But this was equivalent to vehicle levels when osteoclast surfaces were normalized to trabecular bone surfaces due to increased trabecular bone with OPG:Fc treatment at weeks 11 and 13, as was also demonstrated with MicroCT analysis (Figure S4).

Osteoblast number and surfaces were also quantified in this region of interest. Osteoblast numbers followed a similar pattern to osteoclasts during OPG:Fc treatment and rebound bone loss, with significantly lower numbers following treatment, starting to rise thereafter. When total osteoclast numbers were significantly higher than control at week 11, total osteoblast numbers remained equivalent to vehicle levels. By week 13, osteoblast numbers and surface were both significantly increased compared to control, but both number and surface were equivalent to control levels when normalized to trabecular bone surfaces (Figure S5).

In the most distal region of the metaphysis of the femur, quantification of osteoclasts was not possible owing to the difficulty in defining trabecular bone surfaces due to the retention of the primary spongiosa in mice treated with OPG:Fc. Nevertheless, images of this region show clearly that TRAP+ osteoclasts were absent at the end of treatment and abundant in numbers at weeks 8, 11, and 13 compared to vehicle (Figure 5E). On the endosteal surface, osteoclast parameters (number and surfaces) were not different between groups (data not shown).

Higher local and circulating RANKL levels provide a pro-osteoclastogenic environment prior to rebound bone loss

Serum RANKL measurement by ELISA demonstrated significantly higher levels of circulating RANKL following treatment with 2 wk of OPG:Fc, with levels 17.6-fold higher than vehicle levels at week 2 ($P < .001$, Figure 5C). Serum RANKL was maximal at week 8 with serum RANKL levels 14.7-fold higher compared to week 2 levels ($P < .0001$), indicating an abundance of circulating pro-osteoclastogenic factors just prior to BMD loss (Figure 5C). As rebound BMD loss was occurring, serum RANKL levels decreased. Serum RANKL levels were equivalent to vehicle levels once hindlimb BMD was equivalent.

We then performed quantitative PCR to measure mRNA expression of *Rankl* and *Opg* in marrow-depleted femora to examine the changes in osteoclastogenic factors in the bone microenvironment at week 8, when serum RANKL levels were highest. This showed significantly higher *Rankl* expression in OPG:Fc-treated bones, while *Opg* expression remained equivalent to control, leading to a significant shift in the *Rankl:Opg* expression, favoring osteoclastogenesis (Figure 5D).

Discussion

RANKL inhibition with denosumab has revolutionized the treatment of osteoporosis. However, the overshoot of bone resorption and rapid loss in BMD following its discontinuation presents an important clinical challenge in the long-term management of osteoporosis. This phenomenon remains incompletely understood. Combined with a lack of robust

randomized control studies to define optimal management approaches, this has led to uncertainty around how to manage patients who have ceased or plan to cease denosumab therapy.

Animal models facilitate the direct examination of longitudinal changes in bone structure, bone cell activity, and local and serum markers of osteoclast activity during rebound bone loss following treatment withdrawal.

OPG:Fc treatment in mice models denosumab treatment and discontinuation

We used OPG:Fc to inhibit RANKL and model denosumab treatment and discontinuation. This approach models observations seen following denosumab discontinuation in clinical practice where gains in BMD on treatment are lost within 12 mo of discontinuation and a large overshoot in bone turnover markers PINP and CTX are detected.^{3,17} Importantly, we showed a similar pattern of response in hindlimb BMD, trabecular architecture, and serum TRAP in mice treated with OPG:Fc and murine anti-RANKL, confirming the relevance of OPG:Fc when modelling this scenario.

Longer duration of treatment with denosumab has been identified as a risk factor for increased bone loss and fractures.¹⁸ Our results align with this, with longer duration of RANKL inhibition with OPG:Fc leading to greater gains in hindlimb BMD and greater rates of BMD loss once treatment was discontinued: 24% (long) versus 12% (short) over 4 wk. Our model also showed a more sustained overshoot in bone resorption as measured by serum TRAP.

Patients discontinuing denosumab are at increased risk of fractures. Evaluation of iliac crest bone biopsy following discontinuation of denosumab showed a return to bone remodeling parameters similar to those observed in untreated postmenopausal women with osteoporosis.¹⁹ This was also observed in our study where femoral microCT parameters were equivalent between mice treated with OPG:Fc, murine anti-RANKL antibody, or saline at week 17 (Figure 1D). However, analysis of femora harvested while rebound bone loss was occurring showed a relative deterioration of BMD and trabecular bone microarchitecture (week 13), and a deficit in cortical thickness with widening of the cortical structure at weeks 11 and 13 (Figures 4C and S3).

Overshoot in serum TRAP occurs before a rise in serum P1NP and CTX during the rebound phenomenon

Bone turnover markers are used to predict fracture risk and monitor treatment response in the management of patients with osteoporosis. In 2010, the International Osteoporosis Foundation and International Federation of Clinical Chemistry and Laboratory Medicine recommended the use of the bone formation marker (P1NP) and bone resorption marker (CTX) as reference markers measured by standardized assays, and the use of these markers has guided clinical practice and trials since.²⁰ In the setting of denosumab discontinuation, overshoot above control levels is seen in both P1NP and CTX,¹⁴ and a rise in CTX has been used to guide sequential therapy in randomized studies examining the use of zoledronate following denosumab to prevent bone loss.⁴

We demonstrated that serum TRAP, a marker of osteoclast enzymatic activity, rises prior to these bone turnover markers used in clinical practice. During bone resorption,

type 1 collagen is digested by enzymes, and the degradation products of type 1 collagen (such as CTX) is released into circulation once bone resorption and breakdown of bone have already occurred. In our study, CTX and P1NP were only higher than vehicle levels once BMD loss had already occurred, and this may explain why studies intervening at a time of CTX rise failed to prevent BMD loss following denosumab discontinuation^{4,5,7} as the intervention was too late.

In comparison, TRAP is an enzyme produced by the osteoclast during osteoclast differentiation and bone resorption^{21,22} and is detectable earlier during osteoclastogenesis as well as during the process of bone resorption. This phenomenon was also seen in hRANKL mice receiving denosumab, where serum TRAP was suppressed below vehicle levels during treatment, then rose to vehicle levels before a significant overshoot in serum CTX was detected.²³

TRAP is a useful marker to monitor response to antiresorptive treatment including denosumab, decreasing with treatment and correlating to changes in BMD and serum CTX.²⁴⁻²⁶ TRAP is also unaffected by food intake, whereas CTX and P1NP levels decrease after feeding, reducing diagnostic accuracy, and must be measured on a fasting sample.²⁷ Therefore, a rise in serum TRAP from on-treatment levels may provide a more useful marker in the setting of denosumab discontinuation. Clinical investigations are required to determine the potential utility of this finding to inform timing of earlier intervention with sequential osteoclast-directed therapy in patients.

Elevated serum RANKL precedes an overshoot in serum TRAP and BMD loss following withdrawal of RANKL inhibition

Following confirmation that a rapid formation of osteoclasts was driving the bone loss in our model, we aimed to define what was driving this response. Serum levels of RANKL were elevated 17-fold in mice following treatment with OPG:Fc and were significantly elevated before a rise in osteoclast number, serum TRAP, and BMD loss were detected. Our data align with cross-sectional clinical analyses of serum RANKL and TRAP at 6, 9, and 12 mo following the last dose of denosumab.²⁶ In this clinical study, higher RANKL was observed 6 mo following the last denosumab dose, compared to levels measured at 9- and 12-mo, whereas serum TRAP was highest in the 9- and 12-mo groups,²⁶ though the temporal relationship to changes in BMD was not examined.

This supports our observation that following withdrawal of RANKL inhibition with OPG:Fc, there is a rise in serum RANKL, which leads to a rise in serum TRAP and rebound bone resorption, releasing CTX into the circulation at the time of clinically detectable BMD loss.

However, this finding was not observed in another clinical study by Fassio and colleagues,²⁸ who measured serum RANKL longitudinally following denosumab discontinuation and found a progressive increase in RANKL, which only reached statistical significance at 12 mo following denosumab discontinuation. Why a difference in the timing of elevated RANKL exists between these clinical studies is unclear. Sølling and colleagues hypothesized that this difference may be due to the difference in the number and mean age of participants and the RANKL assay utilized.²⁶ TRAP was not measured in the study by Fassio and colleagues so the temporal relationship

between RANKL and TRAP following denosumab discontinuation could not be examined in this study.

Notably, in our study, serum RANKL had returned to control levels by the end of our study once bone loss had completed and BMD also returned to control levels. Serial measurements of serum RANKL could be considered in future clinical studies examining denosumab discontinuation to further elucidate the pattern of change in osteoclastogenic factors. Nevertheless, our pre-clinical study provides a clear temporal pattern of accelerated osteoclast formation and activity in the lead up to BMD loss and elevated fracture risk.

Changes in Rankl expression promote osteoclast formation during rebound

Osteoclast precursors have been observed to accumulate during denosumab treatment and suggested to play a role in the rapid formation of osteoclasts following withdrawal.²⁹ Our previous work using OPG:Fc showed osteoclasts undergoing fission to form daughter cells termed “osteomorphs,” which accumulated during OPG:Fc treatment.¹⁰ These RANK-positive cells were then capable of undergoing re-fusion to form mature osteoclasts following withdrawal of RANKL inhibition in a process called “osteoclast recycling.” The increase in RANKL following withdrawal of RANKL inhibition with OPG:Fc could therefore stimulate this pool of accumulated RANK-positive osteoclast precursors and osteomorphs to undergo differentiation, fusion, and activation to form a large number of osteoclasts and undergo bone resorption *en masse*.³⁰ This is also supported by our previous work, where isolated bone marrow cells from OPG:Fc-treated mice were cultured in vitro with RANKL and M-CSF. The same number of bone marrow cells from OPG:Fc-treated mice produced more osteoclasts than cells from vehicle mice, and these cells were capable of forming resorption pits on dentine slices.¹⁰

To examine this mechanism further in our model and overcome limitations of not being able to assess protein levels of OPG, we examined local production of RANKL via quantification of RANKL and OPG mRNA. Indeed, a significant shift in the *Rankl:Opg* gene expression ratio in the marrow depleted bone prior to increased osteoclast formation and activity and BMD loss was demonstrated. A significant increase in *Rankl* expression was also observed in hRANKL mice receiving denosumab for 2 wk, though there was also a significant reduction in *Opg* expression, which was not observed in our study. Nevertheless, our local mRNA expression data indeed confirm our finding of elevated circulating sRANKL, providing an additional mechanism for the rapid formation of osteoclasts in our model.

In contrast to our previous findings, an increase in osteoclast progenitors, as determined by primary bone marrow cultures, was not detected in a study of hRANKL mice treated with denosumab.²³ Single cell RNA sequencing of bone marrow harvested 2 wk following cessation of denosumab treatment in hRANKL mice revealed no change in myeloid lineage cells with denosumab. However, a trend toward more cells expressing osteomorph markers (such as *Acp5*, *Axl*, and *Cadm1*) was noted. The lack in significant increases in precursors and osteomorphs in this hRANKL mouse study may be due to technical isolation challenges, the timing of analysis post denosumab treatment, or may be influenced by the modified mouse model utilized.

A humanized RANKL mouse has been previously developed by Amgen, and denosumab was able to completely inhibit the chimeric RANKL, thereby increasing BMD.³¹ However, the baseline phenotype of this mouse was altered, with significantly lower serum TRAP levels and decreased osteoclast and osteoblast surfaces (despite equivalent trabecular volume) compared to wildtype.³¹ Although this novel hRANKL mouse demonstrated equivalent cortical thickness and trabecular volume to wild-type mice, bone cell activity and endogenous mouse RANKL/RANK/OPG signaling were not examined, therefore it is unclear if this would influence the differences observed in *Rankl:Opg* expression and osteoclast precursor populations following denosumab treatment.

Nevertheless, the conclusion that downregulation of OPG production by osteoblast and osteocytes in response to denosumab is sound and is supported by our observations showing a reduction in osteoblast parameters and the suppression of the osteoblast marker P1NP following OPG:Fc treatment, indicating decreased osteoblast number and activity in our model. These are complementary to our finding that elevated RANKL provides a local pro-osteoclastogenic environment

prior to and during rebound bone loss. Additional studies examining changes in OPG in the bone microenvironment and osteocyte populations in our model using OPG:Fc to inhibit RANKL would be informative.

It is also important to note that other than bisphosphonates, which display a sustained effect on bone turnover following discontinuation, other bone-directed therapies also display a pattern of rise in bone resorption and loss of BMD following discontinuation. This has been observed following the discontinuation of hormone replacement therapy with estrogen,³² selective estrogen receptor modulators,³³ odanacatib,³⁴ and romosozumab.³⁵ Although increases in fracture risk have not been associated with these reductions in BMD during off treatment periods, further pre-clinical studies employing a similar design to the present study and examining changes to RANKL/OPG signaling and serum TRAP would expand our understanding of this phenomenon across other treatments.

Our data provide the first model of denosumab discontinuation using OPG:Fc in mice with the aim to define the temporal cellular and molecular mechanisms driving the rebound

Key resources table

Reagent or resource	Source	Identifier
Antibodies		
Anti-mouse RANKL antibody	BioXcell	Cat#: BE0191
Chemicals, peptides, and recombinant proteins		
Ambion Nuclease-Free Water	Thermo Fisher Scientific	Cat#: AM9937
Chloroform	Sigma-Aldrich	Cat#: C2432
EDTA	Sigma-Aldrich	Cat#: E5134
Ethyl alcohol, Pure	Sigma-Aldrich	Cat#: E7023
Isopropanol (2-Propanol)	Sigma-Aldrich	Cat#: I9516
Osteoprotegerin:Fc	Amgen Inc	N/A
Paraformaldehyde	Thermo Fisher Scientific	Cat#: ACR416785000
PBS, pH 7.4	GIBCO/Thermo Fisher Scientific	Cat#: 10010049
TriReagent RNA Isolation Reagent	Sigma-Aldrich	Cat#: T9424
Critical commercial assays		
Mouse TRANCE/RANKL/TNFSF11 Quantikine ELISA Kit	R&D Systems	Cat#: MTR00
Serum RatLaps (CTX-I) EIA	Abacus ALS Pty Ltd	Cat#: IDSAC06F1
Serum P1NP ELISA -Mouse	Abacus ALS Pty Ltd	Cat#: IDSAC33F1
Serum TRAP 5b ELISA – Mouse	Abacus ALS Pty Ltd	Cat#: IDSBTR103
Taqman Gene Expression Assay	Thermo Fisher Scientific	Cat#: 4331182
TaqMan Gene Expression MasterMix	Thermo Fisher Scientific	Cat#: 4369016
Tetro cDNA Synthesis Kit	Meridian Life Science Inc	Cat#: BIO-65043
Experimental models: Organisms/strains		
C57BL/6J	Australian BioResources	ABR:000664
C57BL/KaLwRij	Australian BioResources	ABR: 3076
Software and algorithms		
BioQuant Osteo Ver v21.5.60	Bioquant Life Science	https://www.bioquant.com/ RRID:SCR_016423
CTAn	Skyscan	https://www.bruker.com/
Drishti-2.4	³⁶	https://github.com/nci/drishti; RRID:SCR_017999
Vision DXA	Faxitron Bioptics/Hologic	https://www.faxitron.com/
NRecon	Skyscan	https://www.bruker.com/
Life Technologies QuantStudio 7 Real Time PCR System	Applied Biosystems	https://www.thermofisher.com/order/catalog/product/4485701#/4485701 RRID:SCR_020245
Other		
Polytron PT1200E Homogenizer	Kinematica AG	P/N: 9112017

phenomenon. Moreover, this is the first study to demonstrate that longer treatment with OPG:Fc drives a greater rebound stimulus of osteoclast activity and more rapid bone loss. It would be important to determine whether lower doses of OPG:Fc, which may be considered more physiologically relevant, would lead to similar outcomes; however, we did demonstrate a similar pattern of temporal bone gain and rebound loss with our OPG:Fc dosing protocol compared directly to a murine anti-RANKL antibody. In addition, we used intact growing mice in our studies. It would be important to explore our model in aged or mice following ovariectomy to truly mimic the post-menopausal bone microenvironment.

Importantly we also showed the potential for serum TRAP measures to be utilized to predict imminent BMD loss and guide timing of sequential therapy following denosumab discontinuation. At the cellular and molecular level, we revealed aberrant RANKL signaling and osteoclast formation in the weeks following OPG:Fc withdrawal, providing evidence to support our previous conclusion that osteoclast precursor accumulation and osteoclast recycling drive the rebound phenomenon following denosumab discontinuation.

Our studies were performed in growing and eugonadal mice, which is a limitation in the clinical translation of these findings as postmenopausal women represent the majority of patients receiving denosumab. Whether these changes in gene expression and osteoclast precursor and osteomorph populations are also seen in humans receiving denosumab is unclear and warrants further investigation.

Taken together, this study provides a novel framework for the biological mechanisms underpinning the rebound phenomenon and the potential use of alternative markers of bone resorption (serum RANKL and TRAP) to guide sequential therapy. Ultimately, this work will lead to an improved capacity to track rebound response to denosumab withdrawal and therefore our ability to initiate sequential therapy strategies to prevent bone loss and fractures in patients following denosumab discontinuation.

Acknowledgments

OPG:Fc used in this study was provided by Amgen Inc.

Author contributions

Albert S. Kim (Conceptualization, Data curation, Formal analysis, Investigation, Methodology, Writing—original draft, Writing—review & editing), Victoria E. Taylor (Data curation, Formal analysis), Ariel Castro-Martinez (Data curation, Methodology), Suraj Dhakal (Data curation, Formal analysis), Amjad Zamerli (Data curation), Sindhu Mohanty (Data curation), Ya Xiao (Data curation), Marija K. Simic (Data curation, Methodology), Jinchen Wen (Data curation), Ryan Chai (Supervision), Peter I. Croucher (Funding acquisition, Supervision, Writing—review & editing), Jacqueline R. Center (Conceptualization, Investigation, Supervision, Writing—review & editing), Christian M. Girgis (Conceptualization, Investigation, Writing—review & editing), and Michelle M. McDonald (Conceptualization, Formal analysis, Funding acquisition, Investigation, Supervision)

Supplementary material

Supplementary material is available at *Journal of Bone and Mineral Research* online.

Funding

A.S.K. is supported by the UNSW Sydney University Postgraduate Award and the Australian Government Research Training Program Scholarship. This work is supported by the Mrs. Janice Gibson and the Ernest Heine Family Foundation and Cancer Council NSW project grant R20-05, American Society of Bone and Mineral Research Rising Star Award and Bone Health Foundation an Australia and New Zealand Bone and Mineral Society Grant in Aide.

Conflicts of interest

None declared.

Data availability

All raw data files can be provided on request.

References

1. Boyce BF, Xing L. The RANKL/RANK/OPG pathway. *Curr Osteoporos Rep.* 2007;5(3):98–104. <https://doi.org/10.1007/s11914-007-0024-y>.
2. Bone HG, Wagman RB, Brandi ML, et al. 10 years of denosumab treatment in postmenopausal women with osteoporosis: results from the phase 3 randomised FREEDOM trial and open-label extension. *Lancet Diabetes Endocrinol.* 2017;5(7):513–523. [https://doi.org/10.1016/S2213-8587\(17\)30138-9](https://doi.org/10.1016/S2213-8587(17)30138-9).
3. Bone HG, Bolognese MA, Yuen CK, et al. Effects of denosumab treatment and discontinuation on bone mineral density and bone turnover markers in postmenopausal women with low bone mass. *J Clin Endocrinol Metab.* 2011;96(4):972–980. <https://doi.org/10.1210/jc.2010-1502>.
4. Sølling AS, Harsløf T, Langdahl B. Treatment with Zoledronate Subsequent to Denosumab in Osteoporosis: a Randomized Trial. *J Bone Miner Res.* 2020;35(10):1858–1870. <https://doi.org/10.1002/jbmr.4098>.
5. Anastasilakis AD, Papapoulos SE, Polyzos SA, Appelman-Dijkstra NM, Makras P. Zoledronate for the prevention of bone loss in women discontinuing denosumab treatment. a prospective 2-year clinical trial. *J Bone Miner Res.* 2019;34(12):2220–2228. <https://doi.org/10.1002/jbmr.3853>.
6. Anastasilakis AD, Polyzos SA, Yavropoulou MP, et al. Comparative effect of zoledronate at 6 versus 18 months following denosumab discontinuation. *Calcif Tissue Int.* 2021;108(5):587–594. <https://doi.org/10.1007/s00223-020-00785-1>.
7. Everts-Graber J, Reichenbach S, Ziswiler HR, Studer U, Lehmann T. A single infusion of zoledronate in postmenopausal women following denosumab discontinuation results in partial conservation of bone mass gains. *J Bone Miner Res.* 2020;35(7):1207–1215. <https://doi.org/10.1002/jbmr.3962>.
8. Anastasilakis AD, Polyzos SA, Makras P, Aubry-Rozier B, Kaouri S, Lamy O. Clinical features of 24 patients with rebound-associated vertebral fractures after denosumab discontinuation: systematic review and additional cases. *J Bone Miner Res.* 2017;32(6):1291–1296. <https://doi.org/10.1002/jbmr.3110>.
9. Burckhardt P, Faouzi M, Buclin T, Lamy O, The Swiss Denosumab Study G. Fractures after denosumab discontinuation: a retrospective study of 797 cases. *J Bone Miner Res.* 2021;36(9):1717–1728. <https://doi.org/10.1002/jbmr.4335>.
10. McDonald MM, Khoo WH, Ng PY, et al. Osteoclasts recycle via osteomorphs during RANKL-stimulated bone resorption. *Cell.* 2021;184(5):1330–47.e13. <https://doi.org/10.1016/j.cell.2021.02.002>.
11. McDonald MM, Morse A, Mikulec K, et al. Matrix metalloproteinase-driven endochondral fracture union proceeds independently of osteoclast activity. *J Bone Miner Res.* 2013;28(7):1550–1560. <https://doi.org/10.1002/jbmr.1889>.

12. Dempster DW, Compston JE, Drezner MK, et al. Standardized nomenclature, symbols, and units for bone histomorphometry: a 2012 update of the report of the ASBMR Histomorphometry Nomenclature Committee. *J Bone Miner Res.* 2013;28(1):2–17. <https://doi.org/10.1002/jbmr.1805>.
13. Livak KJ, Schmittgen TD. Analysis of relative gene expression data using real-time quantitative PCR and the 2- $\Delta\Delta$ CT method. *Methods.* 2001;25(4):402–408. <https://doi.org/10.1006/meth.2001.1262>.
14. Bossen C, Ingold K, Tardivel A, et al. Interactions of tumor necrosis factor (TNF) and TNF receptor family members in the mouse and human. *J Biol Chem.* 2006;281(20):13964–13971. <https://doi.org/10.1074/jbc.M601553200>.
15. Morony S, Warmington K, Adamu S, et al. The inhibition of RANKL causes greater suppression of bone resorption and hypercalcemia compared with bisphosphonates in two models of humoral hypercalcemia of malignancy. *Endocrinology.* 2005;146(8):3235–3243. <https://doi.org/10.1210/en.2004-1583>.
16. Samadifam R, Xia Q, Goltzman D. Co-treatment of PTH with osteoprotegerin or alendronate increases its anabolic effect on the skeleton of oophorectomized mice. *J Bone Miner Res.* 2007;22(1):55–63. <https://doi.org/10.1359/jbmr.060915>.
17. McClung MR, Wagman RB, Miller PD, Wang A, Lewiecki EM. Observations following discontinuation of long-term denosumab therapy. *Osteoporos Int.* 2017;28(5):1723–1732. <https://doi.org/10.1007/s00198-017-3919-1>.
18. Everts-Graber J, Reichenbach S, Gahl B, Ziswiler HR, Studer U, Lehmann T. Risk factors for vertebral fractures and bone loss after denosumab discontinuation: A real-world observational study. *Bone.* 2021;144(1):115830. <https://doi.org/10.1016/j.bone.2020.115830>.
19. Brown JP, Dempster DW, Ding B, et al. Bone remodeling in postmenopausal women who discontinued denosumab treatment: off-treatment biopsy study. *J Bone Miner Res.* 2011;26(11):2737–2744. <https://doi.org/10.1002/jbmr.448>.
20. Vasikaran S, Eastell R, Bruyère O, et al. Markers of bone turnover for the prediction of fracture risk and monitoring of osteoporosis treatment: a need for international reference standards. *Osteoporos Int.* 2011;22(2):391–420. <https://doi.org/10.1007/s00198-010-1501-1>.
21. Mira-Pascual L, Patlaka C, Desai S, et al. A novel sandwich ELISA for tartrate-resistant acid phosphatase 5a and 5b protein reveals that both isoforms are secreted by differentiating osteoclasts and correlate to the type I collagen degradation marker CTX-I in vivo and in vitro. *Calcif Tissue Int.* 2020;106(2):194–207. <https://doi.org/10.1007/s00223-019-00618-w>.
22. Janckila AJ, Yam LT. Biology and clinical significance of tartrate-resistant acid phosphatases: new perspectives on an old enzyme. *Calcif Tissue Int.* 2009;85(6):465–483. <https://doi.org/10.1007/s00223-009-9309-8>.
23. Fu Q, Bustamante-Gomez NC, Reyes-Pardo H, et al. Reduced OPG expression by osteocytes may contribute to rebound resorption after denosumab discontinuation. *JCI insight.* 2023;8(18). <https://doi.org/10.1172/jci.insight.167790>.
24. Nenonen A, Cheng S, Ivaska KK, et al. Serum TRACP 5b is a useful marker for monitoring alendronate treatment: comparison with other markers of bone turnover. *J Bone Miner Res.* 2005;20(10):1804–1812. <https://doi.org/10.1359/JBMR.050403>.
25. Mori Y, Kasai H, Ose A, et al. Modeling and simulation of bone mineral density in Japanese osteoporosis patients treated with zoledronic acid using tartrate-resistant acid phosphatase 5b, a bone resorption marker. *Osteoporos Int.* 2018;29(5):1155–1163. <https://doi.org/10.1007/s00198-018-4376-1>.
26. Sølling AS, Harsløf T, Jørgensen NR, Langdahl B. Changes in RANKL and TRAcP 5b after discontinuation of denosumab suggest RANKL mediated formation of osteoclasts results in the increased bone resorption. *Osteoporos Int.* 2023;34(3):599–605. <https://doi.org/10.1007/s00198-022-06651-0>.
27. Gossiel F, Ugur A, Peel N, Walsh J, Eastell R. The clinical utility of TRACP-5b to monitor anti-resorptive treatments of osteoporosis. *Osteoporos Int.* 2022;33(6):1357–1363. <https://doi.org/10.1007/s00198-022-06311-3>.
28. Fassio A, Adami G, Benini C, et al. Changes in Dkk-1, sclerostin, and RANKL serum levels following discontinuation of long-term denosumab treatment in postmenopausal women. *Bone.* 2019;123(1):191–195. <https://doi.org/10.1016/j.bone.2019.03.019>.
29. Fontalis A, Gossiel F, Schini M, Walsh J, Eastell R. The effect of denosumab treatment on osteoclast precursor cells in postmenopausal osteoporosis. *Bone Reports.* 2020;13(Supplement):100457. <https://doi.org/10.1016/j.bonr.2020.100457>.
30. Kim AS, Girgis CM, McDonald MM. Osteoclast recycling and the rebound phenomenon following denosumab discontinuation. *Curr Osteoporos Rep.* 2022;20(6):505–515. <https://doi.org/10.1007/s11914-022-00756-5>.
31. Kostenuik PJ, Nguyen HQ, McCabe J, et al. Denosumab, a fully human monoclonal antibody to RANKL, inhibits bone resorption and increases BMD in knock-in mice that express chimeric (murine/human) RANKL. *J Bone Miner Res.* 2009;24(2):182–195. <https://doi.org/10.1359/jbmr.081112>.
32. Tremollieres F, Pouilles J-M, Ribot C. Withdrawal of hormone replacement therapy is associated with significant vertebral bone loss in postmenopausal women. *Osteoporos Int.* 2001;12(5):385–390. <https://doi.org/10.1007/s001980170107>.
33. Naylor K, Clowes J, Finigan J, Paggiosi M, Peel N, Eastell R. The effect of cessation of raloxifene treatment on bone turnover in postmenopausal women. *Bone.* 2010;46(3):592–597. <https://doi.org/10.1016/j.bone.2009.10.043>.
34. Eisman JA, Bone HG, Hosking DJ, et al. Odanacatib in the treatment of postmenopausal women with low bone mineral density: three-year continued therapy and resolution of effect. *J Bone Miner Res.* 2011;26(2):242–251. <https://doi.org/10.1002/jbmr.212>.
35. McClung MR, Brown JP, Diez-Perez A, et al. Effects of 24 months of treatment with romosozumab followed by 12 months of denosumab or placebo in postmenopausal women with low bone mineral density: a randomized, double-blind, phase 2, parallel group study. *J Bone Miner Res.* 2018;33(8):1397–1406. <https://doi.org/10.1002/jbmr.3452>.
36. Limaye A. Drishti: a volume exploration and presentation tool. *Developments in X-ray Tomography VIII.* SPIE, 2012;8506:191–199. <https://doi.org/10.1117/12.935640>.

Denosumab Discontinuation in the Clinic: Implications of Rebound Bone Turnover and Emerging Strategies to Prevent Bone Loss and Fractures

Shejil KUMAR*^{1,2,3}, Mawson WANG*^{1,3,4}, Albert S KIM^{1,5,7}, Jacqueline R CENTER^{5,6,8}, Michelle M MCDONALD^{5,7} Christian M GIRGIS^{1,3}

*** Joint first authors**

- 1. Department of Diabetes & Endocrinology, Westmead Hospital, Sydney, Australia**
- 2. Department of Diabetes & Endocrinology, Royal North Shore Hospital, Sydney, Australia**
- 3. Faculty of Medicine & Health, University of Sydney, Sydney, Australia**
- 4. Department of Diabetes & Endocrinology, Concord Repatriation General Hospital, Sydney, Australia**
- 5. Faculty of Medicine and Health, University of New South Wales, Sydney, Australia**
- 6. Garvan Institute of Medical Research, Sydney, Australia**
- 7. Cancer Ecosystems Theme, Garvan Institute of Medical Research, Sydney, Australia**
- 8. St Vincent's Hospital Clinical School, UNSW, Sydney, Australia**

© The Author(s) 2025. Published by Oxford University Press on behalf of the American Society for Bone and Mineral Research. All rights reserved. For permissions, please email: journals.permissions@oup.com

Corresponding author: Christian M GIRGIS

Christian.girgis@sydney.edu.au

Department of Diabetes & Endocrinology, Westmead Hospital, Cnr Hawkesbury Rd and Darcy Rd, NSW, Australia, 2145

Data availability statement: No datasets were generated in preparation for this manuscript.

Funding statement: The authors have no funding to disclose.

Conflict of interest disclosure: **Shejil Kumar** has received honoraria for advisory board participation from Kyowa Kirin and Sandoz. **Mawson Wang** has no conflicts of interest. **Albert S Kim** has no conflicts of interest. **Jacqueline R Center** has received honoraria for speaking engagements and advisory board participation from Amgen. **Michelle M McDonald** has received honoraria for speaking engagements and advisory board from Angitia Bio and AmgenIn. **Christian M Girgis** has received honoraria for speaking engagements and advisory board participation from Gedeon Richter, Kyowa Kirin and Sandoz.

Acknowledgement: The authors would like to acknowledge and thank Dr Matti Gild and Dr Sue-Lynn Lau for their valuable feedback and comments on Figure 3.

Abstract

Denosumab is a highly effective treatment for osteoporosis, and its long-term use is associated with incremental gains in bone mineral density (BMD) and sustained fracture risk reduction. Stopping denosumab, however, results in rebound increase in bone turnover, loss of treatment-associated BMD gains, and in the worst case, spontaneous vertebral fractures (VFs). Insights into the risk factors and the underlying mechanisms for rebound-associated bone loss and true incidence of rebound VFs are emerging. Conventional strategies using bisphosphonates to mitigate post-denosumab rebound display mixed success. Bisphosphonates may preserve bone

density following short-term denosumab but the optimal sequential approach after longer-term denosumab remains elusive. Patients at particular risk of are those with prevalent VFs or greater on-treatment BMD gains. To greater understand these risks and strategies to preserve bone after denosumab, an emerging body of translational and pre-clinical work is shedding new light on the biology of RANKL inhibition and withdrawal. Discovering an effective ‘exit strategy’ to control rebound bone turnover and avoid bone loss after denosumab will improve confidence amongst patients and clinicians in this highly effective and otherwise safe treatment for osteoporosis. This perspective characterizes the clinical problem of post-denosumab rebound, provides a comprehensive update on human studies examining the use of bisphosphonates following denosumab and explores mechanistic insights from pre-clinical studies that will be critical in the design of definitive human trials.

Keywords: Denosumab; Discontinuation; Rebound; Bone Turnover; Bone Mineral Density; Bone Resorption; Fracture; Bisphosphonates; Osteoporosis; Sequential therapy

Lay Summary

Osteoporosis is common and results in reduced bone strength (low bone density) and increased fracture risk. Denosumab is one of the most common osteoporosis medications proven to increase bone density and reduce fracture risk. Denosumab reduces the number of cells which break down bone (osteoclasts), however is only effective so long as treatment is continued. If denosumab is stopped, its beneficial effects on bone health are rapidly reversed. This ‘rebound effect’ involves a rapid increase in bone breakdown by osteoclasts, loss of all bone density improvement and sometimes cause spine fractures.

Several studies have explored whether switching to a bisphosphonate (another osteoporosis treatment) could prevent this rebound. Although these strategies work well when denosumab has been given for a short time, they are less effective after long-term denosumab use (> 3-years). Exciting new experiments in the laboratory are improving our understanding of the biology of osteoclasts and denosumab rebound which should help in finding a way to safely stop denosumab in the clinic. This would make doctors and patients more comfortable with using this highly effective treatment in the long-term.

In this article, we discuss the latest evidence regarding denosumab rebound and consider new innovative ways to tackle this problem.

“Pride goes before the fall... [the higher you go, the harder you fall]”

- Proverbs 16:18, paraphrased

Introduction

Osteoporosis affects over 200 million people globally and is characterized by low bone mass, deterioration in bone microarchitecture and increased risk of fragility fractures. Over the last 15 years, denosumab has become established in osteoporosis treatment algorithms worldwide.

Denosumab is a fully human monoclonal antibody which mimics endogenous actions of

osteoprotegerin (OPG), neutralizes receptor activator of nuclear factor- κ B ligand (RANKL), and thereby inhibits RANKL-mediated osteoclast differentiation and proliferation¹. Denosumab rapidly and exquisitely suppresses bone turnover, an effect sustained with ongoing use.

In the original pivotal trial, three years of denosumab effectively increased bone mineral density (BMD) by 9.2% at the lumbar spine (LS) and 6.0% at the total hip (TH) in postmenopausal women with osteoporosis, with significant lowering of fracture risk (68% reduction for vertebral, 40% for hip and 20% for non-vertebral fractures). BMD continued to increase and fracture risk reduction was maintained up to 10 years of use^{2,3}. Denosumab has also shown robust efficacy in the ‘real-world’ setting⁴ and several clinical indications beyond postmenopausal osteoporosis (**Table 1**)⁵⁻⁹. Long-term denosumab is safe, with an estimated 281 and 40 clinical fractures prevented for every case of atypical femur fracture (AFF) and osteonecrosis of the jaw (ONJ), respectively^{3,10}.

The potent therapeutic effects of denosumab are reversible, relating to the transient activity of this circulating monoclonal antibody on bone remodelling compartments, and subsequent clearance by the reticuloendothelial system and nonspecific endocytosis¹¹. Treatment discontinuation results in loss of the RANKL inhibitory effect and an exaggerated overshoot in bone turnover; the so-called *rebound phenomenon*^{12,13}. Hazardous effects of rebound include rapid losses of treatment-associated BMD gains and vertebral fractures (VFs)^{14,15}.

With increasing use of denosumab worldwide, clinicians are faced with challenging questions: How and when can we safely stop denosumab? Can denosumab be used as a treat-to-target agent which can then be safely maintained by a bisphosphonate? What is the safety of long-term use

beyond 10 years? In which patients should stopping denosumab be reconsidered? What is the role, if any, of osteoanabolic therapy in facilitating denosumab cessation?

To date, clinical studies have provided mixed answers to these critical questions, limited by the observational nature of studies. This article seeks to extrapolate from current clinical studies and draw on emerging pre-clinical insights into osteoclast biology to define the clinical equipoise and forge much needed guidance in the field. In understanding the rebound phenomenon with greater clarity, we could begin to surmise effective strategies to ‘safely control the rebound’ in the post-denosumab patient, improving the longevity of its clinical utility.

Understanding the Post-denosumab Rebound Phenomenon

Despite its long-term safety and efficacy, denosumab may be discontinued for a variety of reasons. Patients achieving treatment targets or those with adverse events such as hypocalcaemia may be advised to stop treatment¹⁶. Unintended treatment lapses are common¹⁷ as are misconceptions on the risk of rare side-effects. Conversely, bisphosphonates exhibit prolonged skeletal retention and thus do not result in a similar rebound phenomenon following discontinuation. In fact, supervised treatment breaks are a reasonable strategy to optimize the risk versus benefit profile with long-term bisphosphonate use¹⁸.

The *rebound phenomenon* is most pronounced in the first year following denosumab discontinuation, characterized by an exaggerated increase in bone turnover as evidenced by rising serum cross-linked C-telopeptide of type I collagen (CTX) coupled with procollagen type 1 N-propeptide (P1NP) concentrations^{13,19}. However, this rebound bone turnover is not simply a reversal of the antiresorptive effect. Rather, there is an early *overshoot* with serum CTX exceeding

pre-treatment values at 3 months post-discontinuation and peaking at 6 months (~70% greater than baseline), before returning to pre-treatment concentrations by 24 months^{13,19}. Patients typically experience rapid loss of all treatment-associated BMD gains at the LS and TH by 12 months, after which bone loss stabilizes and parallels that in untreated patients^{13,16,19,20} (**Figure 1**). Translational studies are uncovering the dynamic cellular and molecular biology underpinning the withdrawal of RANKL inhibition (see “**Mechanistic Insights and Future Directions**”).

Concerns that rapid bone loss may precipitate fractures were initially allayed by a post-hoc analysis of FREEDOM where discontinuing denosumab did not increase fracture rates versus discontinuing placebo²¹. However, early analyses were limited by the inclusion of short-term denosumab users only (≤ 5 doses), brief median follow-up of 8 months and lack of morphometric VF assessment. Several cases subsequently emerged of multiple spontaneous clinical VFs occurring on average 4-5 months following denosumab cessation^{22,23}. A further FREEDOM extension post-hoc analysis including ~1000 women with morphometric vertebral data showed that although annualized VF risk rebounded from 1.2% to 7.1% after ceasing denosumab, these rates did not exceed those in controls stopping placebo. However, in those who sustained VFs, the proportion with multiple VFs was higher after discontinuing denosumab (61% vs. 39%, $p=0.049$)¹⁵.

Taken together, clinical trials and observational studies suggest an upper risk threshold of rebound VFs of 10% in patients ceasing denosumab without subsequent bisphosphonate treatment²⁴⁻²⁶.

Whether this phenomenon represents an overshoot in fracture risk or a rapid return to baseline risk is worth considering. Do patients ceasing denosumab face a cumulatively greater fracture risk in the critical post-treatment phase than they would have otherwise faced if they never received treatment? The FREEDOM extension study, despite its limitations, suggests this may be the case

for **multiple** VFs but not necessarily for single VFs¹⁵. A large real-world database also suggested an increased, rebound risk for all fragility fractures after denosumab²⁶.

Another important question is why denosumab rebound appears to be more specifically associated with VFs, despite substantial BMD losses occurring also at the hip? Rapid changes in remodelling may exert differential effects across bone compartments in systemic conditions (e.g. immobilization, glucocorticoid or aromatase inhibitor therapy). This may be no different for the post-denosumab phase in which rebound bone turnover places the trabecular compartment at particular risk of microarchitectural deterioration and spontaneous fractures¹⁵. Apart from the relatively greater proportion of trabecular bone in vertebrae, spontaneous fractures occur here due to biomechanical and gravitational forces placed on the vertebral column during everyday activity. In the clinic, red flags for impending critical bone loss in patients stopping denosumab are an important consideration in stratifying the risk of life-altering VFs.

Rebound-associated Bone Loss and Vertebral Fractures: Risk factors and Red

Flags

A body of observational data posit a number of clinical risk factors for rebound-associated complications. These include prevalent history of VFs, longer denosumab treatment and greater BMD gains during treatment.

The most robust indicator for rebound-associated VFs is a **prevalent history of VFs** sustained before or during denosumab^{15,16,22}. This unsurprising risk factor, demonstrated by the post-hoc FREEDOM analysis, identifies a specific cohort of patients with critical background microarchitectural degradation. The distribution and morphology of rebound-associated VFs are

similar to osteoporotic VFs, but multiple VFs are over-represented during rebound, underlying the heightened microarchitectural instability in the more severe form of this phenomenon^{22,23}. VFs post-denosumab occur in the setting of exaggerated osteoclastogenesis with greater bone resorption and acute bone loss²⁷. Screening for prevalent VFs when considering denosumab cessation would therefore be prudent.

Longer denosumab treatment, particularly beyond 5 years, is associated with greater BMD loss, not only at the lumbar spine²⁸, but also at the hip²⁹, as opposed to patients treated for <2 years¹⁹. This may be explained by greater BMD gains with prolonged treatment and risk of greater absolute bone loss over a similar post-treatment period^{20,30,31}. Rebound bone turnover may also be *more exaggerated* after stopping longer-term denosumab, as indicated by higher CTx levels^{28,30,31}. Longer denosumab treatment >2-3 years also predicted subsequent VFs in a post-hoc analysis of FREEDOM and case series^{14,22}. Following denosumab discontinuation, there is a cumulative increased risk of multiple VFs with each year off-treatment and with greater losses in total hip BMD^{14,15}.

Greater BMD gains on treatment was an important risk factor for significant post-denosumab bone loss in post-hoc analyses of FREEDOM and other studies^{20,30,31}, which persisted after adjusting for treatment duration^{29,30}. In a recent retrospective study, patients with persistent high bone turnover requiring sequential zoledronic acid post-denosumab cessation had greater on-treatment BMD gains in LS and femoral neck (FN) despite similar duration of denosumab use²⁹. These studies have not defined a threshold of BMD gain beyond which there is increased risk of post-denosumab bone loss but emphasizes the principle that greater gains lead to greater falls. Interestingly, in another study, despite having greater BMD gains, patients who experienced post-denosumab bone loss still had significantly lower LS BMD values at the time of cessation

compared to those who did not experience bone loss³¹. These patients also had lower LS BMD at treatment initiation. Hence, it remains unclear whether greater on-treatment BMD gains is an independent risk factor for rebound bone loss, or whether this relationship is mediated by longer duration of treatment or regression to a more severely osteoporotic setpoint. Regardless, clinicians should review pre-denosumab BMD results to ascertain on-treatment BMD gains to assist in risk stratification prior to considering or planning treatment withdrawal. Potential theories underpinning the relationship between greater BMD gains and subsequent BMD loss are explored later (see “**Mechanistic Insights and Future Directions**”).

Other baseline risk factors for BMD loss following denosumab cessation included younger age^{28,30,31}, lower baseline LS BMD³¹, higher baseline CTx³¹, lower bodyweight or BMI^{30,32} and lack of preceding osteoporosis treatment³⁰. Younger perimenopausal females, including those receiving aromatase inhibitors, may represent a higher risk cohort with higher baseline CTx and more dynamic bone turnover²³. The presence of CKD (eGFR <60 mL/min) and history of parental hip fracture were both associated with doubling of VF risk in separate studies^{24,26}. Due to the prolonged anti-osteoclastic action of bisphosphonates, exposure prior to denosumab was hypothesized to protect against rebound-associated VFs. However, this was only supported by two retrospective studies^{22,24}, but not in a large registry-based study²⁶.

Table 2 summarizes risk factors for VFs and/or BMD loss and may help clinicians in formulating an individualized risk assessment in patients considering denosumab withdrawal. The main limitation is that these risk factors are derived from retrospective data rather than prospective, controlled studies.

Strategies to Mitigate Rebound after Denosumab Cessation

In patients ceasing denosumab without subsequent bisphosphonate therapy, BMD rapidly reverts back to baseline^{16,19,20} with an elevation in VF risk^{30,33}. Thus, sequential treatment regimens following denosumab have been examined for their efficacy in attenuating the rebound phenomenon and its clinical consequences. Duration of denosumab is the single greatest factor that influences the efficacy of these strategies. Most studies have focused on stopping short-term denosumab (≤ 2.5 -3.0 years). Higher risk patients ceasing medium-to-long term denosumab (> 2.5 -3.0 years) represent a particularly challenging group in whom standard approaches using bisphosphonates offer mixed success.

Mitigating denosumab rebound after short-term use

Various studies have examined strategies to address cessation of short-term denosumab (< 2.5 years). The majority are retrospective in nature and lack adequate control groups (**Table 3**). A single infusion of zoledronic acid was effective in three prospective studies and in several small retrospective studies to maintain or preserve majority of BMD gains at the spine and hip after short-term denosumab^{32,34-40}. The durability of this approach was also demonstrated in a 5-year extension of an open-label prospective study (AfterDmab) in which approximately half of the patients had maintenance of BMD following a single dose of zoledronic acid after a 2.5 year denosumab course^{34,41}. If repeat zoledronic acid treatment was required, this was typically at the 3-year mark post denosumab cessation. Hip BMD and majority of spine BMD were also maintained 27-months after a single zoledronic acid infusion in another prospective study following 12-months denosumab (overlapped with 9-months teriparatide)⁴⁰.

Alendronate also appears to be an effective alternative to maintain BMD after short-term denosumab. Two RCTs provided reassurance that after one-year denosumab, short-term

alendronate maintained BMD gains and suppressed bone turnover. However, inter-individual variability was significant^{42,43}. BMD maintenance after ceasing alendronate was demonstrated in a small extension study, however patients were excluded if they had significant BMD loss during alendronate⁴⁴.

Although direct comparisons between bisphosphonate strategies are sparse, one real-world study found similar efficacy of alendronate (n=34) and zoledronic acid (n=32) in preserving BMD gains following an average 2.5-3.0 years of denosumab, whilst risedronate (n=22) was relatively less effective with loss of half BMD gains³⁷. This is consistent with a small case series of subjects exiting the FRAME trial (n=5) in which a similar proportion of BMD gains were lost after transitioning from denosumab (2 years) to risedronate (1-2 years)⁴⁵. Another small study found that risedronate had no effect on the initial early phase of rebound-associated bone loss⁴⁶.

Raloxifene, a selective oestrogen receptor modulator (SERM), has also demonstrated suboptimal efficacy in this context. In one prospective study, raloxifene resulted in ~50% loss of BMD gains at the spine and total hip despite only 1 year of denosumab, while femoral neck BMD was maintained⁴³. Two observational studies of raloxifene use post-denosumab demonstrated BMD losses at all sites^{47,48}. One real-world study reported the development of clinical VFs (~20%) in patients on raloxifene after discontinuing short-term denosumab³⁸.

Therefore, oral alendronate and intravenous zoledronic acid appear to be the more effective treatment approaches following a short course of denosumab. However, direct comparisons are not possible with existing data; a high degree of inter-individual variability exists and there remains uncertainty around long-term retention of effect after a single treatment course. Greater detail on these studies and others can be found in **Table 3**.

Mitigating denosumab rebound after medium-to-long term use

Longer-term treatment with denosumab poses the risk of more significant rebound with greater absolute bone loss during the critical withdrawal phase. Mitigating rebound after longer denosumab use thus poses unique challenges and requires greater focus in prospective clinical studies (**Table 4**).

The body of evidence suggests that a single dose of intravenous zoledronic acid after medium-term denosumab use preserves only up to half of BMD gains. A multicenter prospective cohort study (n=47) followed women for 1 year after a single zoledronic acid dose after stopping ≤ 3 or >3 years denosumab. Duration of denosumab strongly influenced efficacy of zoledronic acid in preserving BMD. Spine BMD was maintained after short-term denosumab but declined by $\sim 7\%$ in those with longer exposure⁴⁹. Greater BMD loss after >3 years denosumab despite a single dose of sequential zoledronic acid was also demonstrated in a sub-hoc analysis of an RCT³². In the only RCT assessing its use after longer-term denosumab (ZOLARMAB, n=61), zoledronic acid commenced at various timepoints after stopping ~ 5 years denosumab resulted in $\sim 3\text{-}4\%$ BMD decline from the end of denosumab treatment at multiple skeletal sites²⁸. However, data on baseline BMD prior to denosumab initiation were not available, and thus the proportion of treatment-related BMD gains preserved with zoledronic acid could not be quantified. An extension study demonstrated that bone loss was stable in the second year post-denosumab withdrawal, highlighting the importance of close follow-up during the first year⁵⁰.

Retrospective studies also suggest limited BMD preservation with a single dose of zoledronic acid after longer denosumab exposure $>2.5\text{-}3.0$ years^{39,51,52}. In contrast, one retrospective study

reported BMD maintenance in patients receiving either alendronate or zoledronic acid after >2.5 years denosumab (mean 4 years)³⁷. Importantly, these patients had achieved osteopenia at the time of the denosumab-to-bisphosphonate sequence, raising the potential success of a treat-to-target strategy. Two other observational studies reported partial BMD preservation with zoledronic acid after medium-term denosumab. However, there are various limitations of these data including small sample sizes, heterogeneity in treatment schedules, and combined reporting of oral and intravenous bisphosphonates^{16,30}.

Independent of effects on BMD, another study (n=120) demonstrated the efficacy of bisphosphonates, either alendronate or zoledronic acid, in almost quartering the incidence of post-denosumab VFs from 21.1% in those without follow-on treatment to 5.5%³³. VF incidence was independently associated with lack of subsequent bisphosphonates but not with duration of prior denosumab use or prevalent VFs.

The question of optimal sequence after longer-term denosumab (>5 years) is yet more challenging^{28,53}. Six women followed up after completing FREEDOM extension had one dose of zoledronic acid after 7 years denosumab and lost half of LS BMD gains and all of TH BMD gains within the next 2 years⁵³. A real-world study (n=282) provides a hint in suggesting repeat doses of zoledronic acid in short succession may be required to achieve a similar degree of BMD preservation in patients on longer-term denosumab (mean 7.5 years) compared to those on short-to-medium term use⁵¹.

To summarize, bisphosphonates may prevent VFs in patients ceasing denosumab after medium and long-term use, although BMD invariably declines with the various bisphosphonate strategies

and at best, there is partial retention of BMD effect with repeated infusions of zoledronic acid. Complete preservation of BMD in this group is not a consistent finding and patients seeking to stop denosumab after medium to long-term use should expect a degree of bone loss. Further detail on these studies can be found in **Table 4**. Strategies to preserve BMD after >8 years of denosumab have not been examined by any study at this stage, and this evidence-free zone creates uncertainty, particularly as denosumab safety data do not exceed 10 years. A greater understanding of the pharmacobiology of RANKL inhibition and novel strategies to address this are urgently needed for this growing group of patients.

Mechanistic Insights and Future Directions

The latest understanding of cellular biology of denosumab treatment and withdrawal are discussed in the following section. We have also outlined pathways where current and future treatments aim to target rebound bone turnover (**Figures 2 and 3**) which are discussed further in this section.

Long-term denosumab and osteoclast precursors

It remains uncertain why longer denosumab exposure leads to greater difficulty in abating rebound. Pre-clinical studies have recapitulated the rebound phenomenon in normal and ovariectomized mice, a model of post-menopausal osteoporosis^{12,54,55}, and raised several hypotheses for this clinical observation. Prolonged RANKL inhibition may induce a pool of osteoclast precursors, which, after treatment withdrawal, are primed to undergo rapid differentiation and fusion into active osteoclasts^{12,56,57} (**Figure 2B-C**). In contrast, decreases or no changes are observed with bisphosphonate treatment in osteoclast precursor populations^{57,58}. An accumulation of TRAP+

mononuclear cells within the bone marrow may also occur in response to denosumab, another potential source of rapid osteoclast differentiation following treatment withdrawal⁵⁹.

Intravital imaging in mice demonstrated novel evidence for osteoclast recycling, such that osteoclasts appear to undergo fission into newly described ‘osteomorphs’ during prolonged RANKL inhibition which can later re-fuse into active osteoclasts at treatment withdrawal⁵⁶ (**Figure 2C**). However, the presence of osteomorphs in humans is yet to be validated and two small clinical studies suggested rising osteoclast precursors may not be exclusive to denosumab treatment and that serum TRAP concentrations at the end of the dosing interval were not higher during prolonged versus shorter denosumab treatment^{60,61}.

Dysregulated RANKL/OPG signalling may also be implicated in the rebound phenomenon. A humanized RANKL mouse model demonstrated reduced osteocytic OPG expression during prolonged denosumab, which the authors hypothesized was an indirect consequence of suppressed bone turnover⁶². A model utilizing mouse anti-RANKL antibody showed an accumulation of RANKL-bearing extracellular vesicles with treatment, reflected by high circulating RANKL levels, capable of triggering an ‘osteoclastic burst’ following the offset of treatment effect⁵⁷. In humans, elevated serum RANKL concentrations have been reported six months post-denosumab⁶³. In our murine model of rebound, tissue levels of RANKL rose at the end of the therapeutic effect of OPG, reaching over 1000-fold higher than control mice just prior to the significant bone loss that then characterized the withdrawal period⁵⁵.

Longer denosumab exposure may thus lead to a greater pool of osteoclast precursors and heightened tissue levels of RANKL which, following withdrawal, drives greater bone turnover and more critical bone loss (**Figure 2C**). Understanding the chronobiology of these cellular and molecular changes through further pre-clinical studies will lead to better informed, more timely sequential approaches.

Links between on-treatment bone density gains and rebound bone loss

Several studies indicate greater BMD gains during denosumab predict greater rebound BMD loss. Two studies suggest this relationship is not fully explained by a longer period of denosumab exposure^{29,30}. Higher baseline bone turnover may be another confounder for this relationship, as this may result in greater BMD response to treatment but also reversion to a more severe skeletal phenotype after treatment cessation. However, studies exploring this hypothesis are sparse and conflicting. Higher (pre-denosumab) baseline CTx was shown to univariately correlate with rebound bone loss in one study³¹. However these patients had a more severe phenotype (younger, lower baseline BMD) and so there were likely various unadjusted confounding factors. This same relationship was not shown in another prospective study⁴⁰.

Rebound bone loss is a state of particularly high bone turnover and one study showed rapid BMD gains when denosumab was recommenced in this setting, surpassing that seen during initial denosumab treatment¹³. Further studies are required to determine which factors, including baseline bone turnover, may predict BMD response to denosumab and subsequent degree of bone loss after discontinuation.

In earlier studies, denosumab cessation without follow-on treatment resulted in BMD decline back to baseline, potentially to a pre-existing bone mass 'setpoint'. Of interest is the possible involvement of a 'mechanostat' whereby osteocytes respond to local mechanical loads driving BMD back to baseline levels⁶⁴. As an adaptive response to load, osteocytes reduce sclerostin release and increase OPG release to increase bone formation and suppress bone resorption⁶⁵. In the setting of denosumab treatment, RANKL levels are elevated in both humans and mouse models, and OPG levels are reduced in RANKL humanized mice treated with denosumab or C57bkl6 mice treated with OPG:Fc^{62,66}. In patients on denosumab, sclerostin levels are increased and Dkk1 levels decreased⁶⁷. These data suggest denosumab therapy dysregulates mechanosensing pathways which typically regulate bone mass, leading to a load-independent net increase in bone mass. Upon withdrawal of RANKL it is therefore possible that mechanostat pathways reinitiate a high level of bone turnover to return bone mass back to baseline. To support this concept we have shown that upon withdrawal of RANKL inhibition in mice, RANKL levels increase up to 15-fold prior to bone loss⁵⁵. Further pre-clinical studies are needed to determine whether changes in OPG, Dkk1 and sclerostin occur during rebound bone loss to confirm their contributions to this "mechanostat" reset of bone mass. However, the mechanostat, in theory, is not exclusive to post-denosumab bone loss and could be implicated in more gradual withdrawal of BMD gains seen after stopping any reversible osteoporosis treatment. Further, whether bone targeted weight-bearing resistance exercise in addition to sequential therapy could curb rebound bone loss following denosumab has not been studied and may warrant investigation.

'Waves of bone resorption' and timing bisphosphonate doses

How soon should bisphosphonates be commenced to maintain BMD and minimise VF risk following denosumab? Existing clinical evidence suggests this should not be delayed beyond 6 months. The ZOLARMAB study assessed the effect of zoledronic acid at three timepoints: 6 months, 9 months, or when CTx rose to 1.5x the upper reference limit for postmenopausal women and elderly men²⁸. Similar BMD losses occurred regardless of timing, suggesting no benefit to delaying zoledronic acid treatment beyond 6 months. Furthermore, clinical studies indicate rebound VFs may occur as early as 8-9 months after the last denosumab dose, particularly in patients withdrawing from longer-term denosumab^{22,24}.

Our pre-clinical work and that of others demonstrate an early rise in RANKL and TRAP, preceding changes in P1NP and CTx, suggesting even earlier treatment before 6 months may be necessary (**Figure 3**)^{56,62}. Indeed, using our pre-clinical model of denosumab discontinuation, we have recently shown that earlier administration of zoledronic acid, prior to the offset of RANKL inhibition, was able to prevent BMD loss and improved trabecular bone microarchitecture⁶⁸. An overlapping sequential approach between denosumab and bisphosphonates for higher-risk patients may be warranted to prevent the early onset of microarchitectural deterioration^{22,24}.

Understanding differences in the mechanism of action of bisphosphonates versus denosumab is critically important in defining optimal sequencing with these agents. Bisphosphonates primarily target and inhibit osteoclast function upon their engulfment from bone and, unlike denosumab, have little to no impact on osteoclast *formation* (**Figure 2D**). Bisphosphonates therefore may *not* be able to mitigate the rapid flow of osteoclast precursors into newly differentiated osteoclasts (**Figure 3**). It is uncertain whether combining both agents, possibly in alternating doses, could

provide an even more effective approach in extreme cases of rebound. Early evidence for such a strategy is seen in a recent case report in which alternating denosumab and pamidronate in a child with osteogenesis imperfecta type 4 controlled his severe withdrawal rebound phenomenon⁶⁹. However, this approach is untested in adults with osteoporosis. In contrast, tapering of denosumab without intervening bisphosphonates, failed to preserve BMD in a small group of subjects with osteoporosis, but this approach also warrants further investigation (**Figure 2D**)⁷⁰.

The binding of a single dose of bisphosphonates is limited to the bone surfaces available at that point in time. Hence the exacerbated osteoclast formation and activity which takes place during denosumab withdrawal may rapidly expose new unbound surfaces for subsequent osteoclastic resorption. Multiple and regular doses of zoledronic acid may therefore be required to control 'waves of resorption' after longer-term denosumab (**Figure 3**). Indeed, in mice with the complete absence of OPG (-/-) and hence an abundance of osteoclasts, zoledronic acid was less effective in protecting bone mass than in mice with reduced OPG (+/-), suggesting that a single dose of zoledronic acid is inadequate during unregulated osteoclast formation⁷¹. We recently showed that multiple doses of zoledronate, specifically an 'early dose' prior to rise in serum bone turnover markers and a repeat dose during anticipated rebound BMD loss, was able to consolidate BMD gains made during RANKL inhibition and prevent rebound overshoot in osteoclast-mediated bone resorption⁶⁸. Whether these effects are also observed in humans need validation through a clinical trial. The lack of durability of a single dose in humans was highlighted in ZOLARMAB where serum bone turnover increased towards the upper reference limit within 6 months post-zoledronic acid infusion²⁸. Repeated infusions appeared to suppress this rising bone turnover although bone

density declined regardless, potentially suggesting sequential treatment may only be effective if initiated at an optimal threshold of bone turnover (**Figure 3**).

In a recent retrospective study, two doses of zoledronic acid were administered in patients following a mean of 4 years denosumab: the first dose at 6 months and second dose if bone turnover markers increased 6 months later, as supported by current guidelines⁷². Intriguingly, the subgroup of patients who had increased bone turnover at 6 months (CTx > mean reference-range) showed a trend for greater BMD gains on treatment, and despite a second dose of zoledronic acid, lost 5% BMD at spine and alarmingly 10% of this group experienced VFs²⁹. Conversely, achieving CTx below this threshold 6 months after an initial zoledronic acid dose was a reliable indicator for subsequent BMD preservation. This strategy of administering a second dose of zoledronic acid once CTx rises above the mid reference-range, as advocated by current guidelines⁷², may not be effective in a higher risk subgroup. Thus, we advocate clear documentation of BMD gains on treatment before considering denosumab withdrawal for risk stratification (**Figure 4**).

Additional pre-clinical studies examining the impact of denosumab treatment duration, timing of sequential bisphosphonates or the utility of repeated bisphosphonate doses combined with tapered denosumab withdrawal on rebound bone loss are important to define the optimal sequencing approach. It is also important to consider that factors involving other cells, and not just osteoclasts on active remodelling surfaces, may also be at play.

Osteocytes, osteoblasts and osteoanabolic therapy

Pre-clinical work supports a complex interplay of osteocyte and osteoblast dysregulation in the rebound phenomenon. Importantly, osteocytes also express RANKL and its transgenic deletion in these cells leads to significant osteopetrosis in rodents⁷³. In physiological states, osteocyte-derived RANKL attracts osteoclasts to resorb micro-fractures and drive local bone repair. Hence, with prolonged denosumab, micro-fractures may accumulate and the osteocyte mechano-sensory apparatus may be compromised⁷⁴. Local RANKL produced by *both* osteocytes and osteoblasts may promote osteoclastogenesis to different extents during rebound and perhaps at distinctly different timepoints, adding to the complexity of the pro-resorptive state following denosumab withdrawal.

Depletion of osteoblasts at remodelling surfaces occurs during prolonged periods of denosumab treatment due to a loss of coupling signals from the absence of osteoclasts⁶⁴. As established sources of OPG, the absence of osteoblasts, during the early stages of denosumab withdrawal, have also been implicated in the rebound phenomenon (**Figure 2C**). Mice treated with anti-RANKL antibody displayed sustained deficits in osteoblast progenitors, suggesting that suppression of bone formation following treatment withdrawal was due to both a loss of coupling signal and a decrease in osteoblastic lineage cells⁵⁷.

In humanized RANKL mice treated with denosumab, rising levels of RANKL and TRAP5b preceded an increase in OPG following denosumab withdrawal, indicating a greater initial osteoclastic response (\uparrow RANKL/OPG ratio), with osteoblastogenesis lagging behind⁶². Furthermore, production of OPG by “young” osteocytes was also markedly reduced during the early stages of denosumab withdrawal in these mice, implicating osteocytes in the rebound

phenomenon also. In a clinical study of bone biopsies from patients treated with denosumab, osteocyte viability was decreased during denosumab and this persisted during discontinuation⁷⁵. Together with the fact that osteocytes can signal adjacent osteocytes to produce RANKL, it is likely osteocytes play a key role during denosumab withdrawal bone loss⁷⁶. Thus, uncoupling or delayed coupling of osteoclast-osteoblast activity and altered osteocyte signalling in the rebound milieu drives greater resorptive versus anabolic activity. Targeting this ‘uncoupling’ or altered osteocyte and osteoblast signalling may provide novel approaches to managing denosumab withdrawal (**Figure 2D**).

Could a course of osteoanabolic therapy be an answer? Clinical studies have examined this and highlight once again the difficulty of sequencing from denosumab to *any other* agent. These studies predominantly investigated transitioning from denosumab to osteoanabolic treatments to maximise BMD gains during long-term denosumab, rather than to facilitate denosumab cessation. However, insights can still be derived from these treatment sequences involving denosumab. Switching to teriparatide results in exaggerated bone turnover and early rapid bone loss particularly at the hip⁷⁷. This may relate to heightened local RANKL, driven both by PTH activity and denosumab withdrawal, with preferentially deleterious impacts on cortical bone⁷⁸. Indeed, the increase in bone turnover in patients ceasing denosumab is exacerbated by teriparatide⁷⁷. Conversely, transitioning from at least one year of denosumab to romosozumab has resulted in modest BMD gains at the spine (~5%) and maintenance at the hip in several clinical studies (n=163 total patients), despite rising bone turnover during this sequence⁷⁹⁻⁸². However, individual patient responses were highly variable in these studies with the potential for bone loss in patients sequencing directly from long-term denosumab to romosozumab. Given bisphosphonates have

been shown to maintain BMD gains after romosozumab, a denosumab-to-romosozumab-to-bisphosphonate sequence may have a role in mitigating rebound bone loss, although has not specifically been studied. Further, romosozumab is clinically indicated in patients with more severe osteoporosis who may not be suitable for planned denosumab cessation. Early clinical evidence suggests overlapping, combined treatment approaches involving denosumab and romosozumab may be more effective than directly sequencing from denosumab^{83,84}. In our work using an overlapping approach, romosozumab was able to overcome the suppressive effect of denosumab on osteoblast function, as indicated by P1NP levels, however the inevitable increase in CTx following denosumab withdrawal was not controlled by romosozumab⁸³. These strategies require further investigation in prospective controlled studies.

Inflammation, catabolism and the acute-phase reaction

Amongst currently available osteoporosis treatments, denosumab is unique in its ability to progressively increase BMD out to the maximal studied duration of 10 years, with sustained fracture risk reduction. Bisphosphonates reach a plateau in the BMD response and osteoanabolic agents, particularly PTH analogues, have demonstrated an ‘anabolic window’ beyond which further gains are limited. The biological basis of the steady rise in BMD with continued denosumab use may hold important clues for the inevitable bone loss in the rebound, post-denosumab phase. To echo the famous words of Proverbs ‘*pride goeth before a fall*’ and, as shown in this perspective piece, an important precursor for eventful rebound bone loss is a greater BMD response achieved with denosumab. Specific effects on alterations in bone mineralization and biological changes at the cellular level of osteoclast response and activation could hold the keys⁸⁵.

Osteoclasts do not live in isolation. They are an active cellular species, with dynamic, chronologic changes and as discussed, may separate into smaller cell types (osteomorphs) to later drive further bone resorption in regions separated in time and space. They are members of the monocyte/macrophage lineage and inflammatory and immune-mediated components of the post-denosumab rebound may also play an important but as yet undetermined role. Indeed, increased common lymphoid and myeloid progenitors cells as well as higher interleukin-6 and granulocyte colony stimulating factor have been observed in mice treated with anti-RANKL antibody⁵⁷. Interestingly, two studies reported high rates of acute phase reaction following a dose of zoledronic acid in the post-denosumab setting, raising intriguing questions about the role of T-cell dynamics, cytokine release and a potential pro-inflammatory state in patients withdrawing from denosumab with potential flow-on effects to bone^{28,34}.

Systemic disorders which drive inflammatory and catabolic pathways may further heighten the rebound phase. A recent case report published in this journal highlighted newly diagnosed thyrotoxicosis as an exacerbating factor of a severe post-denosumab rebound in a 47-year-old female⁸⁶. This report cautioned clinicians to exclude secondary cases of bone loss in patients withdrawing from denosumab. On a basic level, the potential role of nuclear receptors, such as the thyroid hormone receptor, and other pathways in their modulation of osteoclast activity following denosumab withdrawal was raised.

Conclusions

Denosumab is a highly effective antiresorptive treatment. However, clinicians need to be aware of its Achilles heel; that its withdrawal results in rapid onset of rebound characterized not just by

reversal of treatment effect, but an overshoot in bone turnover, rapid loss of treatment-related BMD gains and increase in VF risk. Strategies such as a single zoledronic acid infusion or short-term alendronate reduce rebound bone loss and potentially VF risk after stopping short-term denosumab (≤ 2.5 years). However, effective approaches to address rebound bone loss after longer-term denosumab remain elusive and repeat doses as suggested by recent guidelines may not prevent VFs in high-risk groups²⁹. In **Figure 4**, we summarize key decision points when considering denosumab withdrawal based on the emerging evidence-base, depicted as a traffic light system; proceed (green), exert caution (amber) and stop and reconsider before ceasing denosumab (red) due to the potential risk of serious harm.

Much remains unclear and existing data are limited, largely observational and intrinsically challenged by ethical concerns of designing 'safe control groups' in patients ceasing denosumab with non-maleficence in mind. Taking this question to the lab and seeking greater insights in osteoclast biology, including withdrawal effects of RANKL inhibition, the chronology of osteoclastogenic markers characterizing the early, potentially modifiable phase of rebound, are shaping future efforts in the clinic. These translational studies are posing critical new questions: could other serum markers, such as TRAP5b or RANKL, better inform optimal timing of sequential therapy? Should we be intervening with bisphosphonates earlier than 6-months after the last denosumab dose with the aim to prevent rebound in its earliest stage? Are bisphosphonates alone the answer or is there a role for gradual denosumab dose tapering or overlapping osteoanabolic treatment?

Ultimately, discovering an effective ‘*exit strategy*’ to prevent rebound bone turnover, bone loss and spontaneous VFs after prolonged denosumab is essential in improving confidence amongst patients and clinicians in this highly effective and otherwise safe treatment for osteoporosis.

UNCORRECTED MANUSCRIPT

Figure Legends

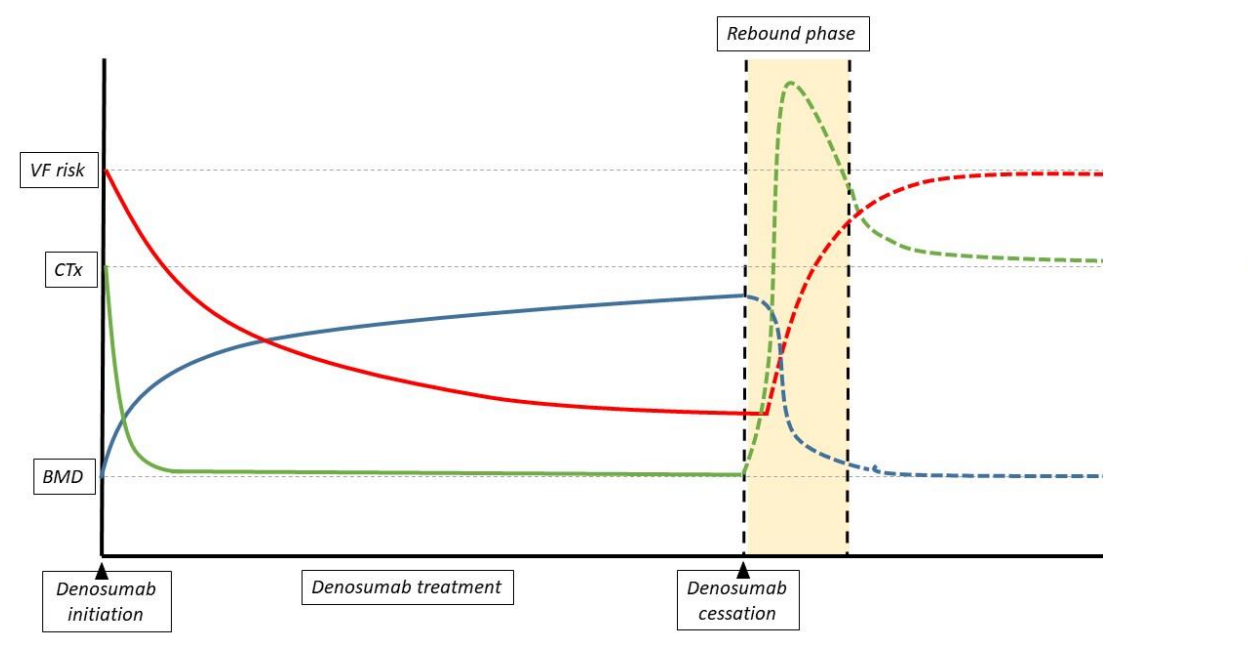


Figure 1: Changes in bone mineral density (BMD), c-terminal telopeptide of type 1 collagen (CTx) and vertebral fracture (VF) risk at baseline, during and post denosumab cessation

CTx falls rapidly with initiation of denosumab treatment and remains suppressed for the duration of treatment. Upon denosumab cessation (defined as 6-months after the last denosumab dose) there is a rapid rebound and *overshoot* in CTx before slowly returning to baseline levels. BMD rises gradually during denosumab treatment. After cessation and along with the rebound in CTx, there is a rapid decline in BMD back towards baseline levels, earlier than the return of CTx to baseline. Fracture risk, including VF risk, falls with ongoing denosumab treatment. In the setting of exaggerated bone turnover and declining BMD, there is a rapid increase in VF risk, particularly

multiple VFs, with a return towards baseline risk. Graphical concepts adapted from Bone et al., 2011 and Miller et al., 2008.

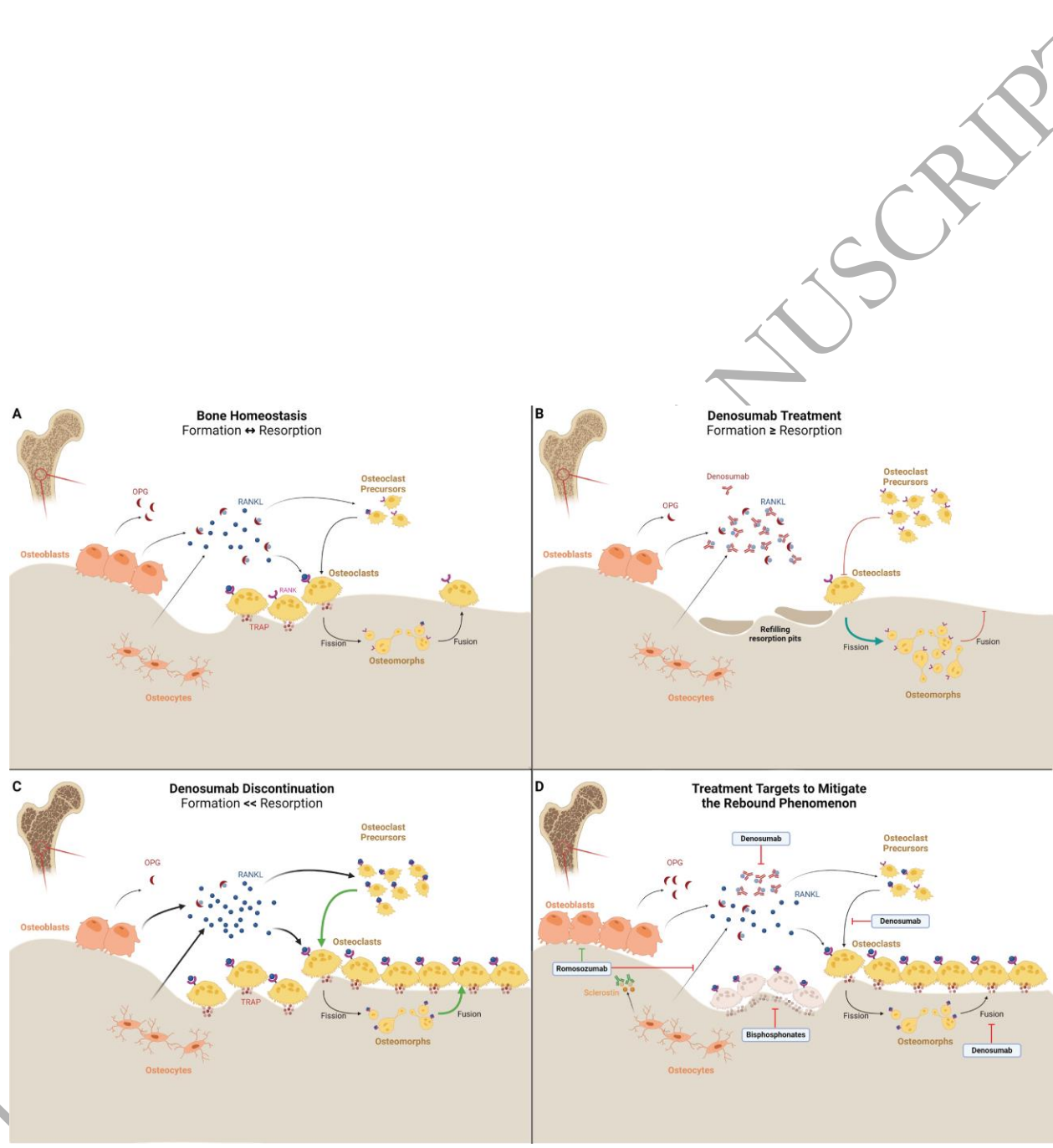


Figure 2: Changes in bone homeostasis during denosumab treatment and discontinuation and targets for sequential therapy

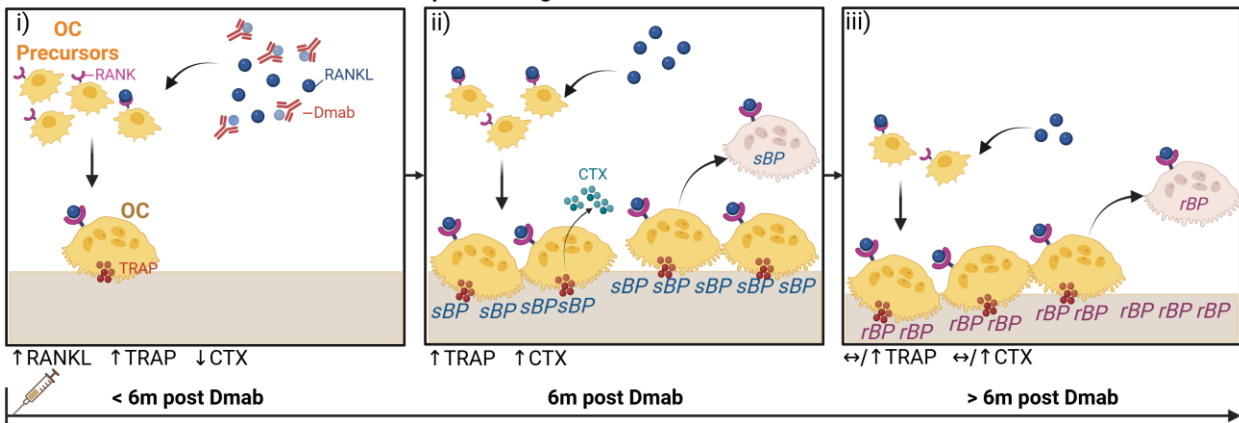
- A) Bone homeostasis is maintained by interaction between bone formation by osteoblasts and bone resorption by osteoclasts which is regulated by RANKL/RANK/OPG signalling. Osteoclasts may undergo ‘recycling’ where, under RANKL stimulation, osteoclasts undergo fission to form osteomorphs which can circulate and fuse to re-form osteoclasts.
- B) Denosumab inhibits RANKL/RANK binding, preventing osteoclast differentiation, and promoting accumulation of osteoclast precursors. Osteoclasts may undergo fission to form osteomorphs but fusion is also inhibited by denosumab, leading to an accumulation of osteomorphs.
- C) Upon denosumab discontinuation and offset of RANKL inhibition, increased RANKL signalling promote differentiation and activation of accumulated osteoclast precursors. Accumulated osteomorphs may also fuse to form active osteoclasts. Bone turnover resumes and osteoblastic bone formation and OPG secretion also restarts but delayed relative to osteoclastogenesis and bone resorption, leading to net bone loss.
- D) Targets for sequential therapy following denosumab discontinuation: bisphosphonates primarily target and inhibit active osteoclasts resorbing bone without impacting osteoclast differentiation and activation. Romosozumab inhibits sclerostin signalling, promoting osteoblast formation and resultant OPG production and bone gains, as well as inhibiting osteoclast formation. Rescue therapy with denosumab reverses the pathophysiology of the rebound phenomenon, targeting RANKL/RANK binding, inhibiting osteoclast formation as well as potentially inhibiting re-fusion of accumulated osteomorphs.

RANKL; receptor activator of nuclear factor kappa beta ligand, RANK; receptor activator of nuclear factor kappa beta, OPG; osteoprotegerin, TRAP; tartrate resistant acid phosphatase.

Created with BioRender.com.

UNCORRECTED MANUSCRIPT

A. Standard 'On Time' Intervention and Repeat Dosing



B. 'Early' Intervention and Repeat Dosing

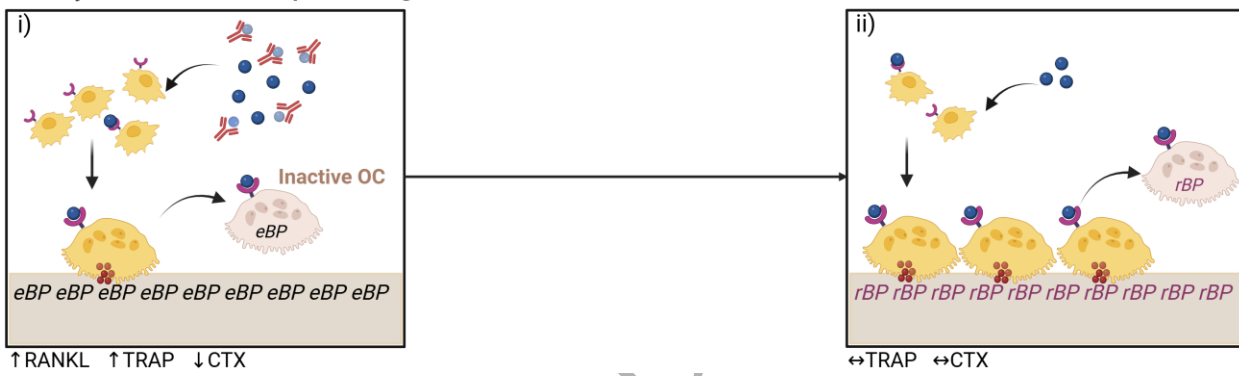


Figure 3: Mechanistic representation of effects of sequential bisphosphonates on targeting rebound bone loss based on concepts extrapolated from preclinical studies

A) Standard 'On Time' Intervention and Repeat Dosing

- i. As the effect of denosumab wanes before the next dose, accumulated osteoclast precursors and osteomorphs form osteoclasts and bone resorption resumes. Serum RANKL and TRAP may become elevated above on-treatment suppressed levels. CTX, however, would likely remain suppressed at this time
- ii. Six-months following the last denosumab dose, bone loss is occurring. Rising TRAP and CTX levels may be seen at this time due to increased bone resorption. 'On Time'

Sequential bisphosphonate (sBP) at this time targets bone resorbing osteoclasts. Standard timing of BPs may mitigate some bone loss, however osteoclasts are more abundant at this stage compared to an earlier intervention window.

- iii. Rebound bone loss continues as accumulated osteoclast precursors and osteomorphs not targeted by the initial bisphosphonate doses are purported to continue to form osteoclasts. Repeat doses of bisphosphonates (rBP) may be required at this time to target these newly formed osteoclasts. Serum TRAP and CTX levels may remain elevated as increased osteoclastic bone resorption continues, or return to baseline levels if resorption is suppressed with repeated BP dosing.

B) 'Early' Intervention and Repeat Dosing

- i. Early bisphosphonate administration (eBP) within 6 months post last denosumab dose may inhibit bone resorption by the initial wave of osteoclasts differentiating from the accumulated pool of precursors.
- ii. Osteoclasts continue to form and repeat bisphosphonate doses (rBP) may be needed to target these newly formed osteoclasts.

OC; osteoclasts, RANK; receptor activator of nuclear factor kappa beta, RANKL; receptor activator of nuclear factor kappa beta ligand, Dmab; denosumab, BP; bisphosphonates, TRAP; tartrate resistant acid phosphatase, CTX; cross-linked C-telopeptide of type I collagen,. Created with BioRender.com.

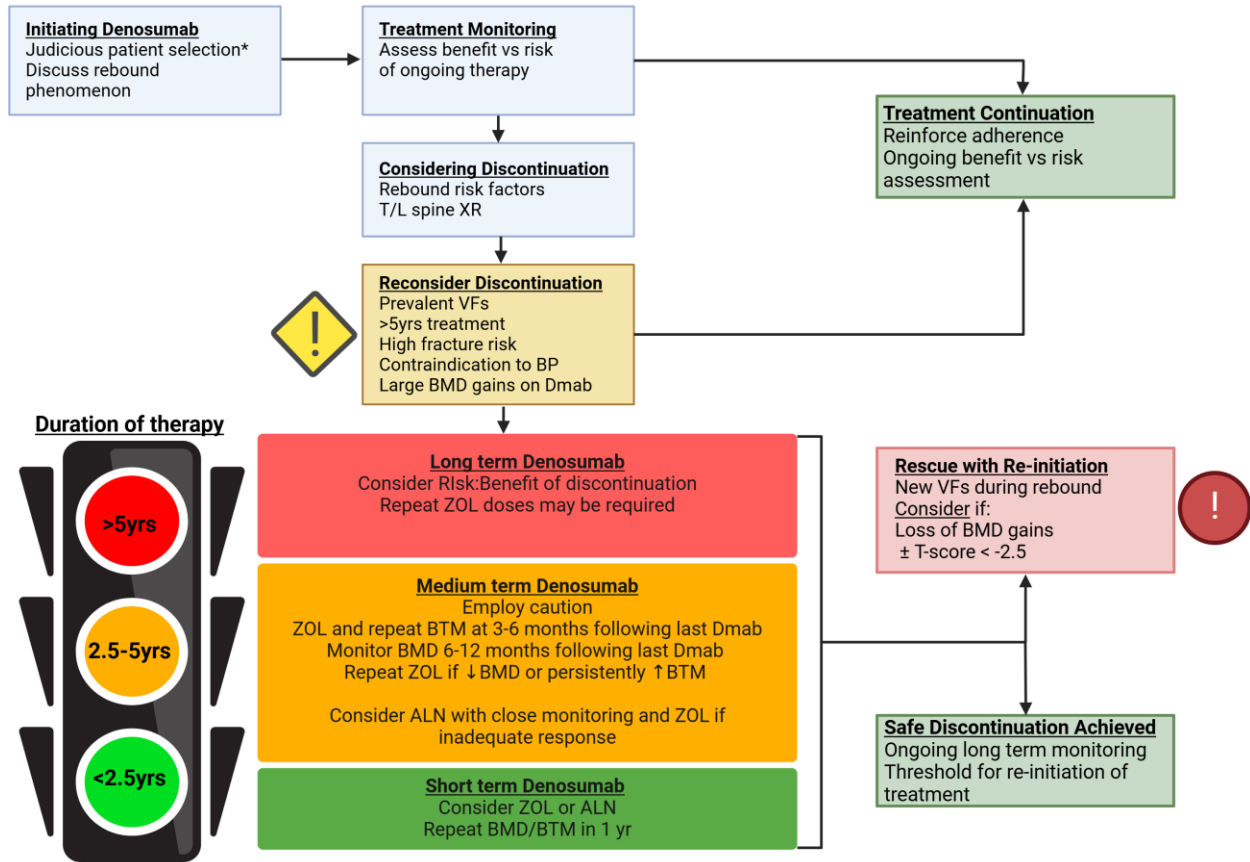


Figure 4: Clinical Considerations for Denosumab Initiation, Discontinuation and Re-initiation

*Prior to initiating denosumab therapy, consider fracture risk and appropriateness for long-term antiresorptive therapy. Stopping denosumab and transitioning to other osteoporosis medications may be more appropriate in cases where long-term antiresorptive therapy is unlikely to be required.

T/L spine XR: thoracolumbar spine X-ray, VF; vertebral fracture, BP; bisphosphonates, ZOL; zoledronate, BTM; bone turnover markers, Dmab; denosumab, BMD; bone mineral density, ALN; alendronate. Created with BioRender.com.

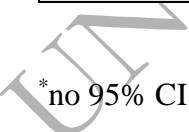
Tables

Table 1: Trial evidence for denosumab efficacy across various clinical indications

Patient population	Trial – participant characteristics	Efficacy	
Postmenopausal osteoporosis ²	N= 7,868 Duration: 3 years Inclusion: Postmenopausal women between 60-90 years BMD T-score between -2.5 and -4.0 SD	BMD gain (vs. placebo)	
		Lumbar spine	9.2% (95% CI: 8.2-10.1)
		Total hip	6.0% (95% CI: 5.2-6.7)
		Fracture risk reduction (vs. placebo)	
		Vertebral	68% (95% CI: 59-74)
		Hip	40% (95% CI: 3-63)
		Non-vertebral	20% (95% CI: 5-33)
Male osteoporosis ⁷	N= 242	BMD gain (vs. placebo)	

	<p>Duration: 1 year</p> <p>Inclusion: Men between 30-85 years</p> <p>BMD T-score between -2.0 and -3.5 SD, or T-score between -1.0 and -3.5 SD with osteoporotic fracture</p>	<p>Lumbar spine</p> <p>4.8% (95% CI: 4.0-5.6)</p> <p>Total hip</p> <p>2.1%*</p> <p>Femoral neck</p> <p>2.1%*</p>	Downloaded from https://academic.oup.com/jbmr/advance-article/doi/10.1093/jbmr/ziaa037/8066440 by University of Sydney user on 12 June 2025	
Osteoporosis in setting of chronic kidney disease ⁹	<p>N= 3,750</p> <p>Duration: 7-10 years</p> <p>Inclusion: Postmenopausal women between 60-90 years with Stage 2 or 3 CKD</p> <p>BMD T-score between -2.5 and -4.0 SD</p>	BMD gain (vs. baseline)		
		Lumbar spine		14.9-23.7%
		Total hip	6.2-9.8%*#	
		Fracture risk reduction at 3 years (vs. placebo)		
		Vertebral	82-100%&	
		Non-vertebral	10-25%&	
Glucocorticoid-induced osteoporosis ⁵	<p>N= 795</p> <p>Duration: 2 years</p> <p>Inclusion: Patients ≥18 years receiving ≥7.5mg prednisolone or equivalent daily</p> <p>Patients ≥ 50 years included if BMD T-score ≤ -2.0 SD, or ≤ -1.0 SD with history of osteoporotic fracture</p> <p>Patients <50 years included if history of osteoporotic fracture</p>	BMD gain (vs. risedronate)		
		Lumbar spine	3.2-4.5% (95% CI: 2.0-5.8)^	
		Total hip	2.5-3.1% (95% CI: 1.3-3.9)^	
		Femoral neck	1.8-2.5% (95% CI: 0.4-3.6)^	

Aromatase inhibitor therapy-induced bone loss ⁶	N= 252 Duration: 2 years Inclusion: Women ≥18 years with hormone receptor positive non-metastatic breast cancer on aromatase inhibitor therapy BMD T-score between -1.0 and -2.5 SD	BMD gain (vs. placebo)	
		Lumbar spine	7.6% *
		Total hip	4.7% *
		Femoral neck	3.6% *
Androgen deprivation therapy-induced bone loss ⁸	N= 1,468 Duration: 3 years Inclusion: Men with non-metastatic prostate cancer on ADT Men ≥ 70 years with any BMD T-score Men <70 years with BMD T-score < -1.0 SD or history of osteoporotic fracture	BMD gain at 2 years (vs. placebo)	
		Lumbar spine	6.7% *
		Total hip	4.8% *
		Femoral neck	3.9% *
		Fracture risk reduction at 3 years (vs. placebo)	
		Vertebral	62% (95% CI: 22-81)
		Any fracture	28% (not significant)

 *no 95% CI provided

#range depending on CKD stage and treatment duration of 7 or 10 years

&range depending on CKD stage

Downloaded from https://academic.oup.com/ajkd/advance-article-abstract/doi/10.1093/ajkd/afz037/8064740 by University of Sydney user on 12 June 2025

^range depending on glucocorticoid-initiating or glucocorticoid-continuing groups

Table 2: Risk Factors for Developing Vertebral Fractures and/or BMD loss After Denosumab Withdrawal

Risk Factors for Vertebral Fractures and/or BMD loss After Denosumab Withdrawal		
Prior to denosumab therapy	During denosumab therapy	After denosumab therapy
<ul style="list-style-type: none">• Prevalent VFs or other fragility fracture• No bisphosphonate therapy• Younger age	<ul style="list-style-type: none">• Prevalent VFs or other fragility fracture• Longer treatment duration (> 2-3 years)• Greater BMD gain	<ul style="list-style-type: none">• No bisphosphonate therapy• Longer duration off-therapy• Greater hip BMD loss• Higher off-treatment CTx

Table summarized from references 14, 15, 16, 20, 22, 26, 28, 29, 30, 31, 32

Table 3: Clinical studies investigating strategies to mitigate rebound after short-term (<2.5-3.0 years) denosumab use

1 st author Year	Study design	Study population	Prior Dmab exposure	Medication	Time since last Dmab	BMD outcomes	BTM outcomes	VF outcomes
Tsai 2024	Extension of open-label RCT (CARD)	N = 18 Postmenopausal osteoporosis Mean age – 66y	1.0 years	ALN 1-year (N=8)	6 months	BMD maintained in both groups at 2-years	BTMs suppressed in both groups	Nil VFs (radiographic)
				ALN 2-years (N=10)				
Anastasilakis 2023	Extension of prospective open-label randomized (AfterDmab)	N = 16 Treatment-naïve postmenopausal osteoporosis Mean age – 65y	Mean 2.5 years	ZOL (N=16)	NR	N=9 – BMD stable for 5 years N=7 – retreated for BMD loss	N/A	Nil VFs (clinical & radiographic)
Ramchand 2023	Open-label RCT (CARD)	N = 51 Postmenopausal osteoporosis Mean age – 66y	1.0 years	ALN (N=26)	6 months	BMD maintained with ALN ~50% decline at LS and TH, maintained at FN with RLX	CTx, P1NP suppressed with ALN and returned to baseline with RLX	One VF (radiographic) with ALN
				RLX (N=25)				
Tutaworn 2023	Retrospective observational (real-world)	N = 121 93% female Mean age – 71y	Mean 2.5 years	ZOL (N=32)	6 months	BMD mostly preserved with ZOL and ALN >50% gains lost with RIS		One VF with ZOL, one VF with ALN (clinical)
				ALN (N=34)				
				RIS (N=22)				
				Nil (N=33)				

Hong 2022	Observational (real-world) Propensity score matching	N = 66 Postmenopausal women Mean age – 69y	0.5-2.0 years	RLX (N=33)	NR	RLX attenuated BMD loss at LS vs nil treatment, but not TH or FN	N/A	Nil VFs (clinical & radiographic)
				Nil (N=33)				
Ha 2022	Retrospective observational (real-world)	N = 61 Postmenopausal women Mean age – 66y	1.0-2.5 years	RLX (N=61)	6 months	Loss of all BMD gains at LS, TH and FN	Overshoot in CTx, P1NP	Nil VFs (radiographic)
Everts-Graber 2022	Retrospective case series	N = 32	0.5 years	ZOL (N=32)	6 months	BMD maintained	BTMs declined	Nil VFs
Ramchand 2021	Extension of prospective open-label randomized (DATA-HD)	N = 53 Postmenopausal osteoporosis Mean age – 66y	1.0 years Overlap with 9-months TPTD	ZOL (N=53)	5.5-8.0 months	BMD maintained at 12-months at LS, TH, FN BMD maintained at 27-months (other than small loss at LS)	BTMs increased but not back to baseline	Nil VFs (clinical)
Ebina 2021	Retrospective multicentre observational (real-world)	N = 64 Postmenopausal osteoporosis Mean age – 73.1 Previously treated with BPs/TPTD for	1.0-1.5 years	RLX (N=13)	Mean 7 months	No sig. diff. in LS BMD Greater FN BMD loss with RLX	Trend to greater rise in serum TRAP5b using RLX	More frequent clinical VFs with RLX (n=3 vs n=1 vs n=0)
				Oral BPs (N=26)				
				ZOL (N=11)				

		mean 18-months						
Kadaru 2021	Retrospective case series	N = 12 Postmenopausal women Mean age – 77y	Median 2.5 years	ZOL (N=12)	Median 7 months	BMD mostly preserved at LS ~50% gains lost at TH, FN	N/A	Nil VFs (clinical)
Kendler 2020	Randomized multicentre open-label cross-over (DAPS)	N = 115 Treatment-naïve postmenopausal women Mean age – 65y	1.0 year	ALN (N=115)	6 months	BMD maintained at LS, TH and FN	Stable CTx and P1NP	Nil VFs (clinical)
Laroche 2020	Prospective cohort study	N = 18 Postmenopausal women Mean age – 70y	Mean 3.0 years	RIS (N=18)	6 months	Loss of ~50% BMD gains at LS and TH	Mean CTx 303 ng/L	One clinical VF
Kondo 2020	Retrospective multicentre observational (real-world)	N = 18 Postmenopausal women Mean age – 76y	Mean 1.5 years	ZOL (N=18)	Mean 9 months	BMD maintained at LS and FN	No increase in TRAP5b	Nil VFs (clinical/radiographic)
Anastasilakis 2019	Prospective open-label randomized (AfterDmab)	N = 27 Treatment-naïve postmenopausal osteoporosis Mean age – 65y	2.0-2.5 years	ZOL (N=27)	Mean 6.5 months	BMD maintained at LS and FN	Stable CTx and P1NP	One clinical VF
			≥1 year	BPs (N=10)	NR			

Zanchetta 2019[#]	Prospective observational (real-world)	N = 33 Postmenopausal women		Nil (N=23)		BMD declined at LS but remained stable at FN with BPs	CTx more than tripled with BPs	Nil VFs (radiographic)
Horne 2018	Observational post-RCT (FRAME)	N = 19 Postmenopausal osteoporosis Rmab/placebo 1-year→Dmab	2.0 years	ZOL (N=11)	Median 8 months	BMD mostly preserved with ZOL Loss of >50% gains with RIS	N/A	Nil VFs
				RIS (N=5)				
				Nil (N=3)				

RCT = randomized controlled trial; DAPS = Denosumab Adherence Preference Satisfaction study; CARD = comparison of alendronate and raloxifene after denosumab study; FRAME = Fracture study in Postmenopausal Women with Osteoporosis study ; Dmab = denosumab; Rmab = romosozumab; BP = bisphosphonate; TPTD = teriparatide; ZOL = zoledronic acid; ALN = alendronate; RIS = risedronate; RLX = raloxifene; BMD = bone mineral density; LS = lumbar spine; TH = total hip; FN = femoral neck; BTM = bone turnover marker; CTx = C-terminal telopeptide of type 1 collagen; P1NP = propeptide type 1 collagen; TRAP5b = tartrate-resistant acid phosphatase 5b; VF = vertebral fracture.

When generating this stable, the following were excluded: single case reports, small case series, conference abstracts or studies where specific treatment to facilitate Dmab cessation was not specified or outcomes were not reported for specific agents.

Green shading = Complete/near-complete preservation of BMD

Amber shading = Partial preservation of BMD

Red shading = Complete/near-complete loss of BMD

#Zanchetta MB, Pelegrin C, Sarli M, & Miechi L. Bisphosphonates Prevent Bone Loss Associated with Denosumab Treatment

Discontinuation. *Journal of the Endocrine Society*. 2019;3(Suppl 1):SAT-532. doi.org/10.1210/js.2019-SAT-532

Table 4: Clinical studies investigating strategies to mitigate rebound after medium-to-long-term (≥3.0 years) denosumab use

1 st author Year	Study design	Study population	Prior Dmab exposure	Medication	Time since last Dmab	BMD outcomes	BTM outcomes	VF outcomes
Lee 2024	Prospective open-label randomized (DST)	N = 76 randomized to ZOL Predominantly women Mean age – 71y	Median 2.0 years	ZOL (N=61)	6 months	BMD maintained in group with <3y Dmab	No sig. diff. in CTx or P1NP between groups	Three clinical morphometric VFs
				ZOL (N=15)		BMD declined by ~3% at LS in group with ≥3y Dmab		
Grassi 2024	Retrospective observational study	N = 52 Predominantly women Mean age – 71y	Mean 4.0 years	ZOL (N=13)	6-7 months	BMD maintained in group receiving one ZOL dose	BTMs at end of follow-up not recorded	Three clinical VFs and one morphometric VF in group needing 2 nd ZOL dose
				CTx <280ng/L 6-months post		BMD declined by ~5% at LS, ~3-4% at TH and FN in group with high bone		
				ZOL (N=39)				
				CTx				

				≥280ng/L 6-months post and needing 2 nd infusion		turnover prompting 2 nd ZOL dose		
Tutaworn 2023	Subgroup analysis of retrospective real-world study	N = 33 Predominantly women Mean age – 73y	Mean 4.0 years	ZOL (N=11)	6 months	BMD maintained at LS, TH and FN with ZOL and ALN other than ~4% decline in LS BMD with ZOL	N/A	N/A
				ALN (N=22)				
Everts-Graber 2022	Single centre prospective observational study (ProOff)	N = 282 Postmenopausal women Mean age – 66y	Mean 2.5 years (N=144)	ZOL (N=144) ~2.5y Dmab	6 months	Greater BMD loss at LS, TH and FN after medium and long-term Dmab cessation	CTx, P1NP increased after first ZOL dose and decreased after subsequent ZOL dose	VF rates post-Dmab - 7.4% after long Dmab - 2.4% after medium Dmab - 2.1% after short Dmab Three out of four cases of multiple VFs occurred in long Dmab group
			Mean 5.0 years (N=84)	ZOL (N=84) ~5y Dmab				
			Mean 7.5 years (N=54)	ZOL (N=54) ~7.5y Dmab				
Makras 2021	Multicentre prospective cohort study (including post-hoc data)	N = 47 Treatment-naïve postmenopausal	≤3.0 years (N=27)	ZOL (N=27) ≤3y Dmab	6 months	BMD maintained at LS and FN after ≤3.0 years Dmab BMD declined	CTx and P1NP increased similarly in both groups	One clinical VF in group with longer Dmab exposure

	from AfterDmab)	osteoporosis Mean age – 65y	>3.0 years (N=20)	ZOL (N=20) >3y Dmab		by ~7% and ~3% after >3.0 years Dmab Longer duration of Dmab correlated with % decline in LS BMD		
Solling 2021, 2020	Prospective open-label randomized (ZOLARMAB)	N = 61 Postmenopausal women and men >50y with osteopenia Mean age – 69y	Mean 5.0 years	ZOL (N=61)	6 months (N=20)	Similar LS BMD loss in all groups (~4-5%) from end of Dmab to 12 months after ZOL BMD stable in second year (although several patients had repeat ZOL or rescue Dmab)	CTx, P1NP and osteocalcin increased in all groups	Two clinical VFs in 9-month group
					9 months (N=20)			
					Treatment threshold or 12 months (N=21)			
Everts-Graber 2021	Retrospective study	N = 219 Women with osteoporosis Mean age – 66y	Mean 2.5 years	ZOL (N=171)	6 months	No sig. diff. in BMD loss between groups Greater BMD loss at LS and TH associated with longer	Greater CTx rise associated with longer Dmab (>2.5 years)	ZOL associated with fewest VFs (HR 0.16, p=0.02) compared to nil treatment Multiple VFs only observed in
				BPs/SERM (N=22)				
				Nil (N=26)				

						Dmab (>2.5 years)		nil treatment group
Grassi 2021	Retrospective real-world single centre study	N = 120 Predominantly women Mean age – 69y	Mean 3.0 years	ZOL (N=73)	NR	No sig. diff. in BMD loss between ZOL and ALN groups Partial loss of LS BMD gains and loss of majority of TH and FN BMD gains	N/A	VF rates: - 5.9% in combined BP treated groups - 21.1% in untreated group
				ALN (N=28)				
				Nil (N=19)				
Reid 2017	Case series post-FREEDOM RCT extension	N = 6 Postmenopausal women Mean age – 83y	7.0 years	ZOL (N=6)	6 months	Loss of >50% LS BMD gains Loss of all TH BMD gains	Mean P1NP 52 ug/L	NR

DST = Denosumab Sequential Therapy; ZOLARMAB = Treatment with Zoledronic Acid Subsequent to Denosumab in Osteoporosis; ProOff = Prolia Off-treatment; FREEDOM = Fracture Reduction Evaluation of Denosumab in Osteoporosis Every 6 Months; RCT = randomized controlled trial; Dmab = denosumab; ZOL = zoledronic acid; BP = bisphosphonate; SERM = selective estrogen receptor modulator; ALN = alendronate; NR = not reported; BMD = bone mineral density; LS = lumbar spine; TH = total hip; FN = femoral neck; BTM = bone turnover marker; CTx = C-terminal telopeptide of type 1 collagen; P1NP = propeptide type 1 collagen; N/A = not applicable; VF = vertebral fracture; HR = hazard ratio.

When generating this stable, the following were excluded: single case reports, small case series, conference abstracts or studies where specific treatment to facilitate Dmab cessation was not specified or outcomes were not reported for specific agents.

Green shading = Complete/near-complete preservation of BMD

Amber shading = Partial preservation of BMD

Red shading = Complete/near-complete loss of BMD

UNCORRECTED MANUSCRIPT

References

1. Kostenuik PJ. Osteoprotegerin and RANKL regulate bone resorption, density, geometry and strength. *Curr Opin Pharmacol*. Dec 2005;5(6):618-25. doi:10.1016/j.coph.2005.06.005
2. Cummings SR, San Martin J, McClung MR, et al. Denosumab for prevention of fractures in postmenopausal women with osteoporosis. *N Engl J Med*. Aug 20 2009;361(8):756-65. doi:10.1056/NEJMoa0809493
3. Bone HG, Wagman RB, Brandi ML, et al. 10 years of denosumab treatment in postmenopausal women with osteoporosis: results from the phase 3 randomised FREEDOM trial and open-label extension. *Lancet Diabetes Endocrinol*. Jul 2017;5(7):513-523. doi:10.1016/S2213-8587(17)30138-9
4. Lai EC, Lin TC, Lange JL, et al. Effectiveness of denosumab for fracture prevention in real-world postmenopausal women with osteoporosis: a retrospective cohort study. *Osteoporos Int*. May 2022;33(5):1155-1164. doi:10.1007/s00198-021-06291-w
5. Saag KG, Pannacciulli N, Geusens P, et al. Denosumab Versus Risedronate in Glucocorticoid-Induced Osteoporosis: Final Results of a Twenty-Four-Month Randomized, Double-Blind, Double-Dummy Trial. *Arthritis Rheumatol*. Jul 2019;71(7):1174-1184. doi:10.1002/art.40874
6. Ellis GK, Bone HG, Chlebowski R, et al. Randomized trial of denosumab in patients receiving adjuvant aromatase inhibitors for nonmetastatic breast cancer. *J Clin Oncol*. Oct 20 2008;26(30):4875-82. doi:10.1200/JCO.2008.16.3832
7. Orwoll E, Teglbjaerg CS, Langdahl BL, et al. A randomized, placebo-controlled study of the effects of denosumab for the treatment of men with low bone mineral density. *J Clin Endocrinol Metab*. Sep 2012;97(9):3161-9. doi:10.1210/jc.2012-1569
8. Smith MR, Egerdie B, Hernandez Toriz N, et al. Denosumab in men receiving androgen-deprivation therapy for prostate cancer. *N Engl J Med*. Aug 20 2009;361(8):745-55. doi:10.1056/NEJMoa0809003
9. Broadwell A, Chines A, Ebeling PR, et al. Denosumab Safety and Efficacy Among Participants in the FREEDOM Extension Study With Mild to Moderate Chronic Kidney Disease. *J Clin Endocrinol Metab*. Jan 23 2021;106(2):397-409. doi:10.1210/clinem/dgaa851
10. Ferrari S, Lewiecki EM, Butler PW, et al. Favorable skeletal benefit/risk of long-term denosumab therapy: A virtual-twin analysis of fractures prevented relative to skeletal safety events observed. *Bone*. May 2020;134:115287. doi:10.1016/j.bone.2020.115287
11. Kendler DL, Cosman F, Stad RK, Ferrari S. Denosumab in the Treatment of Osteoporosis: 10 Years Later: A Narrative Review. *Adv Ther*. Jan 2022;39(1):58-74. doi:10.1007/s12325-021-01936-y
12. Kim AS, Girgis CM, McDonald MM. Osteoclast Recycling and the Rebound Phenomenon Following Denosumab Discontinuation. *Curr Osteoporos Rep*. Dec 2022;20(6):505-515. doi:10.1007/s11914-022-00756-5
13. Miller PD, Bolognese MA, Lewiecki EM, et al. Effect of denosumab on bone density and turnover in postmenopausal women with low bone mass after long-term continued, discontinued, and restarting of therapy: a randomized blinded phase 2 clinical trial. *Bone*. Aug 2008;43(2):222-229. doi:10.1016/j.bone.2008.04.007
14. Cosman F, Huang S, McDermott M, Cummings SR. Multiple Vertebral Fractures After Denosumab Discontinuation: FREEDOM and FREEDOM Extension Trials Additional Post Hoc Analyses. *J Bone Miner Res*. Nov 2022;37(11):2112-2120. doi:10.1002/jbmr.4705

15. Cummings SR, Ferrari S, Eastell R, et al. Vertebral Fractures After Discontinuation of Denosumab: A Post Hoc Analysis of the Randomized Placebo-Controlled FREEDOM Trial and Its Extension. *J Bone Miner Res.* Feb 2018;33(2):190-198. doi:10.1002/jbmr.3337
16. McClung MR, Wagman RB, Miller PD, Wang A, Lewiecki EM. Observations following discontinuation of long-term denosumab therapy. *Osteoporos Int.* May 2017;28(5):1723-1732. doi:10.1007/s00198-017-3919-1
17. Cruchelow KR, Peter ME, Chakrabarti A, et al. Denosumab treatment lapses, discontinuation, and off-treatment fracture risk: A retrospective study of patients with osteoporosis in a real-world clinical setting. *Bone.* Dec 2023;177:116925. doi:10.1016/j.bone.2023.116925
18. Wang M, Wu YF, Girgis CM. Bisphosphonate Drug Holidays: Evidence From Clinical Trials and Real-World Studies. *JBMR Plus.* Jun 2022;6(6):e10629. doi:10.1002/jbm4.10629
19. Bone HG, Bolognese MA, Yuen CK, et al. Effects of denosumab treatment and discontinuation on bone mineral density and bone turnover markers in postmenopausal women with low bone mass. *J Clin Endocrinol Metab.* Apr 2011;96(4):972-80. doi:10.1210/jc.2010-1502
20. Zanchetta MB, Boailchuk J, Massari F, Silveira F, Bogado C, Zanchetta JR. Significant bone loss after stopping long-term denosumab treatment: a post FREEDOM study. *Osteoporos Int.* Jan 2018;29(1):41-47. doi:10.1007/s00198-017-4242-6
21. Brown JP, Roux C, Topping O, et al. Discontinuation of denosumab and associated fracture incidence: analysis from the Fracture Reduction Evaluation of Denosumab in Osteoporosis Every 6 Months (FREEDOM) trial. *J Bone Miner Res.* Apr 2013;28(4):746-52. doi:10.1002/jbmr.1808
22. Anastasilakis AD, Polyzos SA, Makras P, Aubry-Rozier B, Kaouri S, Lamy O. Clinical Features of 24 Patients With Rebound-Associated Vertebral Fractures After Denosumab Discontinuation: Systematic Review and Additional Cases. *J Bone Miner Res.* Jun 2017;32(6):1291-1296. doi:10.1002/jbmr.3110
23. Gonzalez-Rodriguez E, Aubry-Rozier B, Stoll D, Zaman K, Lamy O. Sixty spontaneous vertebral fractures after denosumab discontinuation in 15 women with early-stage breast cancer under aromatase inhibitors. *Breast Cancer Res Treat.* Jan 2020;179(1):153-159. doi:10.1007/s10549-019-05458-8
24. Burckhardt P, Faouzi M, Buclin T, Lamy O, The Swiss Denosumab Study G. Fractures After Denosumab Discontinuation: A Retrospective Study of 797 Cases. *J Bone Miner Res.* Sep 2021;36(9):1717-1728. doi:10.1002/jbmr.4335
25. Lyu H, Yoshida K, Zhao SS, et al. Delayed Denosumab Injections and Fracture Risk Among Patients With Osteoporosis : A Population-Based Cohort Study. *Ann Intern Med.* Oct 6 2020;173(7):516-526. doi:10.7326/M20-0882
26. Tripto-Shkolnik L, Fund N, Rouach V, Chodick G, Shalev V, Goldshtein I. Fracture incidence after denosumab discontinuation: Real-world data from a large healthcare provider. *Bone.* Jan 2020;130:115150. doi:10.1016/j.bone.2019.115150
27. Anastasilakis AD, Yavropoulou MP, Makras P, et al. Increased osteoclastogenesis in patients with vertebral fractures following discontinuation of denosumab treatment. *Eur J Endocrinol.* Jun 2017;176(6):677-683. doi:10.1530/EJE-16-1027
28. Solling AS, Harslof T, Langdahl B. Treatment with Zoledronate Subsequent to Denosumab in Osteoporosis: a Randomized Trial. *J Bone Miner Res.* Oct 2020;35(10):1858-1870. doi:10.1002/jbmr.4098
29. Grassi G, Ghielmetti A, Zampogna M, et al. Zoledronate after denosumab discontinuation: Is repeated administrations more effective than single infusion? *J Clin Endocrinol Metab.* Apr 13 2024;doi:10.1210/clinem/dgae224
30. Everts-Graber J, Reichenbach S, Gahl B, Ziswiler HR, Studer U, Lehmann T. Risk factors for vertebral fractures and bone loss after denosumab discontinuation: A real-world observational study. *Bone.* Mar 2021;144:115830. doi:10.1016/j.bone.2020.115830
31. Liebich G, Lamy O, Aubry-Rozier B, Gonzalez-Rodriguez E. Maintenance of bone resorption markers in the low premenopausal range during the year following denosumab discontinuation is

- associated to bone density preservation. The ReoLaus study. *Bone*. Jul 2023;172:116764. doi:10.1016/j.bone.2023.116764
32. Lee CC, Wang CY, Yen HK, et al. Zoledronate Sequential Therapy After Denosumab Discontinuation to Prevent Bone Mineral Density Reduction: A Randomized Clinical Trial. *JAMA Netw Open*. Nov 4 2024;7(11):e2443899. doi:10.1001/jamanetworkopen.2024.43899
 33. Grassi G, Chiodini I, Palmieri S, Cairoli E, Arosio M, Eller-Vainicher C. Bisphosphonates after denosumab withdrawal reduce the vertebral fractures incidence. *Eur J Endocrinol*. Aug 4 2021;185(3):387-396. doi:10.1530/EJE-21-0157
 34. Anastasilakis AD, Papapoulos SE, Polyzos SA, Appelman-Dijkstra NM, Makras P. Zoledronate for the Prevention of Bone Loss in Women Discontinuing Denosumab Treatment. A Prospective 2-Year Clinical Trial. *J Bone Miner Res*. Dec 2019;34(12):2220-2228. doi:10.1002/jbmr.3853
 35. Kadaru T, Shibli-Rahhal A. Zoledronic Acid after Treatment with Denosumab is Associated with Bone Loss within 1 Year. *J Bone Metab*. Feb 2021;28(1):51-58. doi:10.11005/jbm.2021.28.1.51
 36. Kondo H, Okimoto N, Yoshioka T, et al. Zoledronic acid sequential therapy could avoid disadvantages due to the discontinuation of less than 3-year denosumab treatment. *J Bone Miner Metab*. Nov 2020;38(6):894-902. doi:10.1007/s00774-020-01126-w
 37. Tutaworn T, Nieves JW, Wang Z, Levin JE, Yoo JE, Lane JM. Bone loss after denosumab discontinuation is prevented by alendronate and zoledronic acid but not risedronate: a retrospective study. *Osteoporos Int*. Mar 2023;34(3):573-584. doi:10.1007/s00198-022-06648-9
 38. Ebina K, Hashimoto J, Kashii M, et al. Effects of follow-on therapy after denosumab discontinuation in patients with postmenopausal osteoporosis. *Mod Rheumatol*. Mar 2021;31(2):485-492. doi:10.1080/14397595.2020.1769895
 39. Everts-Graber J, Lehmann T. Bone Mass Gains After One Denosumab Injection Followed by Zoledronate. *J Clin Densitom*. Jul-Sep 2022;25(3):293-298. doi:10.1016/j.jocd.2022.03.001
 40. Ramchand SK, David NL, Lee H, Eastell R, Tsai JN, Leder BZ. Efficacy of Zoledronic Acid in Maintaining Areal and Volumetric Bone Density After Combined Denosumab and Teriparatide Administration: DATA-HD Study Extension. *J Bone Miner Res*. May 2021;36(5):921-930. doi:10.1002/jbmr.4259
 41. Anastasilakis AD, Makras P, Polyzos SA, Papapoulos SE. The Five-Year Effect of a Single Zoledronate Infusion on Bone Mineral Density Following Denosumab Discontinuation in Women with Postmenopausal Osteoporosis. *Calcif Tissue Int*. Oct 2023;113(4):469-473. doi:10.1007/s00223-023-01119-7
 42. Kendler D, Chines A, Clark P, et al. Bone Mineral Density After Transitioning From Denosumab to Alendronate. *J Clin Endocrinol Metab*. Mar 1 2020;105(3):e255-64. doi:10.1210/clinem/dgz095
 43. Ramchand SK, Tsai JN, Lee H, et al. The comparison of alendronate and raloxifene after denosumab (CARD) study: A comparative efficacy trial. *Osteoporos Int*. Feb 2024;35(2):255-263. doi:10.1007/s00198-023-06932-2
 44. Tsai JN, Jordan M, Lee H, Leder BZ. One versus 2 years of alendronate following denosumab: the CARD extension. *Osteoporos Int*. Aug 7 2024;doi:10.1007/s00198-024-07213-2
 45. Horne AM, Mihov B, Reid IR. Bone Loss After Romosozumab/Denosumab: Effects of Bisphosphonates. *Calcif Tissue Int*. Jul 2018;103(1):55-61. doi:10.1007/s00223-018-0404-6
 46. Laroche M, Couture G, Ruyssen-Witrand A, Constantin A, Degboe Y. Effect of risedronate on bone loss at discontinuation of denosumab. *Bone Rep*. Dec 2020;13:100290. doi:10.1016/j.bonr.2020.100290
 47. Ha J, Kim J, Jeong C, et al. Effect of follow-up raloxifene therapy after denosumab discontinuation in postmenopausal women. *Osteoporos Int*. Jul 2022;33(7):1591-1599. doi:10.1007/s00198-022-06388-w
 48. Hong N, Shin S, Lee S, Kim KJ, Rhee Y. Raloxifene Use After Denosumab Discontinuation Partially Attenuates Bone Loss in the Lumbar Spine in Postmenopausal Osteoporosis. *Calcif Tissue Int*. Jul 2022;111(1):47-55. doi:10.1007/s00223-022-00962-4

49. Makras P, Appelman-Dijkstra NM, Papapoulos SE, et al. The Duration of Denosumab Treatment and the Efficacy of Zoledronate to Preserve Bone Mineral Density After Its Discontinuation. *J Clin Endocrinol Metab.* Sep 27 2021;106(10):e4155-e4162. doi:10.1210/clinem/dgab321
50. Solling AS, Harslof T, Langdahl B. Treatment With Zoledronate Subsequent to Denosumab in Osteoporosis: A 2-Year Randomized Study. *J Bone Miner Res.* Jul 2021;36(7):1245-1254. doi:10.1002/jbmr.4305
51. Everts-Graber J, Reichenbach S, Gahl B, et al. Effects of zoledronate on bone mineral density and bone turnover after long-term denosumab therapy: Observations in a real-world setting. *Bone.* Oct 2022;163:116498. doi:10.1016/j.bone.2022.116498
52. Everts-Graber J, Reichenbach S, Ziswiler HR, Studer U, Lehmann T. A Single Infusion of Zoledronate in Postmenopausal Women Following Denosumab Discontinuation Results in Partial Conservation of Bone Mass Gains. *J Bone Miner Res.* Jul 2020;35(7):1207-1215. doi:10.1002/jbmr.3962
53. Reid IR, Horne AM, Mihov B, Gamble GD. Bone Loss After Denosumab: Only Partial Protection with Zoledronate. *Calcif Tissue Int.* Oct 2017;101(4):371-374. doi:10.1007/s00223-017-0288-x
54. Omiya T, Hirose J, Omata Y, et al. Sustained anti-osteoporotic action of risedronate compared to anti-RANKL antibody following discontinuation in ovariectomized mice. *Bone Rep.* Dec 2020;13:100289. doi:10.1016/j.bonr.2020.100289
55. Kim AS, Taylor VE, Castro-Martinez A, et al. Temporal patterns of osteoclast formation and activity following withdrawal of RANKL inhibition. *J Bone Miner Res.* May 2 2024;39(4):484-497. doi:10.1093/jbmr/zjae023
56. McDonald MM, Khoo WH, Ng PY, et al. Osteoclasts recycle via osteomorphs during RANKL-stimulated bone resorption. *Cell.* Apr 1 2021;184(7):1940. doi:10.1016/j.cell.2021.03.010
57. Negishi-Koga T, Ishikawa K, Tani S, et al. Mouse model of uncoupled bone remodeling upon discontinuation of anti-RANKL antibody therapy (Pre-print). *Bone Research.* 2024;doi:<https://doi.org/10.21203/rs.3.rs-4720958/v1>
58. Gossiel F, Hoyle C, McCloskey EV, et al. The effect of bisphosphonate treatment on osteoclast precursor cells in postmenopausal osteoporosis: The TRIO study. *Bone.* Nov 2016;92:94-99. doi:10.1016/j.bone.2016.08.010
59. Kuroshima S, Al-Salihi Z, Yamashita J. Mouse anti-RANKL antibody delays oral wound healing and increases TRAP-positive mononuclear cells in bone marrow. *Clin Oral Investig.* May 2016;20(4):727-36. doi:10.1007/s00784-015-1550-0
60. Kong SH, Kim JH, Kim SW, et al. Effect of Denosumab on the Change of Osteoclast Precursors Compared to Zoledronate Treatment in Postmenopausal Women with Osteoporosis. *J Bone Metab.* May 2022;29(2):93-101. doi:10.11005/jbm.2022.29.2.93
61. Makras P, Yavropoulou MP, Polyzos SA, et al. The relationship between length of denosumab treatment for postmenopausal osteoporosis and serum TRAcP5b measured six months after the last injection. *Osteoporos Int.* Feb 2024;35(2):365-370. doi:10.1007/s00198-023-06931-3
62. Fu Q, Bustamante-Gomez NC, Reyes-Pardo H, et al. Reduced osteoprotegerin expression by osteocytes may contribute to rebound resorption after denosumab discontinuation. *JCI Insight.* Sep 22 2023;8(18)doi:10.1172/jci.insight.167790
63. Solling AS, Harslof T, Jorgensen NR, Langdahl B. Changes in RANKL and TRAcP 5b after discontinuation of denosumab suggest RANKL mediated formation of osteoclasts results in the increased bone resorption. *Osteoporos Int.* Mar 2023;34(3):599-605. doi:10.1007/s00198-022-06651-0
64. Ferrari S, Langdahl B. Mechanisms underlying the long-term and withdrawal effects of denosumab therapy on bone. *Nat Rev Rheumatol.* May 2023;19(5):307-317. doi:10.1038/s41584-023-00935-3
65. Buck HV, Stains JP. Osteocyte-mediated mechanical response controls osteoblast differentiation and function. *Front Physiol.* 2024;15:1364694. doi:10.3389/fphys.2024.1364694

66. El-Masri BM, Andreasen CM, Laursen KS, et al. Mapping RANKL- and OPG-expressing cells in bone tissue: the bone surface cells as activators of osteoclastogenesis and promoters of the denosumab rebound effect. *Bone Res.* Oct 18 2024;12(1):62. doi:10.1038/s41413-024-00362-4
67. Gatti D, Viapiana O, Fracassi E, et al. Sclerostin and DKK1 in postmenopausal osteoporosis treated with denosumab. *J Bone Miner Res.* Nov 2012;27(11):2259-63. doi:10.1002/jbmr.1681
68. Kim AS, Taylor VE, Castro-Martinez A, et al. Early and multiple doses of zoledronate mitigates rebound bone loss following withdrawal of RANKL inhibition. *J Bone Miner Res.* Jan 23 2025;doi:10.1093/jbmr/zjaf008
69. Seale E, Molina MO, Carsen S, et al. Mitigating the Denosumab-Induced Rebound Phenomenon with Alternating Short- and Long-Acting Anti-resorptive Therapy in a Young Boy with Severe OI Type VI. *Calcif Tissue Int.* May 2023;112(5):613-620. doi:10.1007/s00223-023-01065-4
70. Laroche M, Couture G, Degboe Y. Discontinuation of Denosumab: Gradual Decrease in Doses Preserves Half of the Bone Mineral Density Gain at the Lumbar Spine. *JBMR Plus.* Jul 2023;7(7):e10731. doi:10.1002/jbm4.10731
71. Vargas-Franco JW, Castaneda B, Gama A, et al. Genetically-achieved disturbances to the expression levels of TNFSF11 receptors modulate the effects of zoledronic acid on growing mouse skeletons. *Biochem Pharmacol.* Oct 2019;168:133-148. doi:10.1016/j.bcp.2019.06.027
72. Tsourdi E, Zillikens MC, Meier C, et al. Fracture risk and management of discontinuation of denosumab therapy: a systematic review and position statement by ECTS. *J Clin Endocrinol Metab.* Oct 26 2020;doi:10.1210/clinem/dgaa756
73. Nakashima T, Hayashi M, Fukunaga T, et al. Evidence for osteocyte regulation of bone homeostasis through RANKL expression. *Nat Med.* Sep 11 2011;17(10):1231-4. doi:10.1038/nm.2452
74. Martinez-Reina J, Calvo-Gallego JL, Pivonka P. Combined Effects of Exercise and Denosumab Treatment on Local Failure in Post-menopausal Osteoporosis-Insights from Bone Remodelling Simulations Accounting for Mineralisation and Damage. *Front Bioeng Biotechnol.* 2021;9:635056. doi:10.3389/fbioe.2021.635056
75. Jahn-Rickert K, Wolfel EM, Jobke B, et al. Elevated Bone Hardness Under Denosumab Treatment, With Persisting Lower Osteocyte Viability During Discontinuation. *Front Endocrinol (Lausanne).* 2020;11:250. doi:10.3389/fendo.2020.00250
76. McCutcheon S, Majeska RJ, Spray DC, Schaffler MB, Vazquez M. Apoptotic Osteocytes Induce RANKL Production in Bystanders via Purinergic Signaling and Activation of Pannexin Channels. *J Bone Miner Res.* May 2020;35(5):966-977. doi:10.1002/jbmr.3954
77. Leder BZ, Tsai JN, Uihlein AV, et al. Denosumab and teriparatide transitions in postmenopausal osteoporosis (the DATA-Switch study): extension of a randomised controlled trial. *Lancet.* Sep 19 2015;386(9999):1147-55. doi:10.1016/S0140-6736(15)61120-5
78. Saini V, Marengi DA, Barry KJ, et al. Parathyroid hormone (PTH)/PTH-related peptide type 1 receptor (PPR) signaling in osteocytes regulates anabolic and catabolic skeletal responses to PTH. *J Biol Chem.* Jul 12 2013;288(28):20122-34. doi:10.1074/jbc.M112.441360
79. McClung MR, Bolognese MA, Brown JP, et al. Skeletal responses to romosozumab after 12 months of denosumab. *JBMR Plus.* Jul 2021;5(7):e10512. doi:10.1002/jbm4.10512
80. Tominaga A, Wada K, Okazaki K, et al. Effect of the duration of previous osteoporosis treatment on the effect of romosozumab treatment. *Osteoporos Int.* Jun 2022;33(6):1265-1273. doi:10.1007/s00198-021-06261-2
81. Ebina K, Tsuboi H, Nagayama Y, et al. Effects of prior osteoporosis treatment on 12-month treatment response of romosozumab in patients with postmenopausal osteoporosis. *Joint Bone Spine.* Oct 2021;88(5):105219. doi:10.1016/j.jbspin.2021.105219

82. Hong N, Shin S, Kim H, Cho SJ, Park JA, Rhee Y. Romosozumab following denosumab improves lumbar spine bone mineral density and trabecular bone score greater than denosumab continuation in postmenopausal women. *J Bone Miner Res.* Feb 2 2025;40(2):184-192. doi:10.1093/jbmr/zjae179
83. Kumar S, Gild ML, McDonald MM, Kim AS, Clifton-Bligh RJ, Girgis CM. A novel sequential treatment approach between denosumab and romosozumab in patients with severe osteoporosis. *Osteoporos Int.* Jun 5 2024;doi:10.1007/s00198-024-07139-9
84. Adami G, Pedrollo E, Rossini M, et al. Romosozumab added to ongoing denosumab in postmenopausal osteoporosis, a prospective observational study. *JBMR Plus.* Apr 2024;8(4):ziae016. doi:10.1093/jbmrpl/ziae016
85. Martinez-Reina J, Pivonka P. Effects of long-term treatment of denosumab on bone mineral density: insights from an in-silico model of bone mineralization. *Bone.* Aug 2019;125:87-95. doi:10.1016/j.bone.2019.04.022
86. Minisola S, Cipriani C, Colangelo L, Pepe J. Bone loss after discontinuation of denosumab: the devil is in the details. *J Bone Miner Res.* Mar 4 2024;39(1):3-7. doi:10.1093/jbmr/zjad018